# Colour and Colour Vision

## Elementary Colours in Information Technology

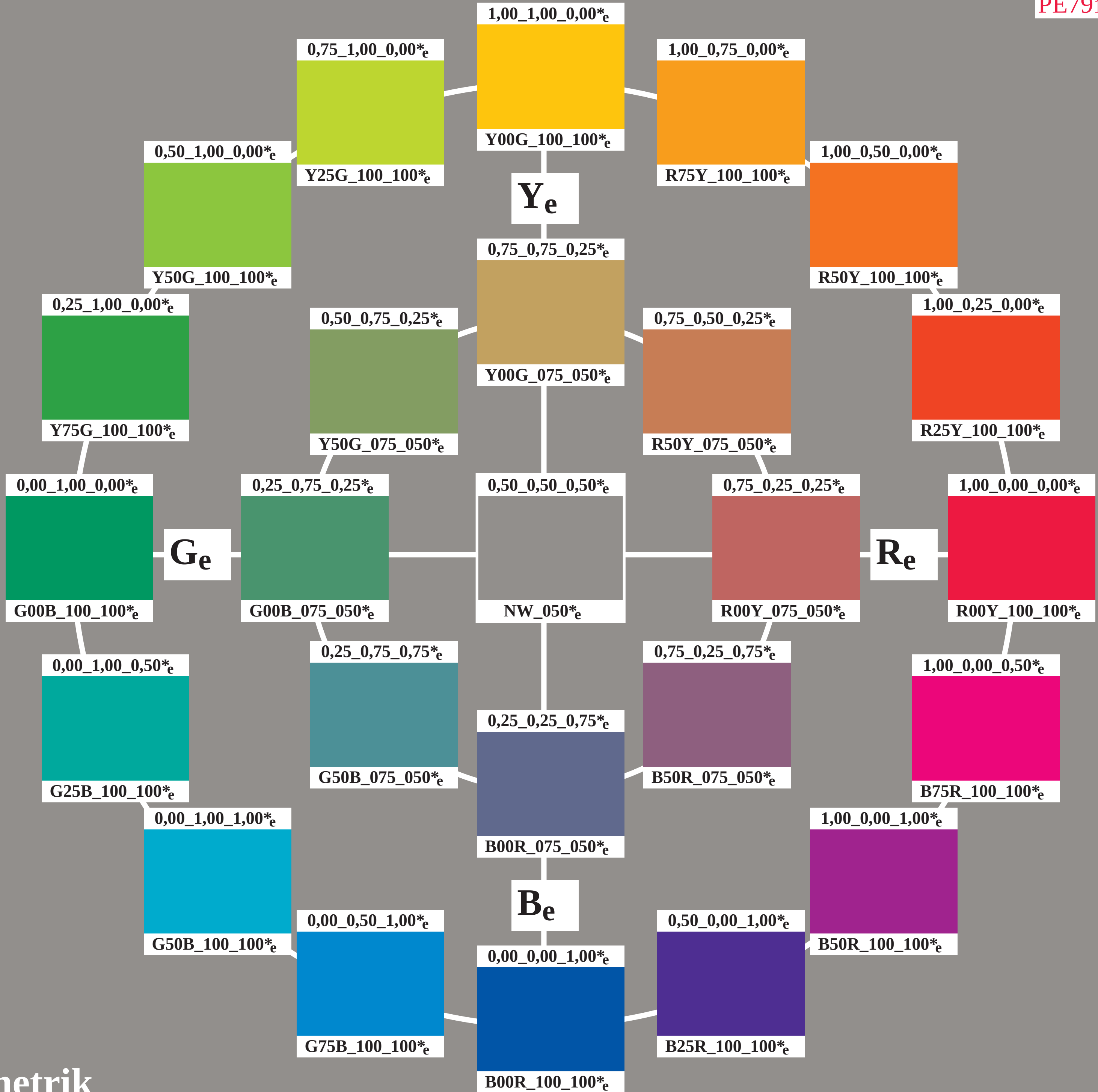


http://130.149.60.45/~farbmetrik

# Colour, Colour Vision and Elementary Colours in Colour Information Technology

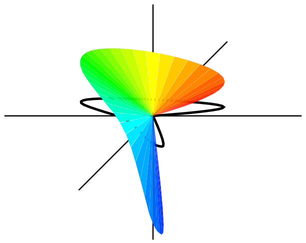

Author:
Prof. Dr. Klaus Richter

Special print for the exhibition
**Colour and Colour Vision (Farbe und Farbsehen)**

at the department Lighting Technology of the
Berlin University of Technology (TU)
Einsteinufer 19
10587 Berlin, Germany

see: http://www.li.tu-berlin.de

This publication (EP_13.PDF) comes with different versions
for monitor (S), offset (L), and printer (P) output, and in
German (G), English (E), Spanish (S), French (F) and Italian (I), see
http://130.149.60.45/~farbmetrik/color



**Content**

**Remarks to the test charts**

The ***test charts no. 1 to 3 for colour rendering*** (PE13, PE23, PE33) are used in lighting and image technology. The following visual evaluations and colorimeric specifications are possible between the real and reference light source (D65, D50, P4000, A) or the real and intended reproduction:
**Colour fidelity:** Colour difference (CIELAB $\Delta E^*_{ab}$) of the reproduction
**Elementary hue location:** Location of the four elementary hues (CIELAB $\Delta h_{ab}$) of the real and the intended reproduction
**Hue scaling:** Shift of the hues (CIELAB $\Delta h_{ab}$) in each hue sector
**Metameric colours:** Colour difference (CIELAB $\Delta E^*_{ab}$) for real and reference light source (D65, D50, P4000, A), or for real and ideal (colorimetric) scanners
**Colour preference:** Colour difference (CIELAB $\Delta E^*_{ab}$) with intended increase in lightness $L^*$ and/or chroma $C^*_{ab}$.

The ***international standards*** ISO/IEC 15775 and ISO 9241-306 as well as the standard series DIN 33866-1 to -5, and DIN 33872-1 to -6 use 5 and 16 step *visual equidistant* colour series for input and output. The equal differences are usually evaluated visually. The colorimetric specification calculates the colour differences between the real and the intended output colours according to CIELAB (ISO 11644-4).

Information to reach the intended output colours is given by a technical description with a table at the two inner cover pages.



# 1 Colour Metric

The colour metric describes the definition and measurement of colours and the colour differences. The colour metric is based on the application of the publication CIE 15 *Colorimetry* of the *International Commission on Illumination (CIE)*.

# 2 Colour and Colour Vision

The description of the quality of colour rendering is only possible on the basis of good knowledge of the properties of the human colour vision. Therefore it is essential to enlarge the basics by visual research. With support of the German Research Foundation *(DFG=Deutsche Forschungsgemeinschaft) K. Richter* (1979, 1985) has edited two BAM research reports. There are many other publications in the field of colour scaling, colour thresholds and elementary hues.

Important separate section of *Colour and Colour Vision* is the psychological order of colours by the human perception. The psycho-physical description of the visual system is based on both the physical measurement and the perception.

In the following sections the basic properties of the field *Colour and Colour Vision* are given.

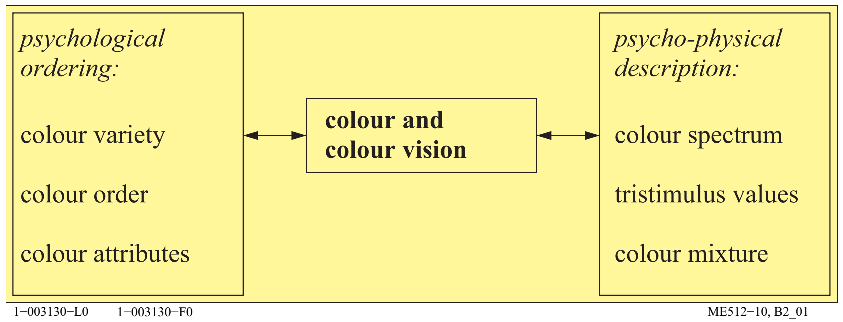


**Fig. 1: Separate sections of colour and colour vision**

Fig. 1 shows the important separate areas of colour and colour vision, which are described in the following by many colour figures.

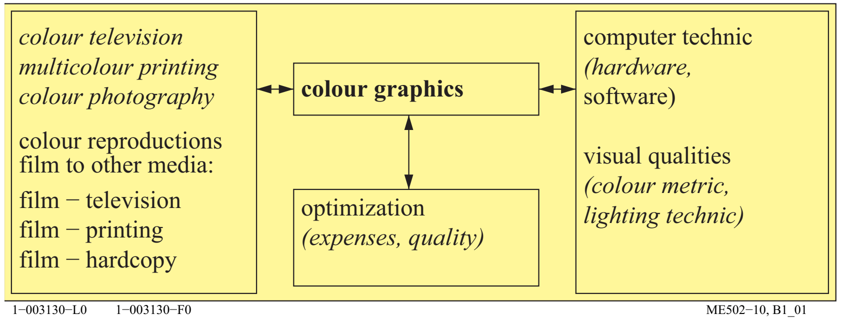


**Fig. 2: Colour graphics as application of the properties of colour vision**

Fig. 2 shows the field of colour graphics, which is essentially based on the properties of colour vision. In addition the properties of the colour reproduction and the computer technic has to be considered to optimise the many applications.

# 3 Colour Multiplicity

All that we see has colour. Colours form the elements of our visual sensations. Different from these sensations are the materials and processes which produce colours. In the following we will order the colour multiplicity. This leads us to colours with equal colour attributes.

According to *Judd* and *Wyszecki* (1975) people with normal colour vision can distinguish about 10 million different colours. A classification by common attributes is thus necessary to order this multiplicity.

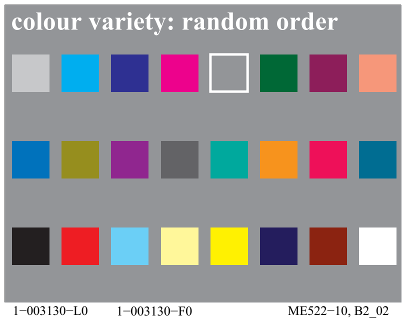


**Fig. 3: Colour multiplicity**

Fig. 3 shows a random arrangement of colour samples which first of all can be separated into groups of achromatic and chromatic colours.



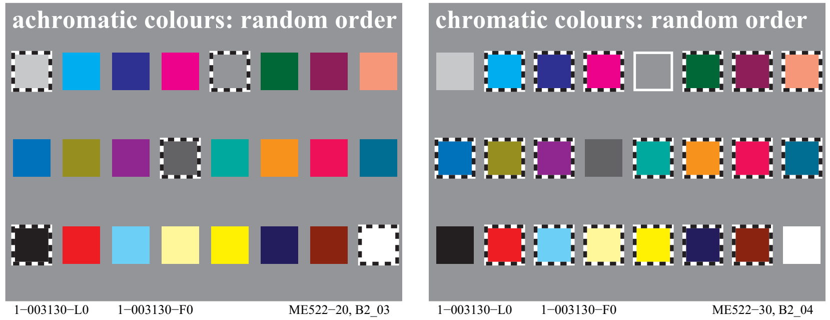


**Fig. 4: Achromatic and chromatic colours**

In Fig. 4 out of the random arrangement of colours, the achromatic group of colours is marked *(left)* and the chromatic group is marked *(right)*.

| **Achromatic colours, intermediate colours** | **Chromatic colours, elementary colours** | **chromatic colours, device colours** |
|---|---|---|
| ***five achromatic colours:*** | ***"neither-nor"-colours*** | ***TV, print (PR), photo (PH)*** |
| *N* black (French noir) | *four elementary (e) colours:* | *six device (d) colours:* |
| *D* dark grey | $R = R_e$ red *neither yellowish nor bluish* | $C = C_d$ cyan blue (cyan) |
| *Z* central grey | | $M = M_d$ magenta red (magenta) |
| *H* light grey | $G = G_e$ green *neither yellowish nor bluish* | $Y = Y_d$ yellow |
| *W* white | $B = B_e$ blue *neither greenish nor reddish* | $O = R_d$ orange red (red) |
| *two intermediate colours:* | | $L = G_d$ leaf green (green) |
| $C_e = G50B_e$ *blue-green* | $J = Y_e$ yellow (French jaune) *neither greenish nor reddish* | $V = B_d$ violet blue (blue) |
| $M_e = B50R_e$ *blue-red* | | |

1–003130–L0 1–003130–F0 ME582–10

**Table 1 Elementary and device colours in information technology**

Table 1 shows the definition of the elementary colours (index e) and the device colours (index d) of the information technology. There are four elementary colours $RGBY_e$ and six device colours $RGBCMY_d$. For some applications the visual intermediate colours $C_e$ (blue-green) and $M_e$ (blue-red) are added to the four elementary colours and produce then six colours (bottom left). Table 1 includes 5 achromatic colours *NDZHW* between black *N* (= French noir) towards mean grey *Z* to white *W*. All others are chromatic colours.

The names *O, L*, and *V* are used in many standard documents, *(for example ISO/IEC 15775, ISO/IEC 24705, ISO 9241-306, DIN 33866-1 to -5, and DIN 33872-1 to -6)*. The names *O, L*, and *V* have the advantages to be short and they represent the appearance. They have the disadvantage to be not used by many applications. In addition the letter *L* is also used for the luminance in all standards of the lighting technology, for example ISO/IEC/CIE 8589.

In the following therefore the letters $R_d$, $G_d$, and $B_d$ will be used instead of the names *O, L,* and *V*. In Table 1 the device colours *(index d)* red $R_d$, green $G_d$ and Blue $B_d$ differ compared to the elementary colours *(index e)* red $R_e$, green $G_e$, and Blue $B_e$. For any undefined colours red, green, and blue the letters *R_*, *G_* and *B_ (letter underscore _)* will be used. The colours RGB_ are usually neither identical to the device colours $R_d$, $G_d$, and $B_d$ nor to the elementary colours $R_e$, $G_e$, and $B_e$. The large advantage of the elementary colours red $R_e$, green $G_e$, and Blue $B_e$ is the *visual definition* and the *device independent property* according to CIE R1-47:2009 "Hue Angles of Elementary colours".

Today in the colour image technology for the specification of colours the digital technic is used. The minimum amount is 4096 colours. The three device colours (index d) $R_d$ (red colour), $G_d$ (green colour) and $B_d$ (blue colour) are used to produce 16 colour steps for each colour. For monitors and data projectors the additive mixture of these colours leads to 4096 (=16x16x16) colours.

The three device colours are usually coded by the hexadecimal system. Therefore the 16 steps with the decimal values 0 to 15 are coded by 0 to 9 and the letters A to F for the values 10 to 15.

For the different colours Fig. 5 shows the appropriate specifications in the hexadecimal system. These specifications correspond to the $rgb_d$-colour data. According to their appearance the three basic colours are named $R_d$=*O* (for orange-red), $G_d$=*L* (for leaf-green), and $B_d$=*V* (for violet-blue).

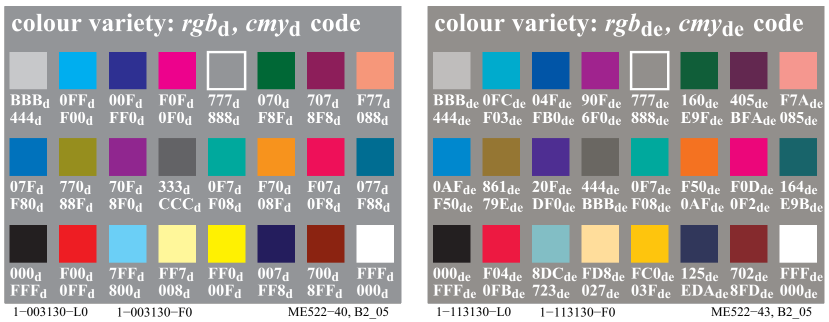


**Fig. 5: *rgb*$_d$, *cmy*$_d$-colour code and *rgb*$_{de}$, *cmy*$_{de}$-colour code**

In Fig. 5 *(left)* the achromatic device colours (index *d=device*) have three equal hex digits. For chromatic colours at least two of the three are different. The device colours $rgb_d$ and $cmy_d$ are transformed between $cmy_d$ and $rgb_d$ data for



the device colour output according to the 1-minus-relation. For example the $rgb_d$-data $00F_d$ for blue are transferred to the $cmy_d$-data $FF0_d$. If in the colour file these two colorimetric definitions are used then equal or different output colours may be produced. With a file according to DIN 33872-4 the equality of the output is tested for both definitions, see http://www.ps.bam.de/De14/10L/L14e00NP.PDF

Fig. 5 *(right)* shows the $rgb_{de}$ and $cmy_{de}$ code for the elementary colour output *(index de = device to elementary data)* by three hex digits. Again the $rgb_{de}$-data are transferred to the $cmy_{de}$-data according to the 1-minus-relation. For example device Blue $B_d$ (first row, third colour) is in Fig. 5 *(left)* defined by the hex number $00F_d$. For the elementary Blue $B_e$ Fig. 5 *(right)* shows the hex digits $09F_{de}$ for the *sRGB* monitor output, $06F_{de}$ for the standard offset output, and $04F_{de}$ for a laser printer output. The device blue $B_d$ and the elementary blue $B_e$ look different. Visually $B_d$ is reddish for all three outputs, and $B_e$ is allways neither reddish nor greenish.

For colour scales, which intent equally spaced visual colour scales, for example an equally spaced 16 step grey series, the symbol * *(star)* for the colour coordinate is used. For example the *visual attribute* lightness *L** uses the symbol * (star) and the measurement term luminance *L* not. Similar one can add to the $rgb_e$ *data* the symbol * *(star)*, and call them $rgb^*_e$ data. The interpretation of this symbol code indicates, that for example the hex-data series $rgb^*_e$ = 000, 111, 222, ... , EEE, FFF produce a *visually equally spaced* grey series.

Instead of the hex data one can use numbers between 0.0 and 1.0. For example for the hex number 5 the decimal number is equal to 0.3333 (=5/F = 5/15). The information technology uses instead of 16 steps between 0 and 9, and from A to F the 256 steps between 00 and 9F, and from A0 to FF. One can transfer these hex numbers to decimal numbers. For example the hex number 55 is equal to the decimal number 0.3333 (=55/FF = 85/255).

For the output of the colorimetric equivalent *rgb*- and *cmy0*-data many problems occur in applications. The display output of the equivalent *rgb* and *cmy0* colour data produces for example with the software products *Adobe Acrobat (all versions above 3 under Mac and Windows) different* output and with *Adobe FrameMaker (Version 8, Windows, 2011) equa*l output. For example *PostScript* colour printers produce often different outputs and *PostScript*-black-white printers equal outputs. With test files according to DIN 33872-4 and -2 the equality of the output is tested, see http://www.ps.bam.de/33872E.

# 4 Colour Solid

*Leonardo da Vinci* (died 1519) ordered the multitude of colours by selecting six ”elementary” colours: one neutral or achromatic pair (white-black) and two chromatic pairs red-green and yellow-blue. The double cone of Fig. 6 serves as a simplified model to illustrate his ideas. The vertical axis corresponding to the array of neutral colours (white to black) and the circumference corresponding to the pure chromatic colours.

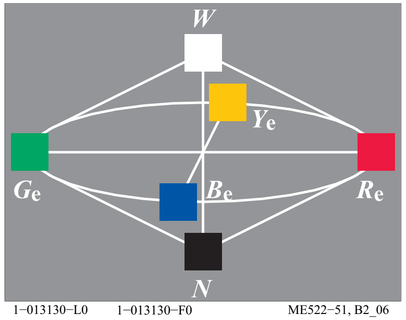


**Fig. 6: Colour double cone**

Fig. 6 shows the double cone with the six “simple” colours. In Fig. 6 the letters stand for:

| | | |
|---|---|---|
| *W* white | $Y_e$ yellow | $R_e$ red |
| *N* black (= noir) | $B_e$ blue | $G_e$ green |

The six “simple” colours are here the six “elementary” colours (index e).

The Technical Committee ISO TC 159/WG2/SC4 *Ergonomics, Visual Display Requirements* has recommended, to produce the four elementary hues $RYGB_e$ with the following four $rgb*_e$-input data 100, 110, 010, and 001, see CIE R1-47. There are at least three methods to calculate the $rgb_{de}$-data (Index de = device to elementary colours) for the output device: by the device manufacturer, the image technology software or a frame file. The frame file method has been used to change all the *rgb*-data of the figures in this publication according to the output device (*sRGB display,* offset print or laser printer). The frame file includes 729 (=9x9x9) *rgb*- and CIELAB-data (colour measurement data) of the output device.



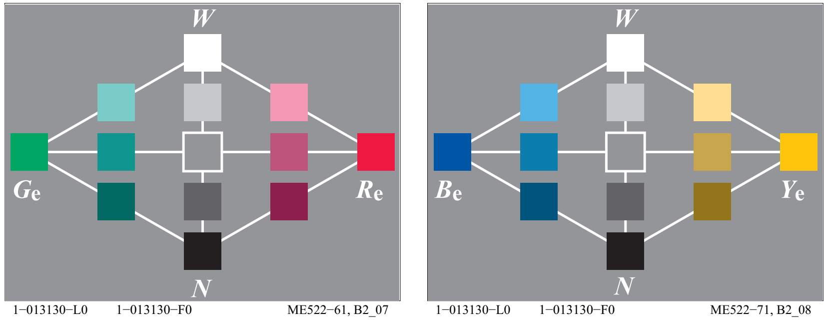


**Fig. 7: $RG_e$- and $YB_e$-hue plane cuts**

Fig. 7 shows the colour double cone with many intermediate steps in the vertical plane cuts red-green *(left)* and yellow-blue *(right)*. The achromatic (white-black) axis is located in the middle.

# 5 Elementary Colours

In any hue circle there are four chromatic colours which are perceptually simple, compare Table 1 on page 6. We call them elementary colours, and we distinguish elementary red, yellow, green, and blue.

Experimentally, bracketing within a hue circle permits easy determination of elementary yellow. Elementary yellow is called a "neither-nor" colour (neither reddish nor greenish) as opposed to yellow-greens which are called "as-well-as” colours (yellow as well as green) in a hue circle. The "neither-nor" colours are often called unique in the literature.

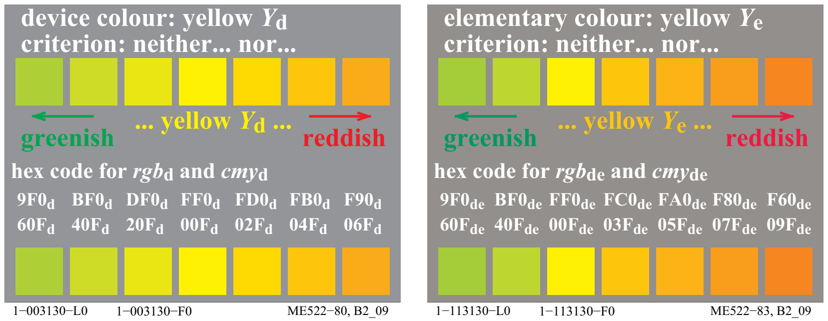


**Fig. 8: Device and elementary colours with criterion for elementary yellow $Y_e$**

Fig. 8 describes the criterion for the determination of the elementary colour yellow $Y_e$ out of a hue circle in the yellow region. For the $rgb_d$-input data $(1\ 1\ 0)_d$ (data separated by spaces) or $FF0_d$ usually the device colour yellow $Y_d$ is produced. The intended elementary yellow $Y_e$ with the visual property *neither greenish nor reddish* is produced with the $rgb_{de}$-input data $(1\ 0{,}86\ 0)_{de} = FD0_{de}$ for the standard *sRGB* monitor, $(1\ 0{,}86\ 0)_{de} = FD0_{de}$ for the standard offset device, and $(1\ 0{,}79\ 0)_{de} = FC0_{de}$ for a laser printer. The hue difference between the device yellow $Y_d$ and the elementary yellow $Y_e$ is largest for a laser printer.

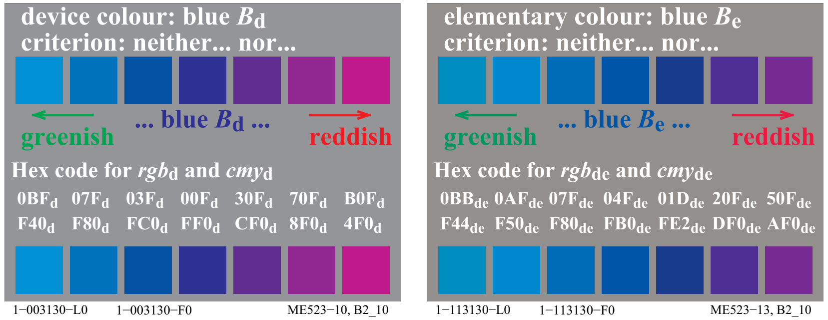


**Fig. 9: Device and elementary colours with criterion for elementary blue $B_e$**

Fig. 9 describes the criterion for the determination of the elementary colour blue $B_e$ out of a hue circle in the blue region. For the $rgb_d$-input data $(0\ 0\ 1)_d$ or $00F_d$ usually the device colour blue $B_d$ is produced. The intended elementary blue $B_e$ with the visual property *neither greenish nor reddish* is produced with the $rgb_{de}$-input data $(0\ 0{,}60\ 1)_{de} = 09F_{de}$ for the standard *sRGB* monitor, $(0\ 0{,}40\ 1)_{de} = 06F_{de}$ for the standard offset device, and $(0\ 0{,}27\ 1)_{de} = 04F_{de}$ for a laser printer. The hue difference between the device blue $B_d$ and the elementary blue $B_e$ is smallest for a laser printer.



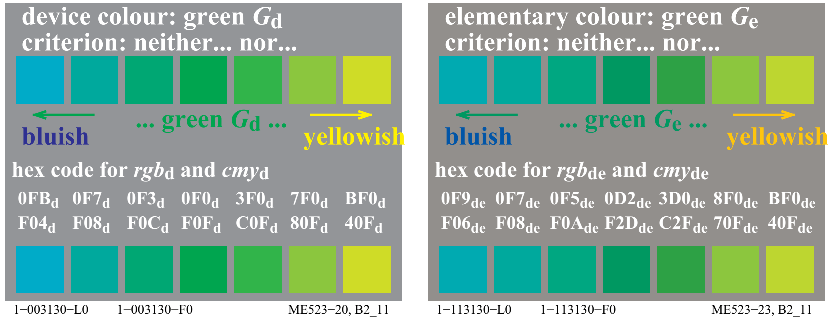


**Fig. 10: Device and elementary colours with criterion for elementary green $G_e$**

Fig. 10 describes the criterion for the determination of the elementary colour green $G_e$ out of a hue circle in the green region. For the $rgb_d$-input data $(0\ 1\ 0)_d$ or $0F0_d$ usually the device colour green $G_d$ is produced. The intended elementary green $G_e$ with the visual property *neither bluish nor yellowish* is produced with the $rgb_{de}$-input data $(0\ 1\ 0{,}67)_{de} = 0FB_{de}$ for the standard *sRGB* monitor, $(0\ 1\ 0{,}07)_{de} = 0F1_{de}$ for the standard offset device, and $(0\ 0{,}87\ 0{,}13)_{de} = 0D2_{de}$ for a laser printer. The hue difference between the device green $G_d$ and the elementary green $G_e$ is smallest for offset print.

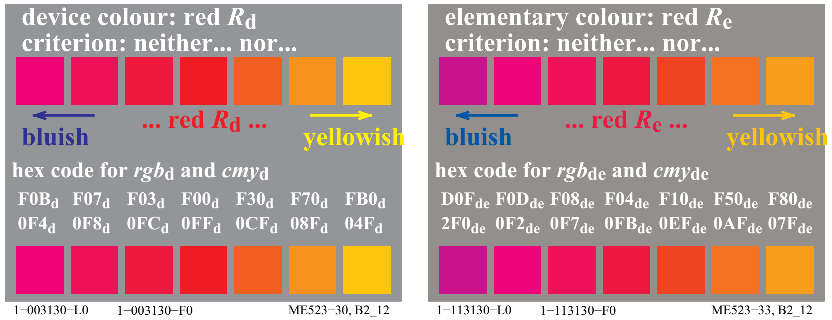


**Fig. 11: Device and elementary colours with criterion for elementary red $R_e$**

Fig. 11 describes the criterion for the determination of the elementary colour red $R_e$ out of a hue circle in the red region. For the $rgb_d$-input data $(1\ 0\ 0)_d$ or $F00_d$ usually the device colour red $R_d$ is produced. The intended elementary red $R_e$ with the visual property *neither bluish nor yellowish* is produced with the $rgb_{de}$-input data $(1\ 0\ 0{,}27)_{de} = F04_{de}$ for the standard *sRGB* monitor, $(1\ 0\ 0{,}20)_{de}$

= F03$_{de}$ for the standard offset device, and (1 0 0,27)$_{de}$ = F04$_{de}$ for a laser printer. The hue difference between the device red $R_d$ and the elementary red $R_e$ is smallest for offset print.

Under daylight and with 28 observers *K. Miescher* (1948) has experimentally determined the elementary colours out of a 400 step hue circle. The standard deviation was 4 steps for $R_e$, $Y_e$ and $G_e$ (1% = 4 of 400 steps) and 8 steps for $B_e$ (2%), see CIE R1-47. The *Miescher* hue circle had a high chroma compared to the CIE-test colours no. 9 to 12, see Fig. 52 on page 53.

## 6 Symmetric Hue Circle

The colours on either side of the two perpendicular elementary hue axis $R_e$-$G_e$ and $Y_e$-$B_e$ become increasingly yellower or bluer, redder or greener respectively, as they depart from the achromatic centre.

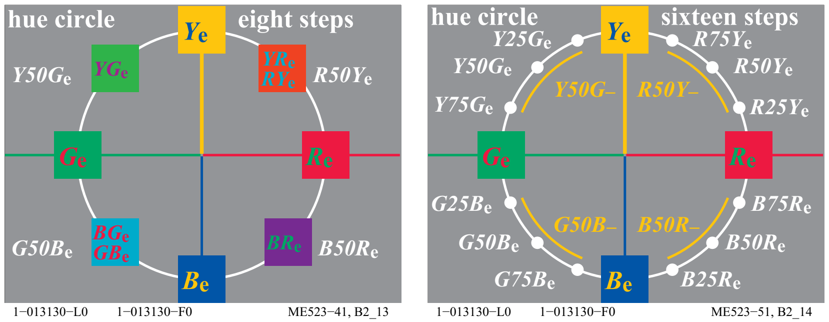


**Fig. 12: Symmetric hue circle and names of intermediate colours**

Fig. 12 shows the symmetric hue circle with the opposing elementary colours red - green and yellow - blue and the intermediate colours.

In most languages (for example German, English, French) yellow and blue is used first in combined colour names: for example yellow-red *YR*, yellow-green *YG*, blue-green *BG*, and blue-red *BR*. This preferred naming in these languages is used in Fig. 12 *(left)* and in addition the naming RY and BG. In Fig. 12 *(right)* the direction of the mathematical angle and the non-preferred continuous naming $RY_e$, $YG_e$, $GB_e$, and $BR_e$ is used. In addition for example $RY_e$ is changed to $R50Y_e$ to allow 100 intermediate steps between 00 to 99.

In addition the CIELAB-colour system (ISO 11664-4/CIE S 014-4) uses for the hue $h_{ab}$ the mathematical angle. The angle count starts at the angle of 0 degree



for elementary red $R_e$ and increases with the angle 90 degree for $Y_e$, 180 degree for $G_e$ and 270 degree for $B_e$.

The CIELAB-colour system uses 100 steps between black and white. One uses 100 hue steps between two elementary colours. This produces in Fig. 12 the names for the intermediate colours. The information technology recommends hue outputs, which shift 25%, 50% and 75% from $R_e$ towards $Y_e$. The output on many devices produce undefined output hues which are located in a large range between $R_e$ and $Y_e$.

Colorimetric information technology recommends to reach the visual intermediate colour with the hue $R50Y_e$. For many of the output devices the output hues for $R50Y_e$ are in a device dependent large range *R50Y_ (yellow range)* and similar for the other intermediate hues $Y50G_e$, $G50B_e$ and $B50R_e$.

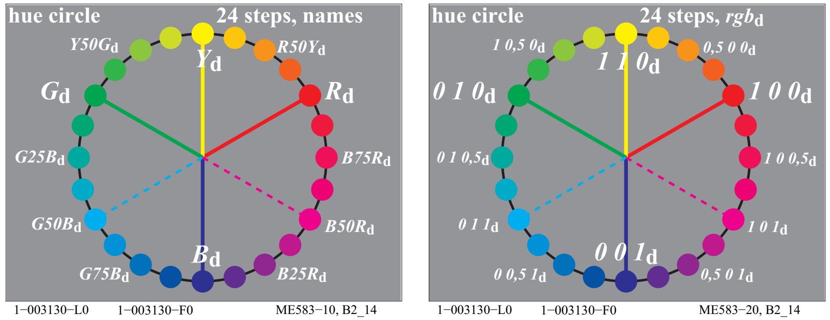


**Fig. 13: 24 steps device-hue circle in information technology**

Fig. 13 shows a 24 step device-hue circle of the information technology. The example device colours $RGB_d$ *(left)* and the corresponding $rgb_d$-input data $(1\ 0\ 0)_d$, $(0\ 1\ 0)_d$, and $(0\ 0\ 1)_d$ *(right)* are given. The intermediate hues $Y_d$, $G50B_d$ and $B50R_d$ of the device have the *rgb*-input data $(1\ 1\ 0)_d$, $(0\ 1\ 1)_d$, and $(1\ 0\ 1)_d$.

For applications in technology, design and art the range of the *lighter* colours between red towards yellow to green is more important compared to the range of *darker* colours between green towards blue to red. In addition in the yellow range the CIELAB chroma $C^*_{ab}$ of surface colours is approximately twice as large compared to the blue range, see the table with $C^*_{ab}$ for 48 hues on the inner back cover. Therefore for *equal* angle difference the *visual hue differences* is twice as large in the yellow range compared to the blue range. Both reasons are used to increase the range between red towards yellow to green from 120 degree to 180 degree, and to decrease the range between green towards blue to red from 240 degree to 180 degree.

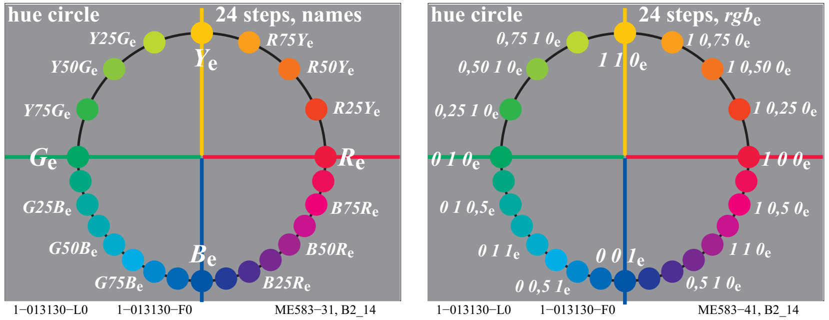


**Fig. 14: 24 steps elementary hue circle of the information technology**

Fig. 14 shows the relation of the elementary hues $RYGB_e$ *(left)* and the $rgb*_e$-input data *(right)* of the information technology for a 24 step hue circle. Fig. 14 produces the elementary hues $RYGB_e$ for the $rgb*_e$-input data $(1\ 0\ 0)_e$, $(1\ 1\ 0)_e$, $(0\ 1\ 0)_e$ and $(0\ 0\ 1)_e$. The workflow *file - output* must produce the $rgb_{de}$-data for the intended output of the elementary hues. In the simplest case the device manufacturer may produce the transformation within his device. DIN 33872-5 includes a test chart in the formats *PDF* and *PS (PostScript)*. The output property *elementary hue* is usually tested visually. In addition it may be specified by colorimetry.

The lower hue discrimination of surface colours in the *darker colour range* between green towards blue to red recommends to use only every second step in this darker area.

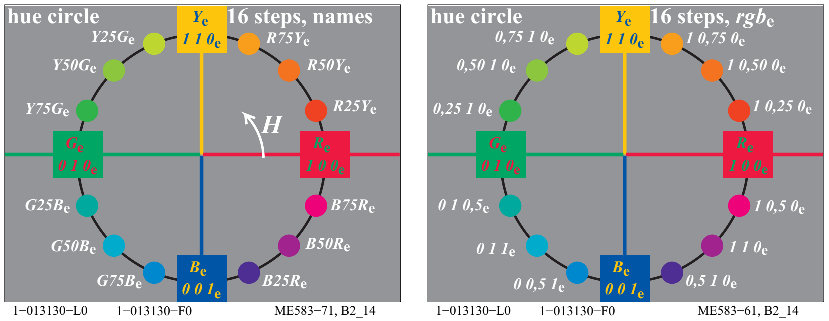


**Fig. 15: 16 steps elementary hue circle of the information technology**

Fig. 15 shows the relation of the elementary hues $RYGB_e$ *(left)* and the $rgb*_e$-input data *(right)* in the information technology in a 16 step hue circle. The elementary hues $RYGB_e$ are produced for $rgb_e$-input data $(1\ 0\ 0)_e$, $(1\ 1\ 0)_e$, $(0\ 1\ 0)_e$ and $(0\ 0\ 1)_e$. The hue changes with the hue angle similar as the hue angle $h_{ab}$ of the CIELAB-colour system (ISO 11564-4). According to CIE R1-47 the elementary hue angles have in the CIELAB-colour system the hue angles $h_{ab} = 26$, 92, 162, and 272 degrees. Especially red $R_e$ and green $G_e$ are not located on the horizontal axis in the CIELAB-colour system.

## 7 Colours with Maximum Chroma

In a colour series with different amount of colorant, leading from whitish colours through chromatic colours to blackish colours, there is one colour that is perceived to exhibit maximum chroma.

Bracketing allows the determination of the "reddest" red in this colour series. This determination is made according to the criterion of whether the colour becomes more achromatic or chromatic, as well as whether it becomes whiter or blacker then the other colours of the series.

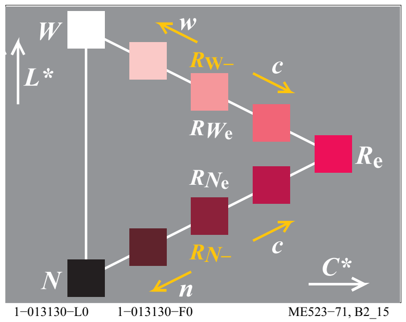


**Fig. 16: Maximum chroma**

In Fig. 16 one can easily determine the most chromatic red colour. The criteria for determining the colour of maximum chroma out of a colour series with different amounts of colorant matter are given. The designations stand for:

| | | |
|---|---|---|
| $R_e$ red | *W* white | *N* black *(= noir)* |
| *c* more chromatic | *w* whiter | *n* blacker |
| $C*$ chroma | $L*$ lightness | |

In the information technology usually the most chromatic colour of any hue (colour of maximum chroma $C*_{ab}$ in the CIELAB-colour system) is mixed with white *W* and black *N*. For the mixture colours between the most chromatic colour $R_e$ and white W the CIE chromaticity difference to white *W* is continuously decreasing, for the mixture of $R_e$ with black *N* the chromaticity is approximately constant. The additive colour mixture on the colour monitor (display), and the often subtractive colour mixture in offset print will be discussed in section 20 on page 67.

In Fig. 16 the visual intermediate colours $R_{We}$ and $R_{Ne}$ shall be produced in the middle between $R_e$ and *W* or *N*. Similar compared to Fig. 12 on page 13 usually the output colours are produced in a large device dependent range *(yellow range)*.

# 8 Colour Attributes Chroma and Lightness

Perceptually, three colour attributes specify a colour. Most colour systems choose hue as the first attribute, for example the *Munsell*-colour system, the colour system DIN 6164, and the *NCS*-colour system. These colour systems differ in the choice of the two other colour attributes. A comparison of the colour systems needs a similar coordinate system. In colorimetry a cut through the colour solid in a plane of constant hue is used. We use on the abscissa the chroma $C^*$ and on the ordinate the lightness $L^*$.

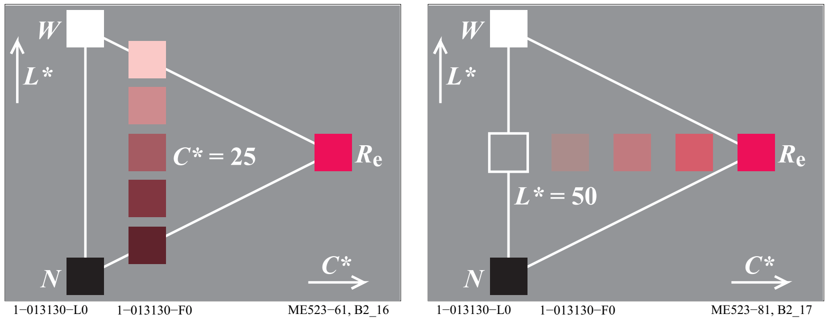


**Fig. 17: Equal chroma $C^*$ and equal lightness $L^*$**

Fig. 17 *(left)* shows colours of constant hue and of the chroma $C^* = 25$. Colours of equal chroma are located on vertical series parallel to the grey axis. In colorimetry for the most chromatic red $R_e$ the chroma $C^*$ =100 may be used. Then in Fig. 17 *(left)* the chroma is $C^* = 25$.

Fig. 17 *(right)* shows colours of constant hue and of the lightness $L^* = 50$. Colours of equal lightness are located on horizontal rows which are perpendicular to the grey axis. Colorimetry defines the lightness $L^*$=100 for white *W*. Then in Fig. 17 *(right)* the colour series has the lightness $L^* = 50$.

At first colour scales of constant hue and equal chroma and lightness were used in the *Munsell*-colour system. This system includes colour samples of 40 different hues. Today in colour metrics the colour spaces ISO 11564-4 and -5 define the coordinates chroma $C^*$ (designations $C^*_{ab}$ in CIELAB and $C^*_{uv}$ in CIE-LUV) and lightness $L^*$.



In the colour order system *RAL-Design* the colour samples of 36 CIELAB-hues $h_{ab}$ = 0, 10, to 350 degrees produce a grid with the chroma differences $\Delta C^*_{ab}$=10 and $\Delta L^*$=10.

# 9 Colour Attributes Brilliance and Whiteness

There are more than three colour attributes hue, chroma, and lightness. In a constant hue plane the further colour attributes blackness (opponent to brilliance) and whiteness (opponent to colour deepness) have a linear relation to chroma and lightness.

The colour attributes blackness and brilliance describe the same property. However, they change their attribute values in opposite directions similar as for lightness and darkness. Further whiteness and colour deepness count in opposite directions. Blackness is chosen as an important colour attribute in *Swedish Natural Color System (NCS)*. The NCS-Colour system chooses the colour attributes hue, blackness, and chroma (called chromaticness). The colour attribute lightness of the *Munsell*-colour system is not used.

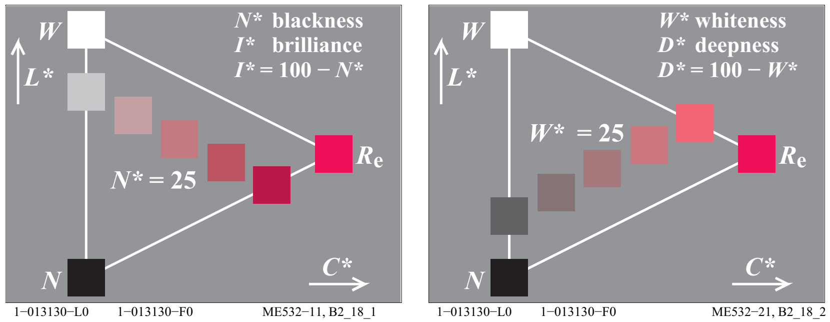


**Fig. 18: Equal blackness $N^*$ and whiteness $W^*$**

Fig. 18 shows colours of equal blackness $N^*$ *(left)* with the blackness $N^* = 25$ and of equal whiteness $W^*$ *(right)* with the whiteness $W^* = 25$. Instead of the blackness $N^*$ the colour attribute brilliance $I^* = 100 - N^*$ may be chosen. Instead of whiteness $W^*$ the colour attribute colour deepness $D^* = 100 - W^*$ may be chosen.

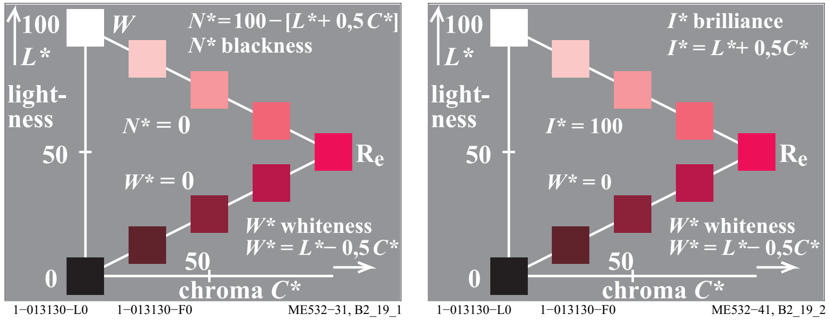


**Fig. 19: Blackness *N**, whiteness *W** and brilliance *I***

Fig. 19 shows the relation of the three colour attributes blackness *N**, whiteness *W**, and brilliance *I** with the two colour attributes lightness *L** and chroma *C**. Fig. 19 shows the relations with linear equations.

It is expected that the linear relations are connected with the physiological achromatic and chromatic signals of Fig. 54 on page 56 and the chromatic values of Fig. 58 on page 64 *(bottom left).*

# 10 Colour Spectrum and Elementary Colours

## 10.1 Luminous Valence and Lightness

The daylight colour spectrum which can be produced by a prism, and which was examined by *Newton* (died 1727), includes the light radiation between the short wave violet-blue (approximately $R60B_e$) and the long wave yellowish red (approximately $Y90R_e$). Colored lights differ in their *spectral power distribution of light radiation*. The spectral distribution of the light radiation which finally falls on the eye is changed by reflection from surfaces which appear colored. for example by use of the pigments of the chemical industry.



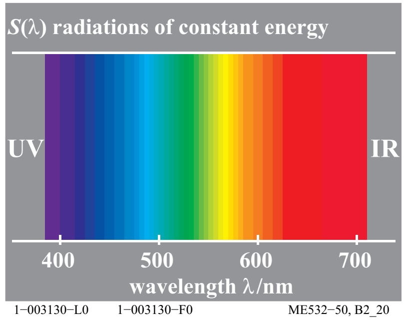


**Fig. 20: Visible spectral region**

Fig. 20 shows schematically the region of light radiation with all wavelength λ in the visible spectrum between approximately λ = 380nm and λ = 720nm (1nm = $10^{-9}$m). The rays beyond these limits are named “ultra-violet” (UV) and “infrared” (IR). Fig. 20 shows a spectrum, which can be produced by a continuous interference filter in the slide plane of a projector. The interference filter has the property of letting through visible light radiation between approximately 380nm and 720nm in a continuous spectrum.

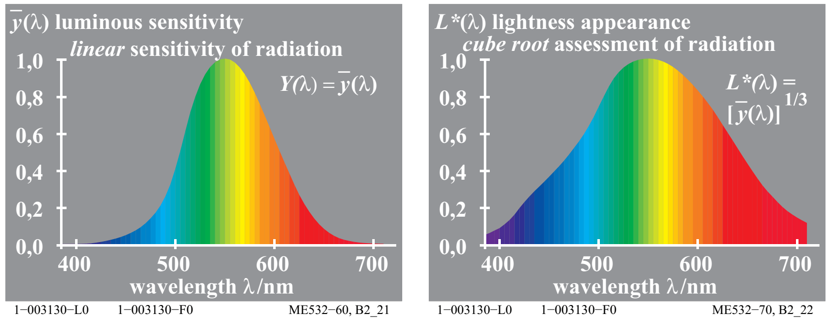


**Fig. 21: Spectral luminous sensitivity and lightness appearance**

In Fig. 21 *(left)* the luminous sensitivity $Y(\lambda)$ of the spectrum decreases from the middle yellow-green region to both ends. This property is a consequence of the spectral luminous efficiency $Y(\lambda)= V(\lambda)=y_q(\lambda)$ of the human eye. This efficiency has a maximum near 555nm and decreases to less than 1% near 400nm and 700nm. The relative spectral luminous efficiency function $y_q(\lambda)$ specifies the *valence* (value) in the colour mixture of the spectral colours, for example of equal energy of light radiation. Therefore the value which is described by the luminous efficiency function $y_q(\lambda)$ may be also called luminous value or luminous valence.

In CIE 15 *Colorimetry* the tristimulus value $Y$ with the normalization $Y_W = 100$ for white $W$ is defined, compare Section 17 on page 49

Different from the *linear* function $Y(\lambda)$ is a *nonlinear* function $L^*(\lambda)$ which describes the lightness appearance of the spectral colours of equal light radiation. This nonlinear function decreases from the middle of the spectrum to both ends by a nonlinear relation which is approximately cubic for grey and quadratic for white backgrounds, compare section 16 on page 44.

Fig. 21 *(right)* shows the lightness appearance $L^*(\lambda)$. The function $L^*(\lambda)$ decreases much less compared to the function $Y(\lambda)$ *(left)*.

Note: CIE 15 defines the following relation between lightness $L^*$ and the tristimulus value $Y$:

$$L^* = 116\ [Y/100\ ]^{1/3} - 16 \quad (Y>0{,}8)$$

Approximations are the relations:
$L^* = 100\ [Y/100]^{1/3}$ and $L^* = Y^{1/3}$ which is used for spectral colours in Fig. 21.

## 10.2 Chromatic Value (Valence) and Chroma

In the colour mixture the spectrum is assessed by "luminous values" and in addition by "chromatic values".

The visible spectrum includes a continuous series of hues, and one can recognize in it three spectral elementary colours. The spectral elementary colours are located close to 475nm for elementary blue $B_e$, 503nm for elementary green $G_e$, and 574nm for elementary yellow $Y_e$.

Elementary red is located outside the visible spectrum and can be produced for example by a suitable mixture of the colours 400nm and 700nm. The purple colours produced in this way are specified by compensatory wavelengths compared to illuminant E (equal energy of light radiation). For elementary red $R_e$ this result is the dominant wavelength $\lambda_{d,E}$ = 494c nm, see Fig. 50 on page 49

Between the end and the beginning of the spectrum the ~~red-green and~~ yellow-blue chromatic values changes the sign from positive to negative. Elementary



red $R_e$ can be mixed by two spectral colours of the yellowish red end and the bluish red beginning of the spectrum.

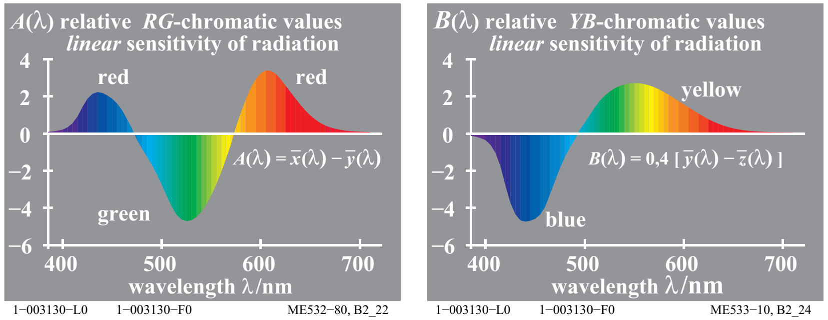


**Fig. 22: *RG*-chromatic values and *YB*-chromatic values**

Fig. 22 *(left)* shows the red-green-chromatic values $A(\lambda)$, which are the red-green-valences (values) in the colour mixture, as function of wavelength. The cero points are near 475nm and 574nm and specify the spectral elementary colours blue $B_e$ and yellow $Y_e$.

Fig. 22 *(right)* shows the yellow-blue-chromatic values $B(\lambda)$, which are the yellow-blue-valences (values) in the colour mixture, as function of wavelength. The cero point is near 503nm and specifies the spectral elementary colour green $G_e$.

For the spectral colours of equal energy the luminous values and the red-green- and yellow-blue-chromatic values produce three numbers (a vector) for any wavelength $\lambda$, for example of the band width 10nm between 380nm and 720nm. In the 3-dimensional space a point is created for the coordinates red-green-chromatic value $A$, yellow-blue-chromatic value $B$ and luminous value or tristimulus value $Y$ of any wavelength. In Fig. 23 the points of all spectral colours are located on a 3-dimensional curve.

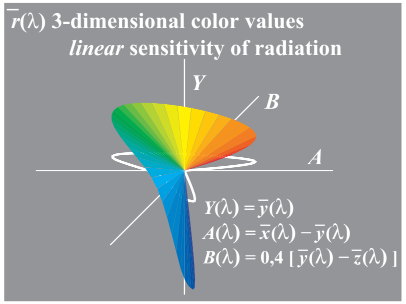


1−003130−L0 1−003130−F0 ME533−20, B2_25

**Fig. 23: 3-dimensional colour values**

Fig. 23 shows the 3-dimensional colour values in the colour space *(A, B, Y),* and the projection in the plane *(A, B) (white curve)*. The 3-dimensional curve cuts the plane *(B, Y)* near 475nm (elementary blue $B_e$) and 574nm (elementary yellow $Y_e$). The plane *(A, Y)* is cut near 503nm (elementary green $G_e$). Fig. 23 includes the linear relation between the luminous and chromatic values $Y(\lambda)$, $A(\lambda)$ and $B(\lambda)$ and the CIE tristimulus values $x_q(\lambda)$, $y_q(\lambda)$, and $z_q(\lambda)$.

There is a difference between chromatic value (valence in colour mixture) and chroma similar compared to the difference between luminous value and lightness.

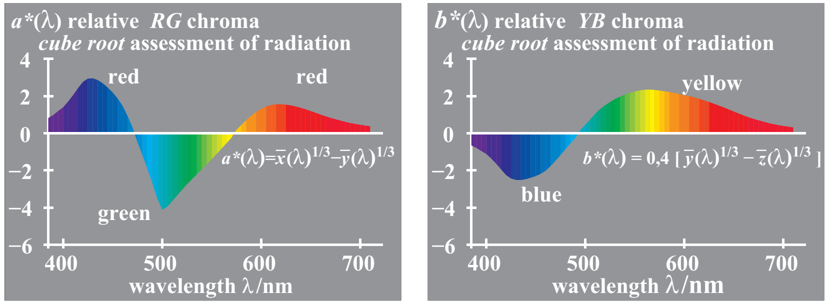


1−003130−L0 1−003130−F0 ME533−30, B2_26 1−003130−L0 1−003130−F0 ME533−40, B2_27

**Fig. 24: *RG*-chroma and *YB*-chroma**

Fig. 24 *(left)* shows the red-green-chroma $a^*(\lambda)$ which describes chroma appearance of reddish and greenish spectral colours. The cero points are near 475nm and 574nm and specify the spectral elementary colours blue $B_e$ and yellow $Y_e$.

Fig. 24 *(right)* shows the yellow-blue-chroma $b^*(\lambda)$ which describes chroma appearance of yellowish and bluish spectral colours. The cero point is near 503nm and specifies the spectral elementary colour green $G_e$.



For the spectral colours of equal energy the lightness and the red-green-, and yellow-blue-chroma produce three numbers (a vector) for any wavelength λ, for example between 380nm and 720nm. In the 3-dimensional space a point is created for the coordinates red-green-chroma $a^*$, yellow-blue-chroma $b^*$ and lightness $L^*$ for any wavelength. In Fig. 25 the points of all spectral colours are located on a 3-dimensional curve.

It is useful to define the group term colourness *(German Farbheit)* which covers the terms lightness, red-green-chroma, yellow-blue-chroma, whiteness, blackness, deepness, and other visual colour attributes. Instead of the term chroma also the term chromaticness is used, for example in the *NCS*-colour system.

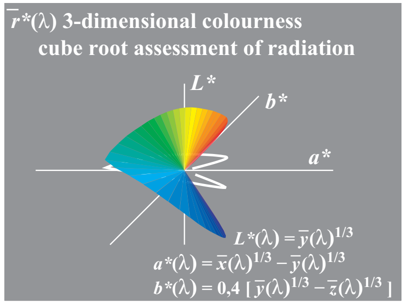


1−003130−L0 1−003130−F0 ME533−50, B2_28

**Fig. 25: 3-dimensional colourness**

Fig. 25 shows the three colourness data $L^*$, $a^*$, $b^*$ in the 3-dimensional colour space *(a*, b*, L*),* and the projection in the plane *(a*, b*) (white curve)*. The 3-dimensional curve cuts the plane *(b*, L*)* near 475nm (elementary blue $B_e$) and 574nm (elementary yellow $Y_e$). The plane *(a*, L*)* is cut near 503nm (elementary green $G_e$).

Fig. 25 includes the nonlinear relation of the spectral lightness and chroma $L^*(\lambda)$, $a^*(\lambda)$, and $b^*(\lambda)$ with the spectral tristimulus values $x_q(\lambda)$, $y_q(\lambda)$, and $z_q(\lambda)$.

## 11 Apparatus for Mixing Spectral Colours and Reflection

With a spectrophotometer one can measure at each wavelength the reflection of the radiation which falls upon a surface. By comparison of the reflection of a surface colour with the reflection of the reference white surface one normally gets a spectral reflection curve with numerical values between 0,0 and 1.0 for each wavelength.

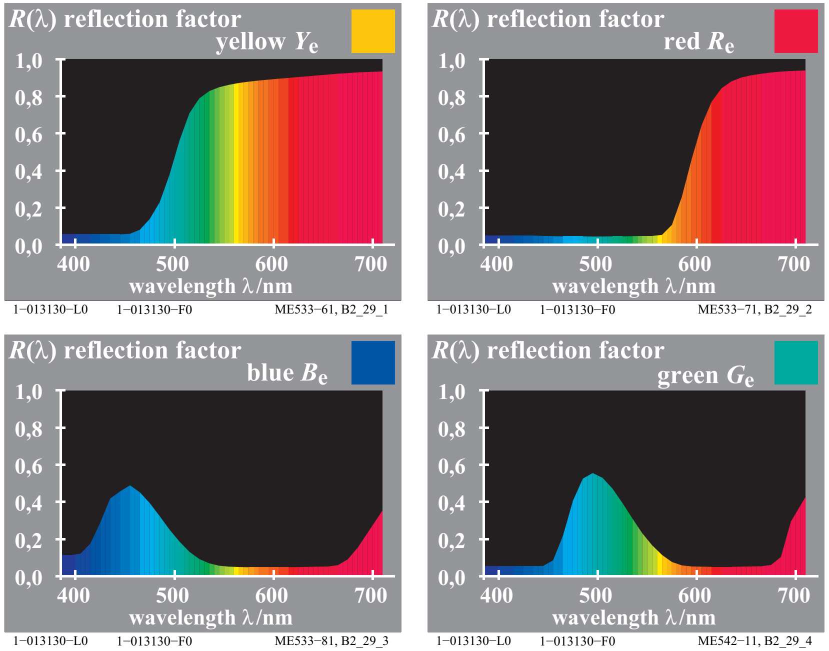


**Fig. 26: Spectral reflection factors of the four elementary colours $RYGB_e$**

Fig. 26 shows spectral reflection factors which are transferred to "masks" with corresponding transmission factors. With a spectral apparatus for mixing spectral colours one can produce optically the elementary colours $RYGB_e$.

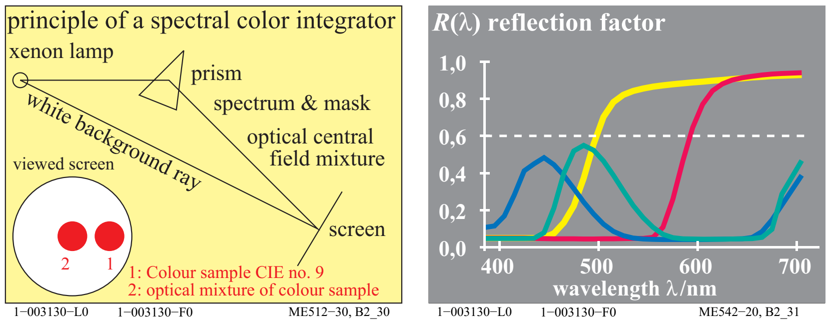


**Fig. 27: Apparatus for mixing spectral colours and the reflection factor masks**



Fig. 27 *(left)* shows the principle of an apparatus for mixing spectral colours. From a white xenon arc lamp two light paths are started.

The background light path produces a white background with the shape of a circular ring on the projection screen.

In the central-field light path the light is split by a prism into a spectrum. This spectrum is mixed optically and produces a circular white central field. The white light of the central and background field are equal at the projection screen.

By the help of masks at the location of the spectrum some spectral colours may be partially or totally masked out. The remaining parts of the spectrum are mixed optically. Different masks will lead to different central field colours, for example to the CIE-test colour no. 9 (elementary red $R_e$ according to CIE R1-47).

Fig. 27 *(right)* shows the masks for the elementary colours $RYGB_e$. The masks are produced according to the reflection factors $R(\lambda)$ of the CIE-test colours no. 9 (red $R_e$), no. 10 (yellow $Y_e$), no. 11 (green $G_e$) and no. 12 (blue $B_e$). According to CIE 13.3 these CIE-test colours and others are used for the specification of colour rendering properties of light sources. In addition a constant reflection factor $R(\lambda) = 0{,}6$ is shown which corresponds to a light grey colour.

## 12 Fluorescence

Fluorescence changes short wave absorption to longer wave radiation. Optical brighteners use this effect. With optical brighteners laundry and paper appears whiter and paints appear more luminous. Luminous red is used as warning colour. The luminous paints or fluorescent colours produce an extension of the normal colour gamut of normal (non-fluorescent) surface colours.

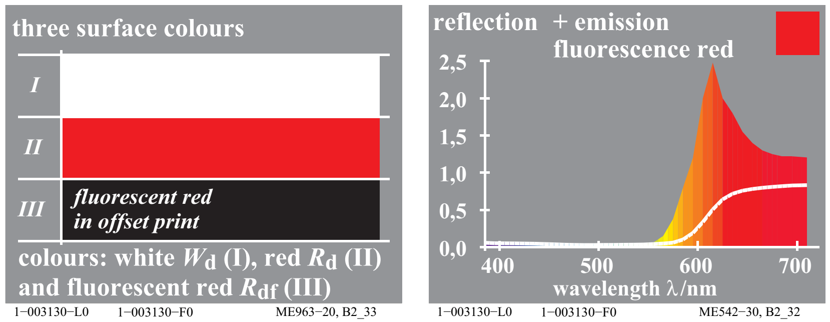


**Fig. 28: Surface colours and reflection and emission of a fluorescent colour**

Fig. 28 shows three surface colours white $W_d$ (I), red $R_d$ (II) and a fluorescent red $R_{df}$ (III) *(left),* and the reflection and emission of a fluorescent colour red $R_{df}$ *(right)*. Fluorescent colours reflect more long wave (red appearing) light than a normal (conventional) red sample with diffuse reflection. In Fig. 28 *(right)* the sum of the spectral emission and reflection is for the fluorescent colour red larger than 1,0 in the long wave spectral region. This surface colour appears especially luminous red. Therefore we call this colour a luminous colour.

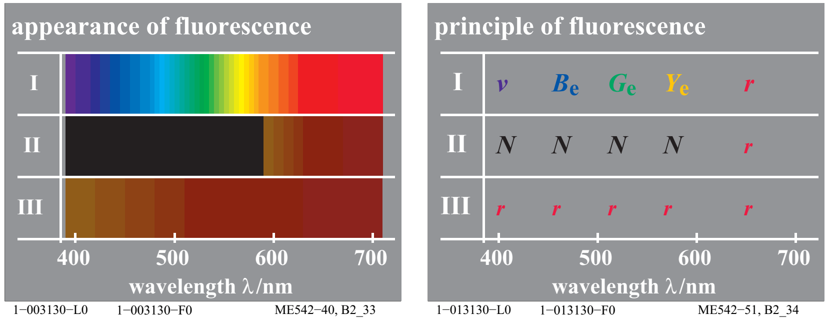


**Fig. 29: Spectral appearance and principle of fluorescence**

Fig. 29 shows the appearance *(left)* and the principle *(right)* of the fluorescence. The spectrum appears on an white surface (I), a normal red surface (II) and a fluorescent red surface (III) very different *(left)*.

The change of the colour appearance of the spectrum can be demonstrated on different colour areas. One produces a spectrum with a continuous interference filter. The spectrum is projected on the three different colour areas I to III:

• The spectrum on the white surface (I) appears as the usual colour series violet-blue $v$, blue $B_e$, green $G_e$, yellow $Y_e$, and red $r$ *(left)*. This is indicated by letters according to the colours *(right)*.

• The spectrum on the red surface (II) appears dark in the range violet-blue $v$ to yellow $Y_e$, and reflects in the red region similar compared to white *(left)*. The letter $N$ (=black) indicates absorption in the range violet-blue $v$ to yellow $Y_e$ and the letter $r$ reflection *(right)*.

• The spectrum on the fluorescent red surface (III) appears red $r$ in the whole spectral range between violet-blue $v$ and red $r$ *(left)*. The letter $r$ for the whole spectrum indicates this reflection property *(right)*.



# 13 Retroreflection

Retroreflective materials appear as particular chromatic and luminous colours under special lighting and observing conditions. The colour is here produced by the daylight illuminant D65, an achromatic (white appearing) material surface with special geometric reflection properties, and a transparent colour layer as a colour filter. This colour filter has different transmission factors depending on its colouring.

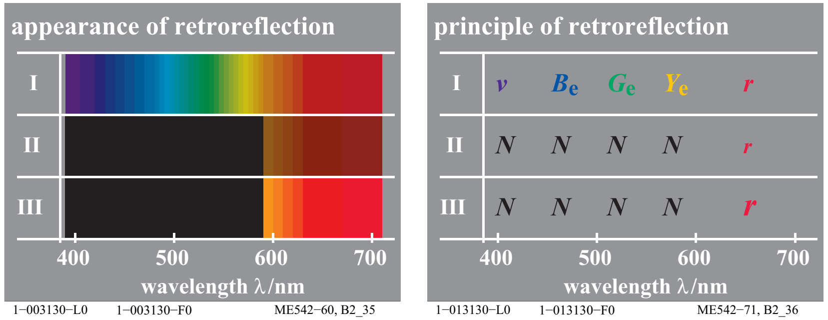


**Fig. 30: Spectral appearance and principle of retroreflection**

Fig. 30 shows the appearance *(left)* and the principle *(right)* of the retroreflection. The spectrum appears on an white surface (I) and the normal red surfaces (II) and a retroreflective red surface (III) very different *(left)*.

The change of the colour appearance of the spectrum can be demonstrated on different colour areas. One produces a spectrum with a continuous interference filter. The spectrum is projected on the three different colour areas I to III:

• The spectrum on a white surface (I) and a normal red surface (II) is already described in Fig. 29.

• The spectrum on a retroreflective red surface (III) appears dark in the range violet-blue $v$ to yellow $Y_e$, and may reflect in the red region more compared to white *(left)*. The letter $N$ (=black) indicates absorption in the range violet-blue $v$ to yellow $Y_e$ and the *large letter* $\boldsymbol{r}$ an increase of reflection *(right)*. This reflection reaches a maximum when the direction of illumination and observation agree.

# 14 Colour Mixture

## 14.1 Dichromatic additive Colour Mixture

*Miescher* has called the additive mixture of two colours a *dichromatic* colour mixture. Similarly one calls a mixture of three colours a *trichromatic* colour mixture. The mixture of two compensatory colours, which may result in an achromatic colour, is according to *Miescher* (1961, 1965) called an *antichromatic* colour mixture.

Colours of any given spectral distribution can be produced by additive colour mixture with an apparatus for mixing spectral colours, compare Fig. 27 on page 25. It is even possible to obtain the *optimal colours*, representing the possible limits of surface colours. Among the optimal colours the *most chromatic* colours, for example the reddest red, are of large importance for image technology, see section 19 on page 64.

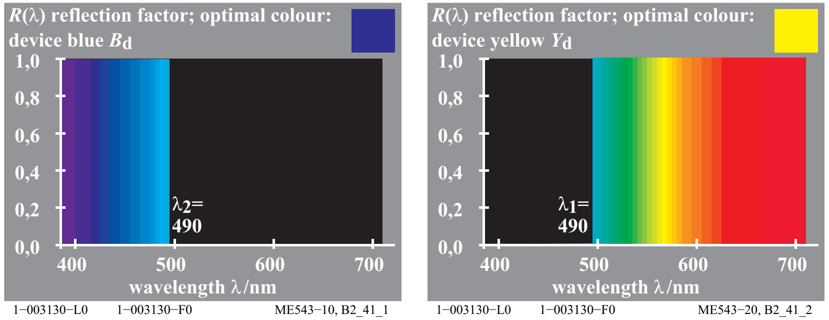


**Fig. 31: Dichromatic additive optimal colours $B_d$, $Y_d$**

Fig. 31 shows the dichromatic mixture of white. White $W$ is produced by additive mixture of any pair of *compensatory* (or complementary) optimal colours (for example blue $B_d$ and yellow $Y_d$). In the following and in reproduction processes a greenish yellow which we call the device yellow $Y_d$ *(Y= yellow, d=device)*, and a reddish blue $B_d$ is usually used.

In Fig. 31 *(left)* the reflection curve of the optimal colour blue $B_d$ has a sharp transition between the value 1,0 and 0,0 at 490nm. The reflection curve has the value 1,0 between 380nm and 490nm and the value 0,0 between 490nm and 720nm.



In Fig. 31 *(right)* the reflection curve of the optimal colour yellow $Y_d$ has the value 0,0 between 380nm and 490nm with a sharp cut off at 490nm. Between 490nm and 720nm the value is 1,0.

The additive mixture of both optimal colours $B_d$ and $Y_d$ results in an achromatic colour with a spectral reflection curve $R(\lambda)$ of the value 1,0 throughout, which appears white.

Fig. 31 shows two device colours yellow $Y_d$ and blue $B_d$ which are different compared to the elementary colours yellow $Y_e$ and blue $B_e$.

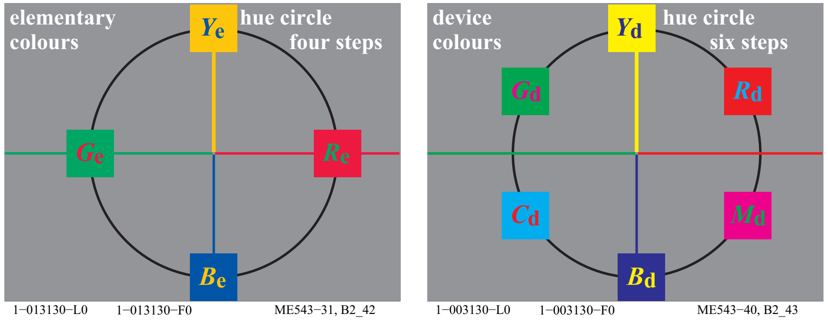


**Fig. 32: Four elementary colours $YRGB_e$ and six device colours $RYGCBM_d$**

Fig. 32 *(left)* shows the four elementary colours red $R_e$, yellow $Y_e$, green $G_e$, and blue $B_e$ in a symmetric elementary colour circle.

Fig. 32 *(right)* shows the six chromatic colours $RYGCBM_d$ of a 6 step hue circle, which serves as basis for the colour reproduction. According to the location in the symmetric hue circle yellow $Y_d$ appears slightly greenish compared to yellow $Y_e$ and blue $B_d$ appears reddish compared to blue $B_e$.

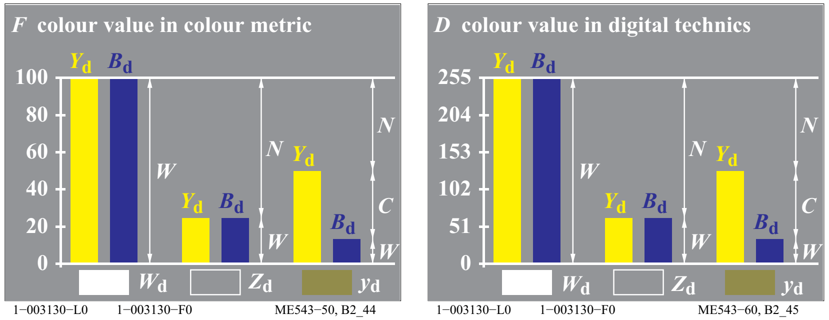


**Fig. 33: Dichromatic colour value in colorimetry and digital technic**

Fig. 33 shows the colour value $F$ in colorimetry *(left),* and the colour values $D$ in the digital technology *(right)*. In colorimetry 100 steps and in digital technic 255 steps are used.

Fig. 33 shows mixture colours between a dominant colour yellow $Y_d$ and the compensatory colour blue $B_d$: white $W_d$, central grey $Z_d$, and a yellow colour $y_d$ *(bottom right).*

If one uses 100% of both the dominant colour $Y_d$ and the compensatory colour blue $B_d$, then the achromatic mixture is the colour white $W_d$ with the spectral reflection factor of the value 1,0 throughout. It is valid in the left part: white value $W = 100$, black value $N = 0$ and chromatic value $C = 0$. The mixture colour $W_d$ is shown *(bottom left).*

If one uses only 25% of both the dominant colour $Y_d$ and the compensatory colour blue $B_d$ , then the achromatic mixture is the colour central grey $Z_d$. With the apparatus for spectral mixtures the masks may have only two jumps between 0,0 and 0,25. It is valid in the middle part for central grey $Z_d$: white value $W = 25$, black value $N = 75$, and chromatic value $C = 0$.

If the dominant colour $Y_d$ is larger compared to the compensatory colour blue $B_d$, then a chromatic colour is produced which has the hue of the dominant colour. It is valid in the right part: white value $W = B_d = 15$, black value $N = 100 - Y_d = 50$, and chromatic value $C = Y_d - B_d = 35$.

The image technology leads to the reproduction of equidistant colour series of the colour attributes. For example equidistant lightness series $\Delta L^*$=constant are described on a white background by the square root of the colour values. For example the CIE tristimulus value $Y$ with the values $Y$=1, 4,9, 16, .., 81, 100 produce the equal distant lightness series $L^*$=10, 20, 30, .., 90, 100.



The coordinates of the colour attributes are the *colourness* $F^*$ in colorimetry or the *colourness* $D^*$ in the digital technic. The group term *colourness* covers the colour attributes lightness, blackness, whiteness, deepness and others. The group term colour values covers the colour values white value, black value, chromatic value and others. There is often a nonlinear (square root) relation between both group terms, for example between lightness $L^*$ and the tristimulus value $Y$ of a sample on a white background (white paper or white monitor).

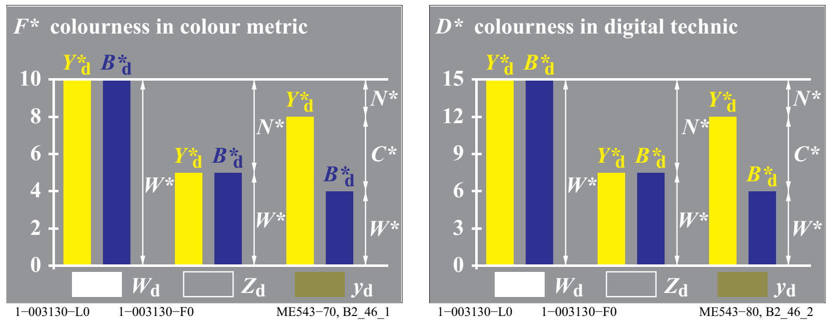


**Fig. 34: colourness in colorimetry and digital technic**

Fig. 34 *(left)* shows the colourness $F^* = Y^*_d$ or $B^*_d$ between 0 and 10 used in colorimetry *(left)*. 10 steps are used in the *Munsell*-colour system. Fig. 34 *(right)* shows the colourness $D^*$ between 0 and 15 in the digital technic. 15 steps are used in the European standard CEPT for Videotext *(Btx)*.

## 14.2 Trichromatic additive Colour Mixture

White $W_d$ may be produced by additive mixture of *three* optimal colours red $R_d$ (or orange-red $O$), green $G_d$ (or leaf-green $L$) and blue $B_d$ (or violet-blue $V$). *Miescher* called this mixture with three basic colours a trichromatic mixture.

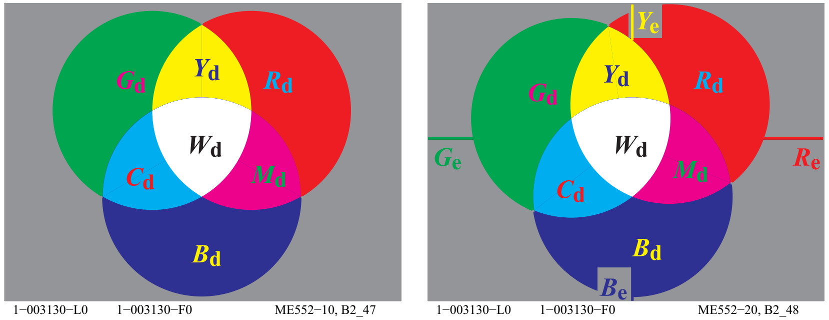


**Fig. 35: Trichromatic additive colour mixture and location of elementary colours**

Fig. 35 *(left)* shows the additive colour mixture with three basic colours red $R_d$ (or orange-red $O$), green $G_d$ (or leaf-green $L$), and blue $B_d$ (or violet-blue $V$). They mix to three dichromatic mixture colours yellow $Y_d$, cyan-blue $C_d$, and magenta-red $M_d$. White $W_d$ is the trichromatic mixture colour with the three basic colours.

Fig. 35 *(right)* shows the location of the additive basic colours, the dichromatic mixture colours $CMY_d$, and the trichromatic mixture colour $W_d$ in relation to the four elementary colours $RYGB_e$. It is necessary to consider the difference between $R_d$ and $R_e$, and between $G_d$ and $G_e$.



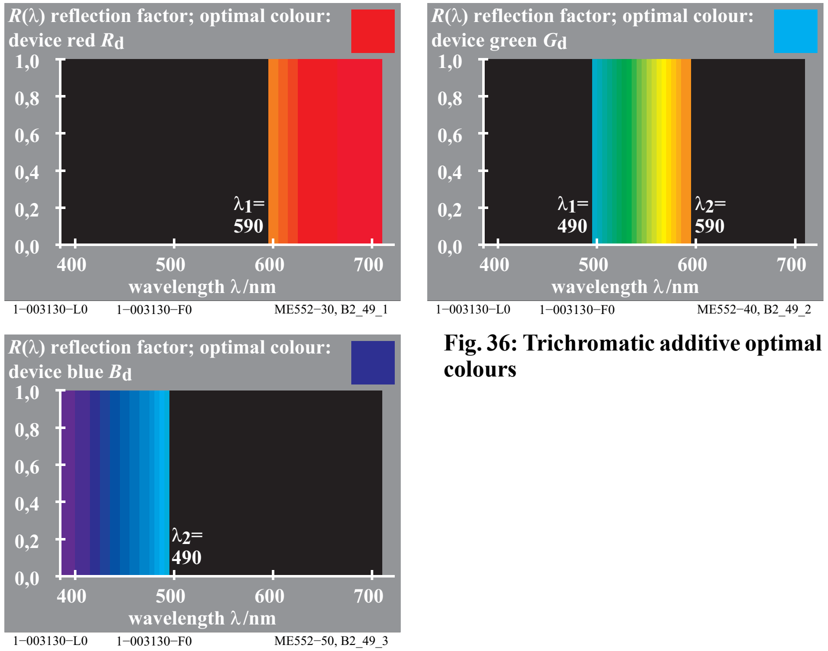


**Fig. 36: Trichromatic additive optimal colours**

Fig. 36 shows the three optimal colours red $R_d$, green $G_d$, and blue $B_d$, which mix additively to white. The additive mixture with different values of the three basic colours red $R_d$, green $G_d$, and blue $B_d$ is of general importance.

In Fig. 37 the three colour values of the device colours red $R_d$, green $G_d$, and blue $B_d$ are ordered according to their values, in the example it is valid $R_d > G_d > B_d$.

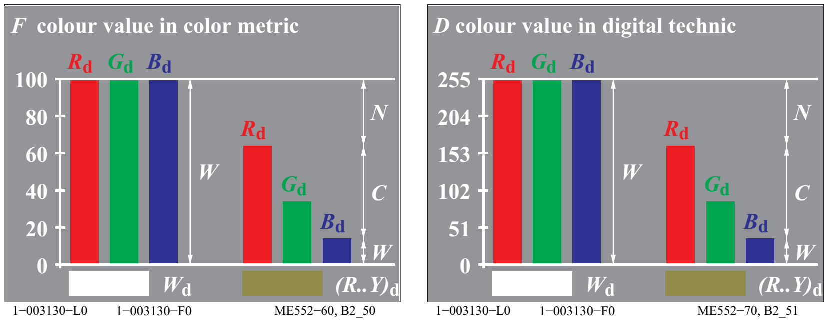


**Fig. 37: Trichromatic colour values $RGB_d$ in colorimetry and digital technic**

Fig. 37 shows the colour values $F = R_d$, $G_d$, and $B_d$ between 0 and 100 in colorimetry *(left)* and the colour values $F = R_d$, $G_d$, and $B_d$ between 0 and 255 in the digital technic *(right)*. The relation with the black value $N$, the white value $W$ and the chromatic value $C$ of colours is shown.

| **colour attributes of low and high colour metric** | | **mode of colour mixture dichromatic** | **trichromatic** |
|---|---|---|---|
| ***low colour- or valence metric*** | | (for $Y_d >= B_d$) | (for $R_d >= G_d >= B_d$ ) |
| white value | $W$ | $B_d$ | $B_d$ |
| black value | $N$ | $100 - Y_d$ | $100 - R_d$ |
| chromatic value | $C$ | $Y_d - B_d$ | $R_d - B_d$ |
| ***high colour- or sensation metric*** | | (for $Y^*_d >= B^*_d$) | (for $R^*_d >= G^*_d >= B^*_d$ ) |
| whiteness | $W^*$ | $B^*_d$ | $B^*_d$ |
| blackness | $N^*$ | $100 - Y^*_d$ | $100 - R^*_d$ |
| chromaticness | $C^*$ | $Y^*_d - B^*_d$ | $R^*_d - B^*_d$ |

1−003130−L0 1−003130−F0 ME982−10

**Table 2: Mode of colour mixture, colour value and colourness in colorimetry**

Table 2 shows the two modes of colour mixture. The relation between the colour attributes and the colour values $Y_d$ and $B_d$ of the dichromatic colour mixture, and the colour values $R_d$, $G_d$, and $B_d$ of the trichromatic colour mixture are given.

The colour attributes of the high colour metric use the group term colourness (whiteness, blackness, chroma). In the table the colourness is specified by the * (star), for example the whiteness $W^* = B^*_d$.

The abbreviations in Fig. 33 on page 31 and in Fig. 37 on page 34 and Table 2 mean:

Fig. 33 on page 31 for $Y_d>=B_d$:

| | | |
|---|---|---|
| $Y_d$ dominant colour | $B_d$ compensatory colour | |
| $W$ white | $Z$ central grey | $y_d$ light yellow |

Fig. 37 on page 34 for $R_d>=G_d>=B_d$

| | |
|---|---|
| $R_d$ red | $G_d$ green |
| $B_d$ blue | $(Y..R)_d$ yellow-red |

In Table 2 the colour values of the dominant colour yellow $Y_d$ and the compensatory colour blue $B_d$ or the three basic colours red $R_d$, green $G_d$, and blue $B_d$ are in a simple relation with the colour attributes: relative white value $w$, relative black value $n$, and relative chromatic value $c$ of *Ostwald*.

It is valid, compare Fig. 33 on page 31, and Fig. 37 on page 34:



| | | |
|---|---|---|
| $w$ relative white value | = white value / 100 | = $W$ / 100 |
| $n$ relative black value | = black value / 100 | = $N$ / 100 |
| $c$ relative chromatic value | = chromatic value / 100 | = $C$ / 100 |

The three colour values $RGB_d$ of colorimetry or of the digital technic may be used to calculate the white value $W$, the black value $N$, and the chromatic value $C$. Based on the nonlinear relation between colour value and colourness the two ratios between white value / black value and whiteness / blackness are different.

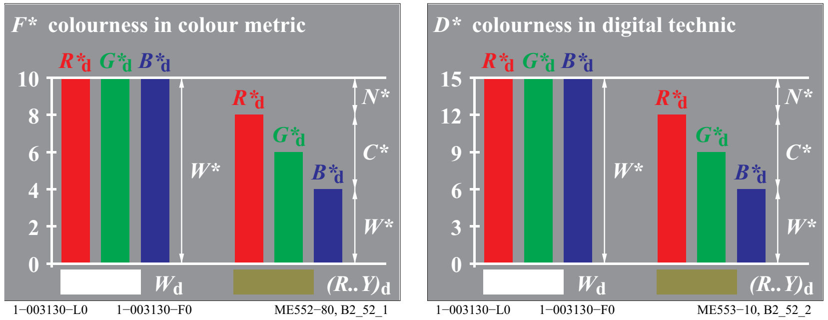


**Fig. 38: colourness $RGB^*_d$ in colorimetry and digital technic**

Fig. 38 shows the colourness $R^*_d$, $G^*_d$ or $B^*_d$ between 0 and 10 in colorimetry *(left)* and between 0 and 15 in the digital technic *(right)*. The relation with the blackness $N^*$, the whiteness $W^*$ and the chroma $C^*$ of colours is given.

Note: In the CIELAB system the lightness $L^*$ and the chroma $C^*$ varies in the range between 0 and 100 instead of 0 and 10, for example in the *Munsell*-colour system.

The most known application of the additive colour mixture is the television and the computer colour monitor. Here the display output is mixed by many raster points red $R_d$, green $G_d$, and blue $B_d$. The luminance of these points is changed by the television signals or the computer image software. On the standard television monitor there are at least 1.2 million luminous points. The points are small and can not be seen separately in a viewing distance of about 3m under normal viewing conditions. An additive raster colour mixture is created on the screen.

## 14.3 Trichromatic subtractive Colour Mixture

The insertion of three appropriate colour filters in the path of the *same* white light source leads (in a white background) to black if nearly all light is absorbed. Contrary to the additive colour mixture described above, filters are put one upon the other in the path of only *one* light source.

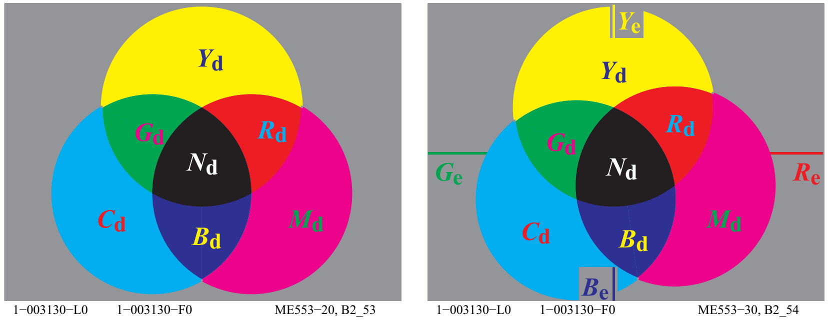


**Fig. 39: Trichromatic subtractive colour mixture, and location of elementary colours**

Fig. 39 *(left)* shows the subtractive colour mixture with the three basic colours cyan-blue $C_d$, magenta-red $M_{d\ and}$, and yellow $Y_d$. The three dichromatic mixture colours red $R_d$, green $G_d$, and blue $B_d$ are produced. Black $N_d$ (= noir) is the trichromatic mixture colour of the three basic colours. For subtractive colour mixture techniques *three* special filters are appropriate with spectral transmission curves similar to the optimal colours yellow $Y_d$, cyan-blue $C_d$ and magenta-red $M_d$, see Fig. 40 on page 38.

Fig. 39 *(right)* shows the location of the subtractive basic colours $CMY_d$, and of the dichromatic mixture colours $RGB_d$, and of the trichromatic mixture colour $N_d$. The relative location compared to the four elementary colours $RYGB_e$ is shown. There is an important difference between $R_e$ and $R_d$ or $M_d$. In the printing area $M_d$ is often named *red* instead of *magenta-red*. In addition there is a difference between $B_e$ and $B_d$ or $C_d$, which is often named *blue* instead of *cyan-blue* in the printing area.



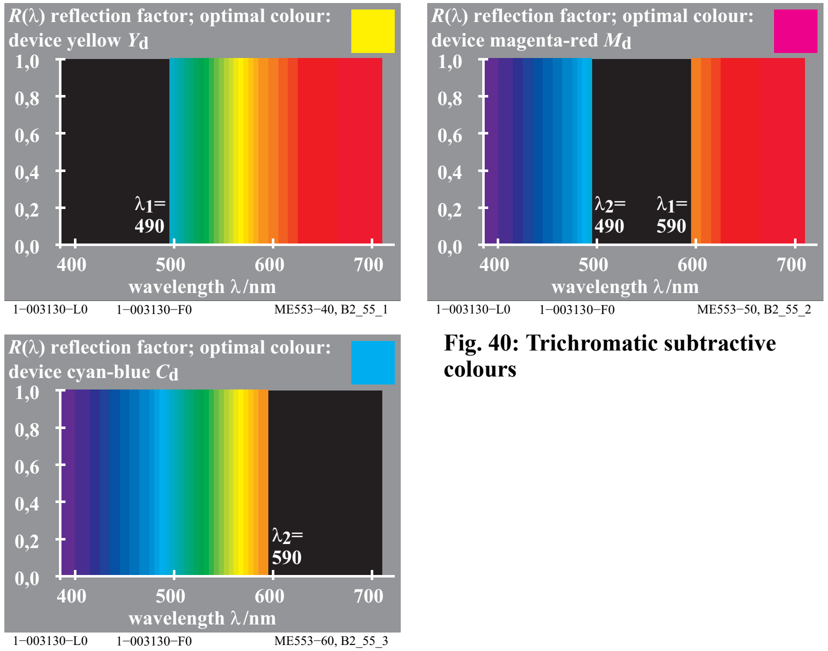


**Fig. 40: Trichromatic subtractive colours**

Fig. 40 shows the spectral reflection factors $R(\lambda)$ (or transmissions factors $T(\lambda)$ of filters) which are appropriate for the subtractive colour mixture: The optimal colour yellow $Y_d$ with $R(\lambda) = 1$ starting at the wavelength 490nm, the optimal colour magenta-red $M_d$ with $R(\lambda) = 1$ up to the wavelength 490nm and starting again at 590nm, and the optimal colour cyan-blue $C_d$ with $R(\lambda) = 1$ up to the wavelength 590nm.

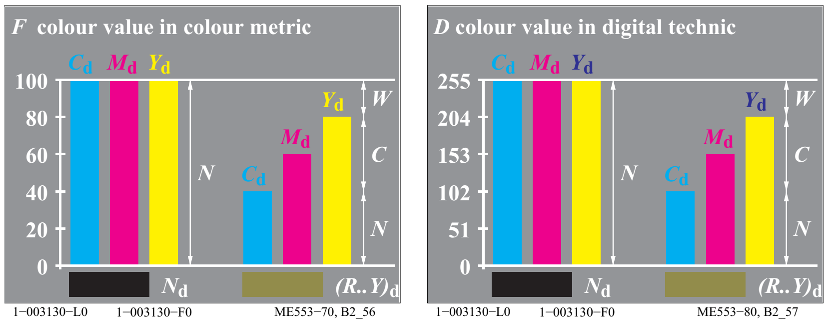


**Fig. 41: Colour values $CMY_d$ in colorimetry and digital technic**

Fig. 41 shows the colour values *F* in the colorimetry *(left)*, and the colour values *D* in the digital technic *(right)* for a trichromatic subtractive colour mixture.

The specification of the mixture colours based on three standard printing colours cyan-blue $C_d$, magenta-red $M_d$, and yellow $Y_d$ is shown. If the colour value of yellow $Y_d$ is dominant compared to the values of magenta-red $M_d$ and cyan-blue $C_d$, then the mixture of $Y_d$ and $M_d$ leads at first to red $R_d$. Because of the large value of yellow $Y_d$, the mixed hue is a yellowish red colour $(R..Y)_d$.

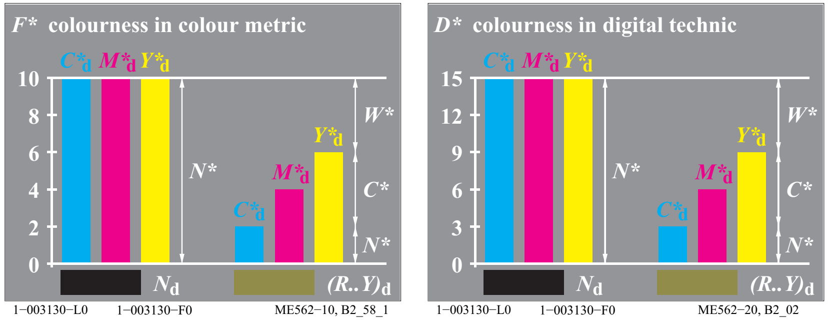


**Fig. 42: colourness $CMY^*_d$ in colorimetry and in digital technic**

Fig. 42 shows the colourness *F** in the colorimetry, and the colourness *D** in the digital technic for a trichromatic subtractive colour mixture.

The most known *technical application* of the *subtractive* colour mixture is in *colour photography*. In a colour reversal film (slide film) there are three filter layers, one after another, with colours cyan-blue $C_d$, magenta-red $M_d$, and yellow $Y_d$. The transmission factors of the layers are controlled by the exposure and the developing process.

In standard multicolour printing both additive and subtractive colour mixtures are involved and this kind of mixture is called an auto-typic mixture. The mixture is additive if two printing colours are printed side by side, and subtractive if the two transparent inks are printed on top of each other.

## 15 Spectral Radiation

Colours with the same appearance can be created by different spectral distribution of light radiation. In modern colorimetry metameric colours can be calculated with special numerical procedures, taking the illuminance into account.



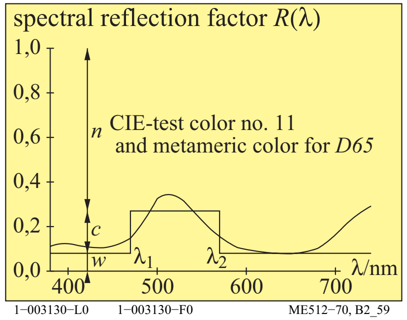


**Fig. 43: Reflection factors of two metameric colours**

Fig. 43 shows the CIE-test colour no. 11 (green) according to CIE 13.3, and a metameric colour of rectangular reflection for the CIE standard daylight D65. Usually one tries to avoid using metameric colours on different parts of an industrial product since such colours will only match under one illuminant. By a change of the illuminant, for example from daylight to incandescent light, *colour differences* appear, the metameric colours no longer match.

Fig. 43 includes the *relative* black value *n*, the *relative* chromatic value *c*, and the *relative* white value *w*. The *Ostwald*-equation $n + c + w = 1$ is valid.

The two compensatory wavelength limits $\lambda_1$=475nm and $\lambda_2$=574nm for D65 belong approximately to an optimal colour with the elementary hue green $G_e$. This optimal colour has the maximum chromatic value $C_{AB}$ and creates a *colour half* according to *Ostwald*.

There are many *dichromatic complementary* colours which mix to white, for example blue $B_d$ in Fig. 36 on page 34 and yellow $Y_d$ in Fig. 40 on page 38. Similar green $G_d$ and magenta-red $M_d$, and red $R_d$ and Cyan-blue $C_d$ of these two figures mix to white. In addition there are special dichromatic complementary colours with compensatory wavelength limits λ1 and λ2 which form a colour half according to *Ostwald*, for example the pairs green - magenta-red with the wavelength limits (λ1, λ2) = (475nm, 574nm), blue - yellow with the wavelength limits (λ1, λ2) = (495nm, 700nm), cyan-blue - red with the wavelength limits (λ1, λ2) = (400nm, 567nm). These wavelength limits are located on lines through the achromatic point E (or approximately D65) in the CIE chromaticity diagram, see Fig. 50 on page 49 (right).

In Fig. 43 the corresponding *linear* $rgb_e$-colour values are for $n$=0.73 and $w$=0.08:

$$rgb_e = (w, (1-n), w) = (0.08, 0.27, 0.08)$$

The corresponding *nonlinear (visual) rgb*$^*_e$-colour values lead to *(for square root relation of white background):*

$rgb^*_e = (w^{1/2}, (1\text{-}n)^{1/2}, w^{1/2}) = (0.28, 0.52, 0.28)$

For the reproduction of the CIE-test colour no. 11 in colour printing or on the colour display the $rgb_{de}$-colour values (*de = device to elementary hue*) must be calculated and may get approximately the following values:

$rgb_{de} = (w, (1\text{-}n), w\text{+}0.20\text{w}) = (0.08, 0.27, 0.10)$

According to Fig. 10 on page 12, and for production of the elementary colour green $G_e$ the *b*-value increases by 20% (=3/F%=3/15%) from 0.08 to 0.10.

For this print output all the calculations shown here are done automatically by the software. The software uses the measurement data of 729 (=9x9x9) colours of the output device for the steering of the output.

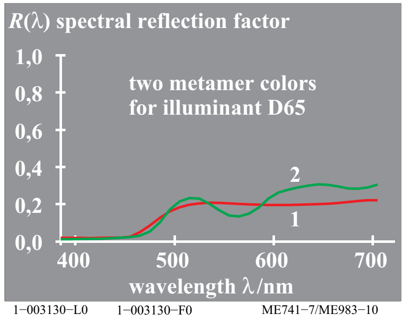


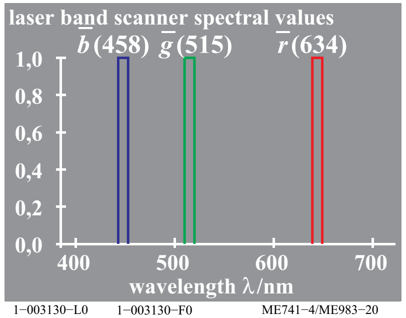


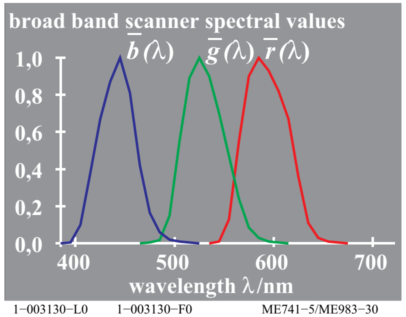


**Colour rendering index Ri of two metameric BAM-scanner test colours**

| scanner | TC | colour rendering index | colour difference |
|---|---|---|---|
| broad band | 1 | 82 | 3 |
| | 2 | 84 | |
| laser | 1 | 63 | 10 |
| | 2 | 69 | |
| ideal | 1 | 100 | 0 |
| | 2 | 100 | |

**D65, colour adjustment with white paper**

1−003130−L0 1−003130−F0 ME741−8/ME983−40

**Fig. 44: Two metameric test colours, scanner values and colour rendering**

Fig. 44 *(top left)* shows two metameric test colours which are scanned by a laser scanner, a broad band scanner, and an ideal scanner with CIE sensitivities. The scanner values are usually normalized for the white paper to *r*=*g*=*b*=1.



Depending on the type of scanner the two colours no. 1 and 2 in Fig. 44 *(top left)* produce usually two different *rgb* data sets. However, the two colours appear equal for the CIE- illuminant D65 and they have equal CIE-XYZ data.

The *rgb*-scan values are usually interpreted in the *sRGB*-colour space according to IEC 61966-2-1, and are then transformed to CIE-*XYZ* data and to colour differences $\Delta E^*$. For the ideal scanner, which has the broad band sensitivities of the CIE tristimulus values, the *rgb* values are equal. Maxima and minima of the spectral reflection curves, and the *real* spectral sensitivities of the scanner type, for example a laser or wide band scanner, determine the differences of the *rgb* scanner values. In Fig. 44 *(bottom right)* the one colour differences $\Delta E^*$ of the two samples no. 1 and 2 are in the range 0 to 10.

In the ideal case the colour rendering index $R_i$ according to CIE 13.3 has the value 100. It decreases according to the formula $R_i$ = 100 - 4,6 $\Delta E^*$. For example $R_i$ = 86 (=100 - 3*4,6) for the colour difference $\Delta E^*$=3. For the two samples there are colour differences $\Delta E^*$ between the scanner data with the ideal CIE sensitivities, and the real laser band or broad band sensitivities. This produces two colour rendering indices $R_i$ for the two samples no. 1 and 2.

In offset print and with colour printers the achromatic colours may be printed only with the achromatic colour black $N_d$ or only with the three chromatic colours cyan-blue $C_d$, magenta-red $M_d$, and yellow $Y_d$, especially in images. The achromatic colours, which are printed by the black ink $N_d$, have approximately a constant reflection curve. The achromatic colours, which are printed by $CMY_d$, have usually up to three maxima and minima, compare Fig. 44 *(top left)*.

Test and metameric colours for the CIE standard illuminants D65 and A, and the CIE-illuminants D50, and a Planckian (P) radiation with the colour temperature T=4000K (P40) are printed as test charts no. 1 to 3 in the annex with the format A4 landscape. The spectral reflection factors of the samples of three test charts are available. The *rgb* data are given and the many CIE data for six illuminants D65, D50, P40, A, C, and E have been calculated. The colour samples are based on the 16-step colour circle of the *Relative Elementary colour system RECS*, compare DIN 33872-1 to -6.

CIE R1-47 defines the elementary hue angles for the CIE standard illuminant D65. Elementary yellow $Y_e$ and blue $B_e$ have the hue angles 92 and 272 degree. However, for CIE standard illuminant A the elementary hue angles may shift from 92 and 272 degree to 82 and 262 degree in CIELAB (for D65 and A). The exact values are unknown. Therefore the elementary hues under D65 appear not any more as elementary hues under the CIE standard illuminant A. For example the elementary blue $B_e$ under the CIE standard illuminant D65 appears reddish under the CIE standard illuminant A. Similar the elementary yellow $Y_e$ under the CIE standard illuminant D65 appears greenish under the CIE standard illuminant A. In future the CIE may define the change of the elementary hue angles for the different CIE illuminants.

If in offset print or with colour printers the achromatic colours are only printed with the three colorants *CMY* instead of *only N*, then this needs 3 times higher material resources. If achromatic colours are *only* printed with *CMY* then the price may increase by a factor 6. The price for the three chromatic inks *CMY* is usually twice compared to the achromatic ink *N*. In addition for the *CMY* print there are up to three maxima and minima of the reflection curves which may produce colour differences $\Delta E^*$=10 for equal (metameric) colours, see Fig. 44 *(bottom right)*.

In the annex, the test charts no. 2 and 3 (*PE231lL* and *PE331lL*) use the above two print technologies for the print of achromatic colours. The offset print of the test charts no. 2 and 3 has produced metameric achromatic colours for the four different CIE illuminants D65, D50, P40 and A. In addition there are metameric colours for a 8 step colour circle with half the maximum CIELAB chroma $C^*_{ab}$ compared to the maximum chroma of offset print.

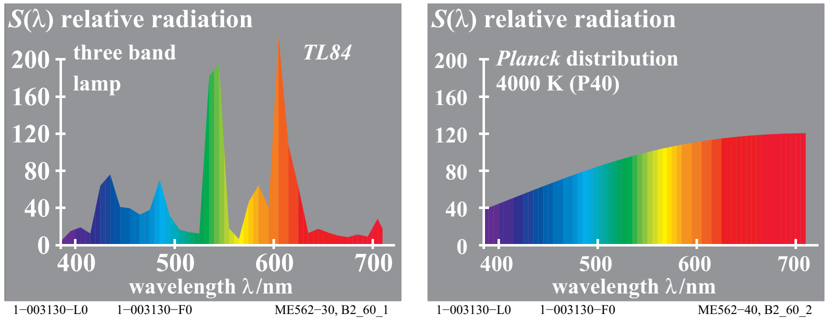


**Fig. 45: Relative spectral distribution of the radiation**

Fig. 45 shows the relative spectral distribution of the radiation $S(\lambda)$ of a three band fluorescent lamp of high luminous efficiency (energy saving lamp), and a (hypothetical) light source of the colour temperature 4000K (P40) according to the radiation law of *Planck* (P). Both light sources appear equal white, although they have different spectral distributions.

Alternative illumination of chromatic test colours under these metameric lamps leads to differences in the colour appearance of the test colours. One speaks of this as *differences in the colour rendering properties*, compare CIE 13.3. The two *metameric* colours in Fig. 43 on page 40, which appear equal for daylight D65, appear *different* under the two illuminants TL84 and 4000K (P40) in Fig. 45.



The test chart no. 1 to 3 in the annex allow both a *visual evaluation* and a *colorimetric specification* of the *colour rendering properties* of *LED* lamps and of the *colour reproduction properties* in the field of information technology. The test charts are based on the *Relative Elementary Colour System RECS*, compare DIN 33872-1 to -6.

# 16 Contrast

Contrast, already known to *Leonardo da Vinci* and described in detail by *Goethe* (1749-1832), is one of *the most important principles of expression* in fine art, arts and crafts, and industrial design. Contrast is conditioned by the mutual influence of different parts of the visual field.

## 16.1 Achromatic contrast

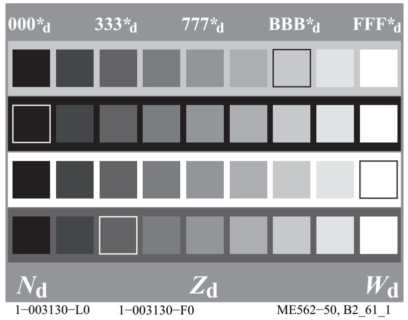


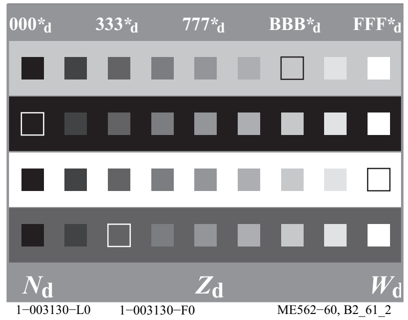


**Fig. 46: Achromatic contrast: background and field size**

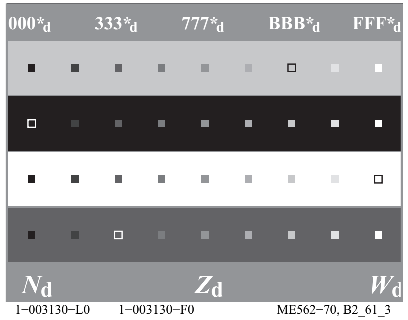


The perceived lightness of a central field in a light background shifts in the opposite sense. For example the lightness of different steps of four *physically identical* grey series changes, depending on the background luminance. Without a lighter reference field there is no grey or black.

Fig. 46 shows four achromatic grey series between black $N_d$ and white $W_d$ viewed against four backgrounds, and different in lightness. A square highlights if the lightness of the sample and the background is equal. The $rgb*_d$ code (with a star) shall indicate, that on a medium grey background the nine-step grey series is equally spaced, and has the CIELAB lightness $L* = 15, 25, 35, .., 95$. In a white background the samples appear *darker* and in a black background *lighter* compared to a medium grey background ($Z_d$ = central grey, here shown as rectangle at top and bottom).

According to *Miescher* (1961) an equally spaced scale with 100 steps on a white, medium grey and a black background obey the following equations for the CIE tristimulus value $Y$:

• white background: $L*_W = 100\ ( Y_W / 100 )^{1/2}$

According to this formula for a medium grey step with $L*_W = 50$ the CIE tristimulus value is $Y_W = 25$.

• medium grey background: $L*_Z = 100\ ( Y_Z / 100 )^{1/2,4}$

According to this formula for a medium grey step with $L*_Z = 50$ the CIE tristimulus value is $Y_Z = 19$.

• black background: $L*_N = 100\ ( Y_N / 100 )^{1/3,0}$

According to this formula for a medium grey step with $L*_N = 50$ the CIE tristimulus value is $Y_N = 12{,}5$.

On a medium grey background the medium grey step with $Y_Z = 19$ in the original has the lightness $L*_Z = 50$. According to the above formulas $Y_W = 19$ has on a white background the lightness $L*_W = 44$, and $Y_N = 19$ has on a black background the lightness $L*_N = 58$.

The formulae given for the ranking of the greys on different backgrounds provides only a first step in describing contrast by taking the background into account. The absolute luminance also influences this ranking.

With increasing luminance, the discrimination of individual grey steps increases. White appears more and more white and black more and more black with increasing luminance. This means that the sensory colour difference between white and black also increases. If the illuminance of the grey series is increased from 500 lux to 5000 lux, then the discrimination increases by approximately 20%. This effect seems small compared to the change of the illuminance by the factor 10 (1000%).



Fig. 46 includes three separate figures with different field size of the central fields compared to the background. The largest contrast influence by the background occur by a central field with a viewing size of about one degree (1°), and if the field size of the background is at least 10 times larger (>10°).

## 16.2 Chromatic contrast

The colour of a chromatic background shifts all the colour attributes of the central field in the opposite direction.

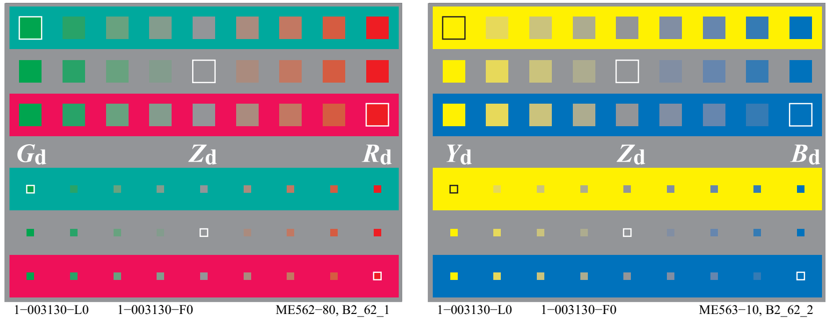


**Fig. 47: Chromatic contrast: background and field size**

Fig. 47 shows three physically identical chroma series with equally spaced steps viewed against a medium grey background $Z_d$ and two backgrounds red $R_d$ and green $G_d$. In Fig. 47 the red samples appear on a green background redder compared to a red background. The green samples appear on a red background greener compared to a green background. In addition the grey samples

$Z_d$ appear in red and green background not achromatic, but are influenced in *opposite directions*.

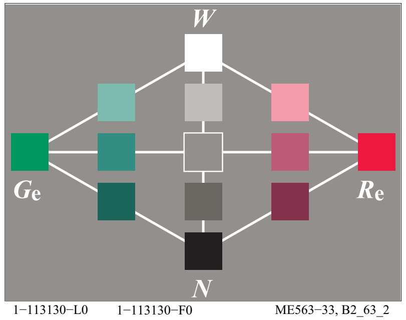


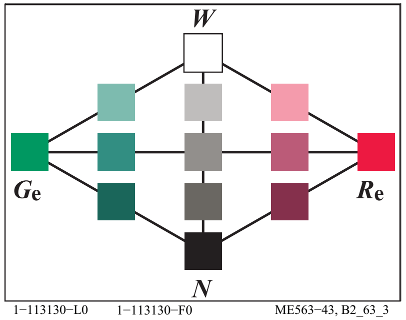


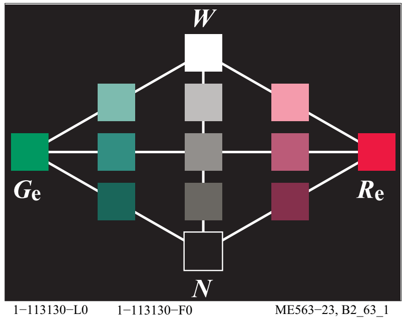


**Fig. 48: Influence of the background on *RG*-colour scaling**

Fig. 48 shows a further important property of the achromatic and chromatic contrast in a hue plane red-green.

The colour multiplicity and the colour gamut appear on a medium grey background larger compared to a white and black background. On a black background many colours appear luminous, and the important component "blackish" is missing. On a white background many colours appear "blackish" and the important attribute "luminous" is missing. On a medium grey background both colour attributes "blackish" and "luminous" are present with an appropriate part compared to the natural viewing.

Fig. 48 shows that all red colours have a better agreement in hue with the elementary red hue $R_e$ compared to Fig. 7 on page 10. In Fig. 48 a 3-dimensional linearization has been used, to calculate (from the undefined *rgb*-input data in the file) the intended $rgb_{de}$-coordinates (*Index de* = device to elementary hue). The $rgb_{de}$-coordinates produce for all red colours the CIELAB-hue $h_{ab}$=26 degrees in the output, which is defined in CIE R1-47 for the elementary hue red $R_e$.



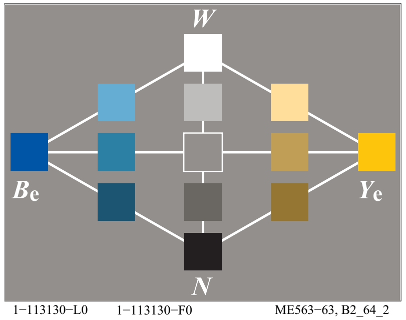


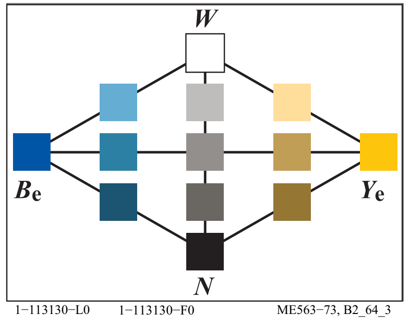


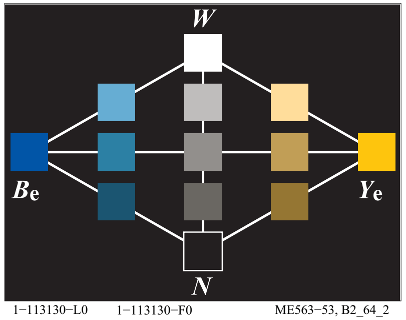


**Fig. 49: Influence of the background on *YB*-colour scaling**

Fig. 49 shows the colour multiplicity and the colour gamut in a hue plane yellow-blue. Similar as for the hue plane red-green, again on a medium grey background the two colour attributes "blackish" and "luminous" are present with an appropriate part compared to the natural viewing.

The appearance change of colours by the background colours depends on physiological processes in the eye. Up to now there are only first steps to describe these processes, compare also the section 18 on page 55.

# 17 Standard Colour Value and Colour Measurement

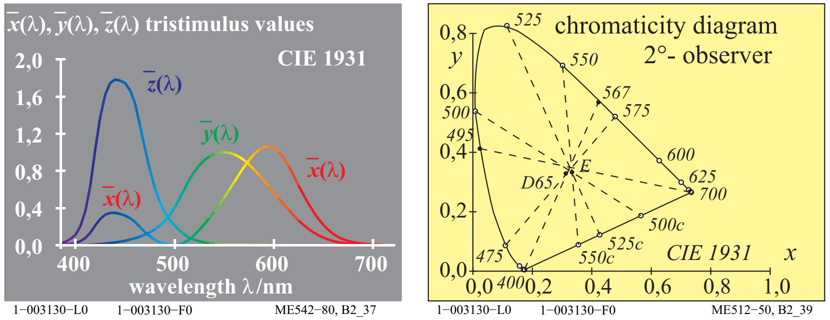


**Fig. 50: CIE tristimulus values and CIE chromaticity diagram for 2° observer**

Fig. 50 shows the three CIE spectral tristimulus values $x_q(\lambda)$, $y_q(\lambda)$, and $z_q(\lambda)$ for CIE illuminant E (equal energy radiation) between 380nm and 720nm. In Fig. 50 the curves show the colour values of the spectral colours. There are three tristimulus functions which may be specified roughly by three colours blue $z_q(\lambda)$, green $y_q(\lambda)$, and red $x_q(\lambda)$.

For the spectral colours the CIE has defined the spectral chromaticity

$$x(\lambda) = x_q(\lambda) / [\ x_q(\lambda) + y_q(\lambda) + z_q(\lambda)\ ]$$
$$y(\lambda) = y_q(\lambda) / [\ x_q(\lambda) + y_q(\lambda) + z_q(\lambda)\ ]$$
$$z(\lambda) = z_q(\lambda) / [\ x_q(\lambda) + y_q(\lambda) + z_q(\lambda)\ ] = 1 - x(\lambda) - y(\lambda)$$

The spectral tristimulus values, the physical spectral radiation, and the spectral reflection of samples allow to calculate the CIE tristimulus values *X, Y* and *Z* and the CIE standard chromaticities *x, y* and *z*.

$$x = X / ( X + Y + Z )$$
$$y = Y / ( X + Y + Z )$$
$$z = Z / ( X + Y + Z ) = 1 - x - y$$

Examples of these calculations for the three additive optimal colours are given by *K. Richter* (1996), pages 276-277, for download see (288 pages, 2,8 MB) http://130.149.60.45/~farbmetrik/BUA4BF.PDF

In Fig. 50 the CIE spectral chromaticities define the border of the CIE chromaticity diagram. Together with the so called purple line a closed area is defined. The purple line is created by the connection of the chromaticities of the short and long wave spectral colours, approximately λ = 400nm and λ = 700nm.



All colours, for example surface colour, spectral, and optimal colours, have chromaticities within or at the edge of the chromaticity diagram.

The chromaticities *x* and *y* and the CIE tristimulus value *Y*, which is normalized to the value 100 for a reference white, specify a colour as well as the CIE tristimulus values *X, Y,* and *Z*. The numerical values of the CIE tristimulus values *X, Y,* and *Z* are between 0 and 100 according to CIE 15 (“Colorimetry”) for the CIE illuminant E. The chromaticity coordinates are always smaller than 1.0. The *x* and *y* coordinates specify chromaticity points on a rectangular *(x, y)* diagram.

In the *(x, y)* chromaticity diagram there is a whole colour series with different CIE tristimulus values *Y* (0<=Y<=100) that belong to each chromaticity point. Therefore colours with a constant chromaticity point in the region “yellow” of the chromaticity diagram can appear either approximately black (for example with *Y*=4) or as a chromatic light yellow (with *Y*=90). Both the chromaticity and the tristimulus value *Y* are required to define a colour stimulus.

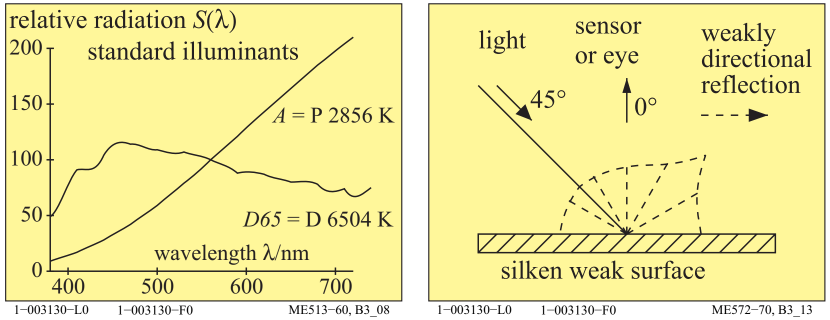


**Fig. 51: Radiation of illuminants D65 and A, and CIE-measurement geometry**

The standard tristimulus values are dependent on the illuminant, for example the CIE standard illuminants D65 or A, see Fig. 51 *(left)*. The illumination angle of the sample surface is usually 45°. *The viewing or measuring* angle is usually 0°, see Fig. 51 *(right)*. The silky weak surface of the standard offset print produces usually a diffuse reflection in all directions. However, there is some more reflection in the mirror or gloss direction -45°. Therefore black colours appear blacker under 0° compared to -45°. The CIE tristimulus value is *Y*=2,5 for the angle 0° and approximately *Y*=5 for the angle -45°.

| colour valence metric (color data: linear relation to CIE 1931 data) | | |
|---|---|---|
| **linear color terms** | **name and relationship to CIE tristimulus or chromaticity values** | **notes** |
| **tristimulus values** | *X, Y, Z* | |
| **chromatic value** | *linear chromatic value diagram (A, B)* | *n=D65* |
| red−green | $A = [\, X / Y - X_n / Y_n \,]\, Y = [\, a - a_n \,]\, Y$ | *(background)* |
| | $= [\, x / y - x_n / y_n \,]\, Y$ | |
| yellow−blue | $B = -\,0{,}4\, [\, Z/Y - Z_n/Y_n \,]\, Y = [\, b - b_n \,]\, Y$ | |
| | $= -\,0{,}4\, [\, z / y - z_n / y_n \,]\, Y$ | |
| radial | $C_{AB} = [\, A^2 + B^2 \,]^{1/2}$ | |
| **chromaticity** | *linear chromaticity diagram (a, b)* | *compare to linear* |
| red−green | $a = X / Y = x / y$ | *cone excitation* |
| yellow−blue | $b = -\,0{,}4\, [Z / Y\,] = -\,0{,}4\, [z / y\,]$ | ***L/(L+M)=P/(P+D)*** |
| radial | $c_{ab} = [\, (\, a - a_n \,)^2 + (\, b - b_n \,)^2 \,]^{1/2}$ | ***S/(L+M)=T/(P+D)*** |

1−003130−L0 1−003130−F0 ME982−70

**Table 3: Colour coordinates of low colour metric or colour valence metric**

Table 3 shows the coordinates of the low colour metric or the colour valence metric. All these coordinates are *linear* transformations of the CIE tristimulus values *X, Y, Z* or the CIE chromaticities *x, y* and the tristimulus value *Y*. The main coordinates are the chromatic values *A, B,* and $C_{AB}$ and the chromaticities *a, b,* and $c_{ab}$. The chromatic values are dependent on the chromaticities of the background (index n). Usually the chromaticity $x_n$=0,3127 and $y_n$=0,3390 of the CIE standard illuminant D65 is used.

The CIE-receptor sensitivities of the human colour vision $l_q(\lambda)$, $m_q(\lambda)$, and $s_q(\lambda)$ according to CIE 170-1 are linear functions of the CIE spectral tristimulus values $x_q(\lambda)$, $y_q(\lambda)$, and $z_q(\lambda)$. The luminous efficiency $y_q(\lambda)$ is approximately the sum of $l_q(\lambda)$ and $m_q(\lambda)$. Section 18 on page 55 shows the CIE-receptor sensitivities.

In Table 3 the chromaticity *a* (red or green content) is roughly equal to the ratio *L/(L+M)* and the chromaticity *b* (blue or yellow content) is equal to the ratio *S/(L+M)*. In the literature instead of the letters *L, M, S* the letters *P, D, T* are



used, according to the three colour vision deficiencies *P=Protanop*, *D=Deuteranop,* and *T=Tritanop*.

Anomalies of colour vision, either of the colour receptors in the retina or in the neural signal transmission, result in partially or totally defective colour vision. Defective colour vision occurs in 8% of men, but only 0,5% of woman (ratio 16:1). Most of these people confuse red and green colours. They appear grey or greyish for these persons.

Persons with colour vision deficiencies shall not take some professions, which depend on normal colour vision, for example pilots, bus or taxi drivers, and print technicians. Only very less people confuse the colours yellow and blue. Even less people perceive all colours as achromatic (white, grey, and black). For tests of defective colour vision there are test charts, for example those of *Ishihara* (1953) in which digits or symbols are used. Observers with normal and defective colour vision see different digits or symbols on these test charts. The anomaloscope of *Nagel* according to DIN 6160 allows the determination the degree of the colour vision deficiency.

| higher colour metric (color data: nonlinear relation to CIE 1931 data) | | |
|---|---|---|
| **nonlinear color terms** | **name and relationship with tristimulues or chromaticity values** | **notes** |
| **lightness** | $L^* = 116\, (\, Y / 100\,)^{1/3} - 16 \quad (Y > 0{,}8)$ | *CIELAB 1976* |
| | approximation: $L^* = 100\, (Y/100)^{1/2{,}4} \;\; (Y > 0)$ | |
| **chroma** | *nonlinear transform chromatic values A, B* | |
| red−green | $a^* = 500\, [\, (\, X / X_n)^{1/3} - (\, Y / Y_n)^{1/3} \,]$ | *CIELAB 1976* |
| | $= 500\, (\, a' - a'_n \,)\, Y^{1/3}$ | |
| yellow−blue | $b^* = 200\, [\, (\, Y / Y_n)^{1/3} - (\, Z / Z_n)^{1/3} \,]$ | *CIELAB 1976* |
| | $= 500\, (\, b' - b'_n \,)\, Y^{1/3}$ | *n=D65* |
| radial | $C^*_{ab} = [\, a^{*2} + b^{*2} \,]^{1/2}$ | *(background)* |
| **chromaticity** | *nonlinear transform chromaticities x/y, z/y* | *compare to log* |
| red−green | $a' = (\, 1 / X_n \,)^{1/3}\, (\, x / y \,)^{1/3}$ | *cone excitation* |
| | $= 0{,}2191\, (\, x / y \,)^{1/3}$ for D65 | ***log[L / (L+M)]*** |
| yellow−blue | $b' = -\,0{,}4\, (\, 1 / Z_n \,)^{1/3}\, (\, z / y \,)^{1/3}$ | ***= log[P / (P+D)]*** |
| | $= -\,0{,}08376\, (\, z / y \,)^{1/3}$ for D65 | ***log[S / (L+M)]*** |
| radial | $c'_{ab} = [\, (\, a' - a'_n \,)^2 + (\, b' - b'_n \,)^2 \,]^{1/2}$ | ***= log[T / (P+D)]*** |

1−003130−L0 1−003130−F0 ME983−70

**Table 4: Colour coordinates of high colour metric or sensation colour metric**

Table 4 shows the coordinates of the high color metric or sensation colour metric. The lightness $L^*$, the chroma coordinates $a^*$, $b^*$, and $C^*_{ab}$, and the chromaticities $a'$, $b'$, and $c'_{ab}$ are the most important coordinates of the high or sensation colour metric. In Table 4 the nonlinear chromaticities $a'$ and $b'$ serve as alternate to calculate the chroma coordinates $a^*$, $b^*$, and $C^*_{ab}$ of the CIELAB-colour space. The chromaticity *(a', b')* for CIELAB is not defined in CIE 15 and ISO 11664-4. The *nonlinear* chromaticity *(a', b')* seems roughly similar compared to the *linear* chromaticity *(u', v')* of CIELUV in CIE 15.

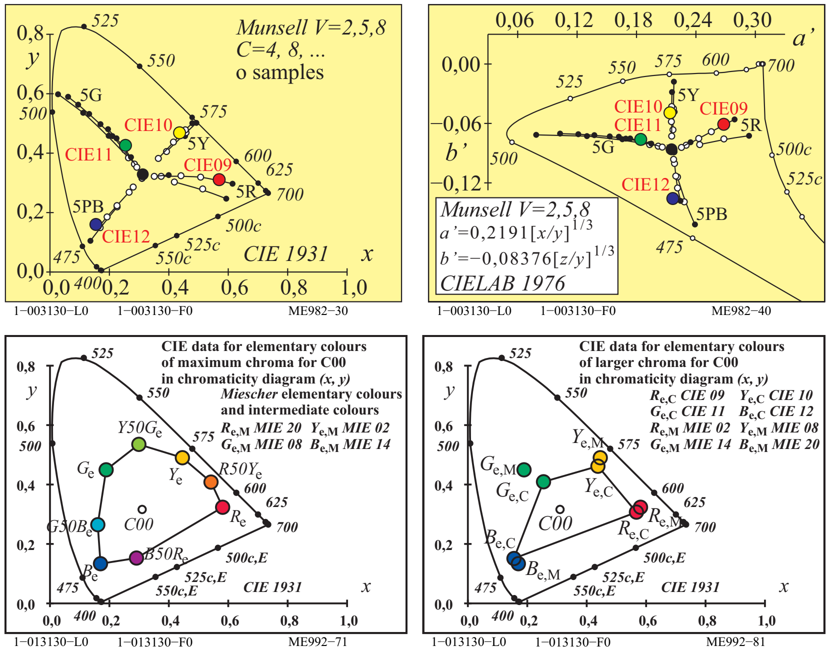


**Fig. 52: *Munsell, Miescher,* and CIE colours in *(x, y) and (a', b')***

Fig. 52 shows the four elementary hues $RYGB_e$ and in addition the *Miescher*-intermediate hues $R50Y_e$, $Y50G_e$, $G50B_e$, and $B50R_e$ *(bottom left)*. The colours of the real (o) and the extrapolated (•) four *Munsell* hues *5R, 5Y, 5G,* and *5PB* of *Value 2, 5,* and *8* are shown *(top left and right)*. In the chromaticity diagram *(a', b')* the location is more on straight lines compared to *(x, y)*. The chroma of the four elementary colours of the *Miescher*-hue circle is larger compared to the four CIE-test colours no. 9 to 12 according to CIE 13.3 *(bottom right)*. The *Miescher*-hue circle has been produced by 11 appropriate colour inks. In addition the chroma is larger compared to the hue circle of the *Relative Elementary Colour System RECS*. This hue circle is produced by the three colours $CMY_d$ of standard offset print, compare Fig. 59 on page 66 *(bottom left and right)*.



The chromaticity diagram *(a', b')* is defined in Table 4. It has a large extension to the chromaticity of the wavelength $\lambda$=400nm. For the application in the information technology this is not a problem, because these colours do usually not exist in both offset printing and on colour monitors. All real surface colours are located within the region of Fig. 52 *(top right)*.

Fig. 52 shows the elementary colours of *Miescher* in the chromaticity diagram *(x, y)*. These colour samples are not located on a circonference around the chromaticity of the CIE illuminant C, which is also used in the *Munsell*-colour system. The chromaticity differences of the CIE illuminants C and D65 are small. The elementary colours yellow $Y_e$ and blue $B_e$, and the achromatic point D65 are approximately on a line. Therefore one can mix additively the colours $Y_e$ and $B_e$ in a appropriate mixture ratio to the achromatic colour D65. The elementary colours red $R_e$ and green $G_e$ are *not* located together with D65 on a line. Therefore $R_e$ and $G_e$ mix additively to yellowish-green, yellowish or yellowish-red colours and never to the achromatic colour D65.

Table 3 on page 51 and Table 4 on page 52 show colour attributes of the low and high colour metric. It is assumed, that the complementary device colours yellow $Y_d$ and blue $B_d$ mix additively to white. Then one can only mix achromatic, yellow or blue hues. If the yellow value is larger compared to the blue value ($Y_d > B_d$), then the colour values white, black and the chromatic values are calculated according to Table 3 on page 51.

The dichromatic and trichromatic mixture is of large importance for the colour information technology. In the information technology for example on a colour monitor, or with a colour projector, or in multicolour printing all colours are reproduced by three basic device colours $RGB_d$ or $CMY_d$. The additive colour mixture on a monitor, and a data projector produces with two basic colours and the third colour a dichromatic mixture, for example

$$W_d = R_d + (G_d + B_d) = R_d + C_d$$
$$W_d = G_d + (B_d + R_d) = G_d + M_d$$
$$W_d = B_d + (R_d + G_d) = B_d + Y_d$$

In the colour information technology usually a large colour gamut in the reproduction is intended. For this the colours with the maximum chromatic value $C_{AB}$ and approximately of the largest chroma $C^*_{ab}$ are produced by complementary optimal colours with compensatory wavelength limits $\lambda_d$ and $\lambda_c$. Then the dichromatic mixture will lead to white. Colorimetric solutions for a large colour gamut in the ouput are given in section 19.

# 18 Special Properties of Colour Vision

The properties of colour vision depend on the properties of the three receptors *LMS* or *PDT* for the daylight vision.

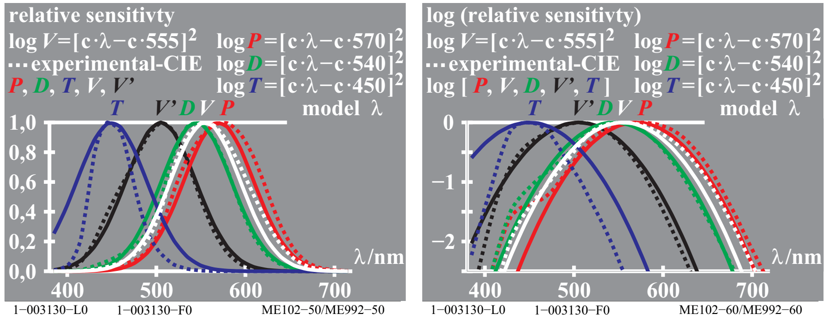


**Fig. 53: Relative receptor sensitivities *PDT* (or *LMS*), $V(\lambda)$, and $V'(\lambda)$**

Fig. 53 shows the receptor sensitivities *PDT* (according to the colour vision deficiencies *P*=Protanop, *D*= Deuteranop, and *T*=Tritanop) or *LMS* (according to CIE 170-1). The maximum sensitivities are near the wavelength 570, 540, and 450nm. A linear combination of the photopic (daylight) sensitivity $V(\lambda)$ and the scotopic (nightlight) sensitivity $V'(\lambda)$ with a maximum near 500nm is used to describe the mesopic vision beween day and night luminances.

The long wave receptor *(L or P)* has the maximum sensitivity *not* in the region red, but in the yellow-green region. The wavelength $\lambda_m$ = 570nm of the maximal sensitivity is smaller compared to the dominant wavelength $\lambda_d$ = 574nm of elementary yellow $Y_e$. If a logarithmic vertical axis is used, then a parable with approximately an equal shape for all receptors is appropriate, see Fig. 53 *(right)*. In this case the sum and the differences have special properties:

$\log V(\lambda) = \log P(\lambda) + \log D(\lambda)$ (new maximum 555nm with 570 and 540nm)
$\log P(\lambda) = \log V(\lambda) - \log D(\lambda)$ (known maximum 570nm with 555 and 540nm)
$\log R(\lambda) = \log P(\lambda) - \log D(\lambda)$ (new maximum 600nm with 570 and 540nm)

Again in the last line a parable shape is created, and in addition the missing *red sensitivity* $R(\lambda)$ with a maximum at 600nm is defined.

The luminous sensitivity $V(\lambda)$ has a large importance for the colour vision. $V(\lambda)$ serves as basic for the definition of the luminance. According to CIE 15 *Colorimetry* $V(\lambda)$ is calculated linearly by the *Grassmann*-law, for example by:

$$V(\lambda) = P(\lambda) + D(\lambda)$$

The calculation according to the above logarithmic formulas leads to



$$V_{\log}(\lambda) = 10^{[\log P(\lambda) + \log D(\lambda)]}$$

The difference between $V(\lambda)$ and $V_{\log}(\lambda)$ is about 1% for the two wavelength 400 and 700nm compared to the maximum near 555nm, see *K. Richter* (1996). The colour threshold is also near 1%. Therefore for many applications both calculation methods are approximately equal. The spectral luminous sensitivity $V(\lambda)$ is of special importance for the lighting technology. The following ratios calculated with $V(\lambda)$ have special importance for the colour field, for example

$A(\lambda) = R(\lambda) / V(\lambda)$ spectral chromaticity red-green

$B(\lambda) = - T(\lambda) / V(\lambda)$ spectral chromaticity yellow-blue

In applications these ratios correspond to the ratios *X* / *Y* and *Z* /*Y*. In Table 3 on page 51 this ratios (together with a weighting factor) are called the red-green and the yellow-blue chromaticities *a* and *b* respectively. Both define the chromaticity diagram *(a, b)*. For the use of the chromaticity diagram *(a, b)* instead of the chromaticity diagram *(x, y)* in applications, and for the description of colour thresholds, see *K. Richter* (1996).

Further properties of colour vision can be described with physiological colour signals in the retina of monkeys. *A. Valberg* (2005) has described many physiological signals as function of chromaticity and luminance of both central and background fields.

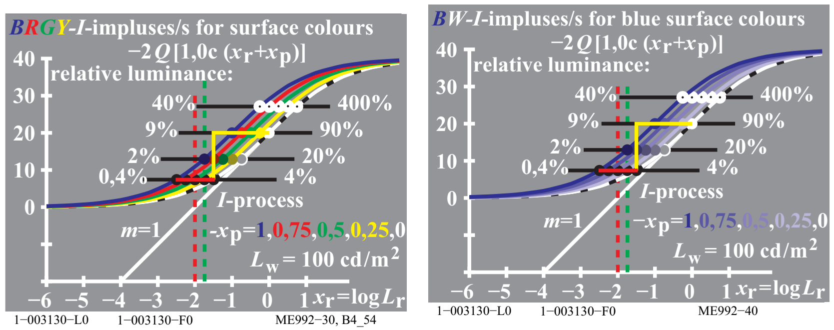


**Fig. 54: Colour signals of chromatic and blue colours**

Fig. 54 shows the measured colour signals of central field colours with increasing luminance in a white background. The white background luminance is 100 cd/m². For the office the illuminance 500 lux is recommended. This corresponds to the luminance
142 cd/m² for the white standard offset paper. This luminance is in the range of *photopic* daylight vision between about 1 cd/m² and 10000 cd/m².

In Fig. 54 the *I*-Signals (*I*=Increment) for achromatic and chromatic colours follow an S-shape curves which saturates at 0,9% and 9000% compared to the white background with the value 90%. The curve for chromatic colours *(left)* are shifted compared to the achromatic colours to the left. The curves for chromatic blue colours *(right)* shift with the chromaticity difference to D65 in the chromaticity diagram *(a, b)* to the left. For all chromatic colours equal signals are therefore created for a lower luminance *L* compared to the background luminance $L_w$=100 cd/m$^2$ *(w= white background)*.

According to *Ostwald* (1920) optimal colours of maximum chroma are defined by a "colour half", which has compensatory wavelength limits. The tristimulus value *Y* and the chromatic value $C_{AB}$ can be calculated according to Table 3 on page 51. The tristimulus value *Y* and the chromatic value $C_{AB}$ are related linearly. The ratio $C_{AB}/Y$ may serve to describe the shift to the left in Fig. 54 on page 56.

The slope of the S-shape signal curve is largest in the middle. Therefore here the largest luminance discrimination $L / \Delta L$ is expected. The threshold for achromatic and chromatic colours is expected at a luminance, which is at maximum by a factor 36 smaller compared to the white background. The number 36 may be calculated by the ratio of the tristimulus values $Y_W$=90 and $Y_N$=2,5 of white *W* and black *N*.

Probably the luminances of the largest luminance discriminability $L / \Delta L$ are similar to the luminances of the $G_0$ colours of *Evans* (1967). The $G_0$ colours appear in a white background neither blackish nor luminous. According to *Evans* the tristimulus value $Y_s$ at the colour threshold (*s=threshold*) is for all colours by the factor 30 smaller compared to the tristimulus value of the $G_0$ colours.

A CIE report of the committee CIE 1-83 *Validity of Formulae for Predicting Small Colour Differences* (Chairman *K. Richter*, DE) with a description of colour thresholds may be produced during 2014. A CIE report CIE R1-57 *Border between blackish and luminous colours* (Reporter *T. Seim*, NO) is planed during 2013.



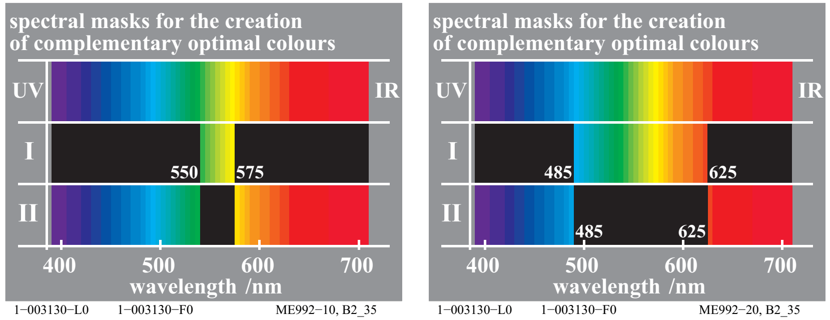


**Fig. 55: Complementary optimal colours of different band width**

Fig. 55 shows complementary optimal colours with different band width *(left and right)*. Such complementary optimal colours are created as edge spectra of white-black and black-white, if one observes the edges of different size with a prism. Already *Goethe (1830)* has observed, that there is equal colour discrimination in the *positive* and *negative* spectrum for neighbouring locations within the continuous complementary colour series.

*T. Holsmark and A. Valberg (1971)* have mixed the spectral colours of a *positive* and *negative* slit with an apparatus for mixing spectral colours. The *negative* and *positive* slit produces very different optimal colours, for example yellow and blue *(left)* or cyan and red *(right)*. For the appearance of a colour difference (threshold) the shift of the slit was approximately equal for the complementary optimal colours.

An improved colour metric for the description of colour thresholds needs therefore equal and anti symmetric coordinates. The chromatic values *A* and *B* of Table 3 on page 51 have this property. The chroma coordinates *a** and *b** of the CIELAB space have *not* this property. A colorimetry for colour thresholds, which shall consider the results, is planed in 2014 in a CIE report of the Committee CIE 1-83.

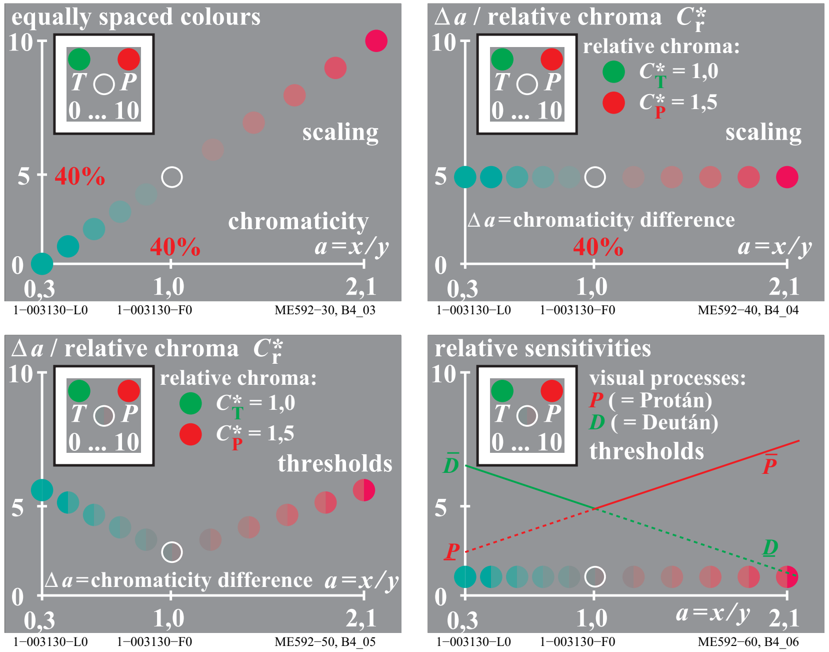


**Fig. 56: colour scaling and colour thresholds of the colour series *T - D65 - P***

Fig. 56 shows in principle some experiments and results about colour scaling and colour thresholds as function of the chromaticity $a = x/y$. The colour scaling and the colour thresholds are shown for colours of equal luminance $L$, in this case with the constant tristimulus value $Y$=18.

Fig. 56 *(top left)* shows a colour series between a very chromatic turquoise colour *T* via grey (*D65* daylight) up to a very chromatic purple-red *P*. This colour series is approximately equally spaced. The experimental situation is shown in Fig. 56 *(top left)*. In a white surround there is a square grey background. In this grey background two “end-colours” were presented, here turquoise *T* and purple-red. In the lower field it was possible to produce colours of equal luminance between the two end-colours *T* and *P*.

The observer gets a fixed scale between the steps 0, 5 and 10 for *T*, *D65* and *P*. By a random process within the experiments digits between 0 and 10 were produced. For 1 the observer shall produce a chromatic turquoise, for 7 a medium chromatic purple, for 5 the achromatic grey of the chromaticity D65. The goal



of the production of a visual equidistant colour scale both between *T* and *D65* and between *D65* and *P* was explained explicitly to the observers.

Fig. 56 *(top right)* shows the results of the experiments in *T - P* direction. The difference Δa shows a straight line as function of the coordinate $a = x / y$ between two neighbouring colour steps (divided by the relative chroma evaluated by the observers as 1,0 for *T - D65*, and 1,5 for *D65 - P)*. Equal chromaticity differences Δ*a* (divided by 1,0 for *T - D65*, and 1,5 for *D65 - P*) correspond to equal chroma differences. There is a simple description of equal chroma differences by equal differences of a coordinate of the low colour metric (here $a = x / y$ ).

In addition the visible colour thresholds, which are just noticeable colour differences, have been determined along the same colour series *T - D65 - P*. At first we assumed, that the chromaticity difference Δ*a* for the threshold may be smaller, for example by a constant factor 30. However, the results are different.

Fig. 56 *(bottom left)* shows the experimental situation. In a white surround there was a grey quadratic background. In this grey background two ”end-colours” were shown, here turquoise *T* and purple-red *P*. In the lower circular field all colours between the two end-colours could be produced. In two half circles equal amounts of *T* or *P* could be added. In general for a colour threshold about 1% of the two end-colour was necessary to recognize a colour difference.

Fig. 56 *(bottom left)* shows the chromaticity difference Δ*a* for colour thresholds as function of the coordinate $a = x / y$ of the low colour metric. The differences Δ*a* for colour thresholds change in the range 1 to 3. The difference Δ*a* is smallest for grey (D65), and increase linearly towards *T* and *P*. At grey about 30 thresholds correspond to a chroma step. At purple-red *P* and turquoise *T* 10 thresholds correspond to a chroma step.

The BAM-research results of *K. Richter* (1985) are in agreement with other results, for example of *Inamura and Yaguchi* (2011). In principle two different kinds of metric are necessary to describe for example the *MacAdam*-ellipses (at threshold) and the colour order systems which apply the colour scaling.

Fig. 56 *(bottom right)* shows the *relative sensitivities* of two colour vision processes in red-green direction. For the two series *D65 - T* and *D65 -P* one of two colour vision processes determines the recognition of colour thresholds. According to this model the chromaticity difference Δ*a* is small for achromatic colours and large for chromatic colours. According to Fig. 56 *(bottom left)* the experimental results are opposite. The colour vision model with the colour signals as function of luminance and chromaticity can explain this property.

Fig. 54 on page 56 shows the colour signals of blue colours with an increasing chromaticity difference Δ*b* compared to the achromatic series *(right)*. The *largest luminance* discrimination *L* / Δ*L* is reached on a *horizontal* line and for *decreasing* luminance of blue colours compared to the achromatic white. This is described by the *largest* slope of all the signals on a *horizontal* line (slope change of the signals). The *luminance* discrimination $L / \Delta L$ on a *vertical* line decreases for these blue colours of *equal* luminance, because the slope of the signal curve decreases. If one in addition assumes a linear relation between $\Delta L$ and $\Delta b$ on a *vertical* line*,* then $\Delta b$ *decreases* for blue colours of *equal luminance* according *to* Fig. 54 on page 56.

Fig. 56 *(bottom right)* seems to show that the *relative sensitivities* increase with the chromaticity difference. This is not true and may be described as follows. The luminance of the black threshold is by a factor 1:36 lower compared to white luminance. According to Evans (1974) the luminance of the chromatic treshold is usually lower compared to the black luminance. This result is in agreement with Fig. 56. However with increasing chromaticity difference, for colours of equal luminance the signal slope decreases and therefore the chomatic threshold decreases which seems opposite to Fig. 56 *(bottom right).*

The research results require at least a colour metric for colour thresholds and a colour metric for scaling, and if possible with transitions. In applications the colour thresholds are important for the determination of small colour differences. The equal spacing of larger colour differences is important for the spacing of colour rendering properties. Colour samples in colour order systems have usually colour differences around 30 colour thresholds (or $\Delta E^*_{ab} = 10$). An example is the colour order system *RAL*-Design (1993), which is based on CIELAB and has sample differences of $\Delta E^*_{ab} = 10$ in any hue plane, and for 36 hues.



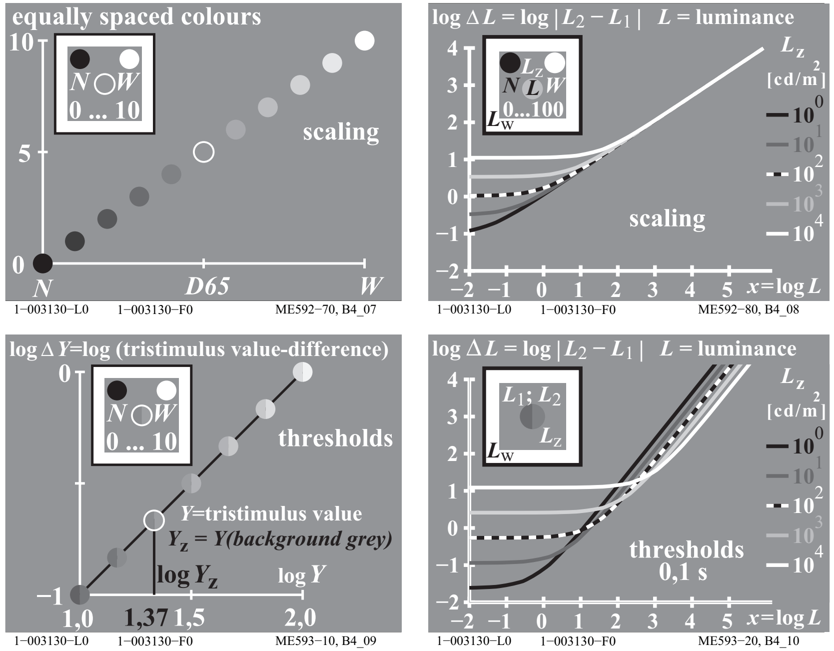


**Fig. 57: Luminance scaling and thresholds of lightness series *N - Z - W***

Fig. 57 shows experiments and results of colour scaling and colour thresholds as function of the luminance *L*. Instead of the luminance *L* one can also use the tristimulus value *Y*, which represents a relative luminance and is always normalized to 100 for white. The formula

$$Y = 100\, L / L_W$$

uses the central field luminance *L* and the surround field luminance $L_W$ (outer white frame in the experimental situation, see Fig. 57).

Fig. 57 *(top left)* shows the equally spaced colour (lightness) scaling for a central field luminance series in the two regions *N - D65* and *D65 - W.*

Fig. 57 *(top right)* shows the measured central field luminance differences $\Delta L$ as function of the central field luminance *L.* A *log* scale is used on both axis. As a parameter the background luminance is given. The black-white curve is valid for the background field luminance $L_z$ = 100 cd/m$^2$ of the grey background *z.* The luminance $L_z$ = 100 cd/m$^2$ corresponds to a medium illuminance of 1500 lux (=5 • π •100 lux). The factor five is used for a medium grey with the reflection factor 0,2.

Fig. 57 *(bottom left)* shows the results of colour thresholds along the grey series. For the central field and only a part of the grey scale the tristimulus value difference $\Delta Y$ (proportional $\Delta L$) is a function of the tristimulus value $Y$. The threshold $\Delta Y$ is constant and 1% of the central field tristimulus value $Y$. The constant slope near the value 1 (or 0,9) is based on the law of *Weber-Fechner* $\Delta Y / Y$ = constant or $\Delta L / L$ = constant.

Fig. 57 *(bottom right)* shows in addition the results for very dark and very light colours for a luminance range of six *log* units (in Fig. 57 *(bottom left)* only one unit is shown). The parameter background-field luminance describes especially the large change of the black threshold with the background-field luminance. For small central-field luminances $L$ a constant black threshold $\Delta L_s$ (*s=threshold*) is reached. Luminance differences smaller than $\Delta L_s$ are not visible.

A comparison of Fig. 57 *(top and bottom right)* shows that the luminance differences $\Delta L_{scaling}$ for equally spaced grey series and $\Delta L_{thresholds}$ for luminance thresholds are not proportional along the same gray scales. The different slopes (about 0,9 and 0,45) are the basis for this statement. One may explain the differences along the grey scale by two visual processes in white-black direction, see *K. Richter* (1996).

Also in Fig. 56 on page 59 for colours of equal luminance along the colour series *T - D65 - P* two different slopes are necessary for the chromaticity differences $\Delta a_{scaling}$ for scaling and $\Delta a_{threshold}$ for thresholds.

A colour vision model for the description of both scaling and thresholds results and the transitions is missing up to now.



# 19 Elementary Colours and Colour Information Technology

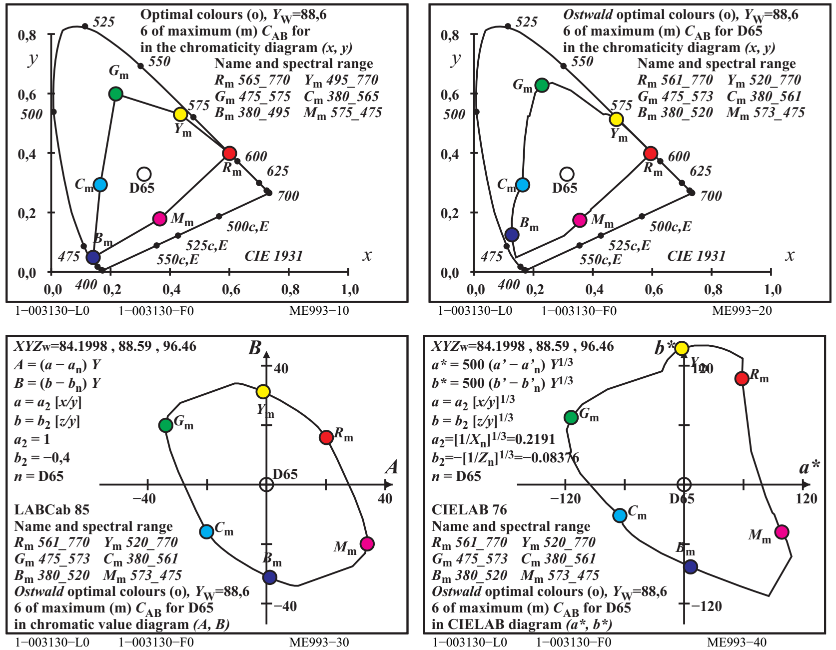


**Fig. 58: Three complementary and all optimal colours of maximum chroma**

Fig. 58 shows three optimal colour pairs $R_m$-$C_m$, $Y_m$-$B_m$, and $G_m$-$M_m$. The two colours of each pair are complementary, mix to white and are called dichromatic. The chromatic values A and B defined in Table 3 on page 51 are shown in Fig. 58 *(bottom left)*. The chromatic value $C_{AB}$ is *equal* for the dichromatic complementary optimal colours of a “colour half”. For example the two wavelength limits ($\lambda_1$, $\lambda_2$) of red $R_m$ = (561, 770) and the complementary colour cyan-blue $C_m$ = (380, 561) are given. All colours of maximum (m) chromatic value $C_{AB}$ are not located on a circle but on an ellipse. The maximum (m) chromatic value $C_{AB}$ is smallest and equal for $R_m$ and $C_m$ and larger and equal for $Y_m$ - $B_m$ and $G_m$ - $M_m$.

For all optimal colours approximately instead of a triangle in the standard chromaticity diagram *(x, y)* now apprimately an ellipse is produced in the chromatic value diagram *(A, B)*.

The anti symmetry in the chromatic value diagram *(A, B)* is a requirement for an efficient description of the *equal* threshold for complementary optimal colours. For this experimental result by *Holtsmark and Valberg* (1969), compare Fig. 55 on page 58.

Dichromatic optimal colours, for example $R_m$ and $C_m$, include for red and cyan-blue the complementary spectral ranges 565nm to 770nm and 380 to 565nm, compare the description in Fig. 58 *(top left)*. For example the wavelength limits $\lambda_1$=380nm and $\lambda_2$=565nm are located with D65 approximately on a line.

The colour cyan-blue $C_m$ of the spectral range 380nm to 565nm ("colour half") has the largest chromatic value $C_{ab}$. For example an additional spectral colour red with $\lambda_r$=600nm mix to a more whitish cyan-blue $C_m$, and the chromatic value $C_{ab}$ decreases.

Fig. 58 *(top left)* shows in addition two optimal colours $G_o$ and $M_o$, which produce a triangle in the standard chromaticity diagram *(x, y)* together with $RYCB_m$. The spectral range 495 to 565nm of the colour $G_o$ is smaller compared to the range 475 to 575nm (with compensatory wavelength limits) of the colour $G_m$. Green $G_o$ is therefore darker compared to $G_m$. In the standard chromaticity diagram (x, y) the chromaticity difference between $G_o$ and D65 is larger as the one between $G_m$ and D65. However, for the chromatic value it is opposite and it is valid $C_{ab,Go} < C_{ab,Gm}$.

The *area* of the basic and mixture colours in any *chromaticity diagram* is therefore *not* appropriate to specify the colour gamut. However, the colour area in a chromaticity diagram is often used to specify the colour gamut in many IEC and ISO standards. A more appropriate specification uses the chromatic value or chroma area.

Experimental results of *Miescher and Weisenhorn* (1961) with optimal colours in a white background have shown, that the dichromatic optimal colours which have all the largest chromatic value, have at the same time the largest chroma. However, in many cases the band width was a little smaller compared to the *colour half* with compensatory wavelength limits.

Fig. 58 *(top right)* shows all dichromatic optimal colours as continuous curve in the standard chromaticity diagram *(x, y)*, the chromatic value diagram *(A, B) (bottom left)* and the CIELAB-chroma diagram *(a*, b*) (bottom right)*. These complementary optimal colours have all the maximum chromatic value $C_{ab}$ *(bottom left)*. The calculated wavelength limits *(top right)* for D65 differ slightly for the three CIE illuminants D65, E, and C *(top left)*.

The CIELAB-colour system is mainly based on colour scaling of the *Munsell*-colour order system and requires *nonlinear* coordinates.



For the description of colour thresholds for example the colour vision models of *Guth* (1972) require only *linear* coordinates.

All pairs of dichromatic optimal colours have the same chromatic value $C_{ab}$. In CIELAB for dichromatic optimal colours the chroma is in the red-yellow region about twice compared to the complementary region cyan-blue. Therefore the CIELAB-definition of chroma $C^*_{ab}$ may be wrong by a factor 2.

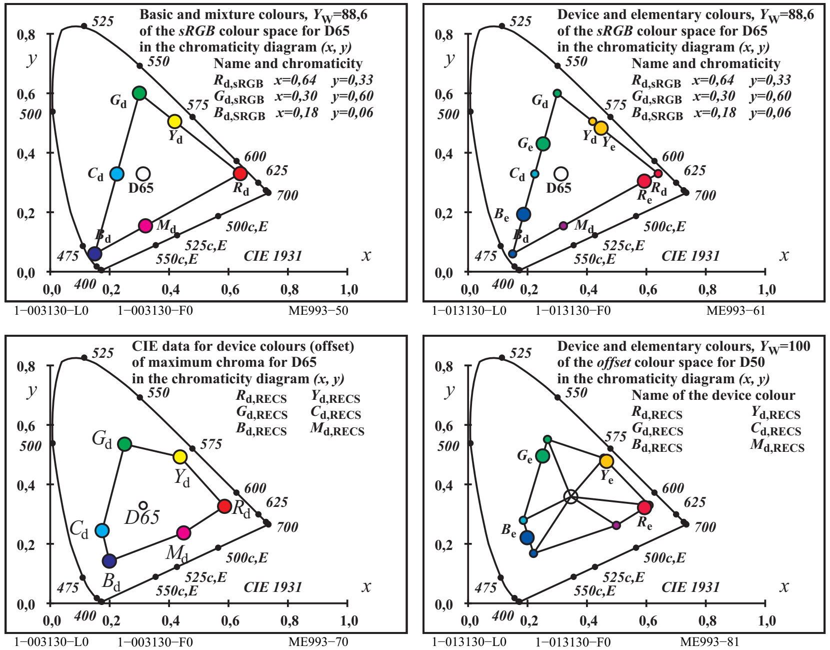


**Fig. 59: Device- and elementary colours of the colour spaces *sRGB and RECS* (Offset)**

Fig. 59 shows the device colours of a *sRGB* standard display, and of the *Relative Elementary Colour System RECS* (standard offset) *(top and bottom left)*. The device independent elementary hues $RYGB_e$ according to CIE R1-47 with the CIELAB-hue angles $h_{ab}$ = 26, 92, 162, and 272 degree (larger balls) may be mixed from six device colours $RYGCBM_d$ (d=device) *(top and bottom right)*.

In the *Relative Elementary Colour System RECS* with about 2000 colours a 16-step hue circle with the four elementary hues $RYGB_e$ as anchor hues is printed, see *RECS*. In each of the four sectors there are three intermediate hues. For the

16 hues there are 5- and 16-step colour series in standard offset printing on standard offset paper.

## 20 *Device independent* Elementary Colour Output

For the elementary colours the report CIE R1-47 defines the hue angles $h_{ab,e}$ = 26, 92, 162 and 272 which allows a device-independent hue output on any colour device. Fig. 59 on page 66 shows the solution for the *sRGB*-colour space (standard display) and the *RECS*-colour space (standard offset). For the visual $rgb*_e$ data $(1\ 0\ 0)_e$ $(1\ 1\ 0)_e$, $(0\ 1\ 0)_e$, $(0\ 0\ 1)_e$ the device colours of maximum chroma $C*_{ab,d}$ with the hue angles $h_{ab,e}$ = 26, 92, 162, and 272 are produced. This leads to device specific values for lightness $L*_d$ and chroma $C*_{ab,d}$.

As a future next step, and in addition to the definition of the CIELAB-elementary hue angles, the definition of a special lightness $L*_e$ and a special chroma $C*_{ab,e}$ for the elementary colours is appropriate. A first definition may be included in 2013 in the report CIE R1-57 “Border between blackish and luminous colours” *(Reporter T. Seim, Norway)*.

For the illuminant D65 the dichromatic optimal colours (index oe) with the largest chromatic value $C_{ab,oe}$, and the CIELAB elementary hue angles $h_{ab,oe}$ = 26, 92, 162, and 272 may be located at the border “neither blackish nor luminous”. These colours have the following *device-independent* lightness $L*_{oe}$ and chroma $C*_{ab,oe}$.

| colour | $rgb*_{oe}$ | $L*_{oe}$ | $C*_{ab,oe}$ | $h_{ab,oe}$ | $x_{oe}$ | $y_{oe}$ | $Y_{oe}$ |
|---|---|---|---|---|---|---|---|
| $R_e$ | (1 0 0) | 75 | 65 | 26 | 0,57 | 0,33 | 48 |
| $Y_e$ | (1 1 0) | 89 | 136 | 92 | 0,47 | 0,51 | 73 |
| $G_e$ | (0 1 0) | 79 | 120 | 162 | 0,19 | 0,52 | 55 |
| $B_e$ | (0 0 1) | 60 | 69 | 272 | 0,17 | 0,19 | 25 |

It is unknown, if the here calculated optimal colours are located on the visual border between “neither blackish nor luminous”. The *fluorescent* red colour printed in Fig. 28 on page 26 and which appears luminous is above this border.

With displays and special software one perhaps may reach the *natural* colour data $LCh*_{oe}$ of CIELAB for the standard display luminance 142cd/m$^2$. This luminance is required for the standard illuminance 500 lux in offices, and the white paper of offset printing with the standard reflection factor $R(\lambda)$ =0.886.

For surface colours (with no fluorescence and retroreflection) it seems impossible to reach the CIELAB values for green $G_e$ and blue $B_e$. The shape of the



reflection factors of these surface colours is too different compared to the reflection factor of the intended optimal colours, compare Fig. 26 on page 25.

## 21 Affine Colour Reproduction

In colour image technology the colour gamut is limited in any hue plane approximately by the triangle white - most chromatic colour - black. Both for displays and printing there is aproximately an additive mixture at the border of this triangle. Solutions for the reproduction of both the border and within the triangle are most important.

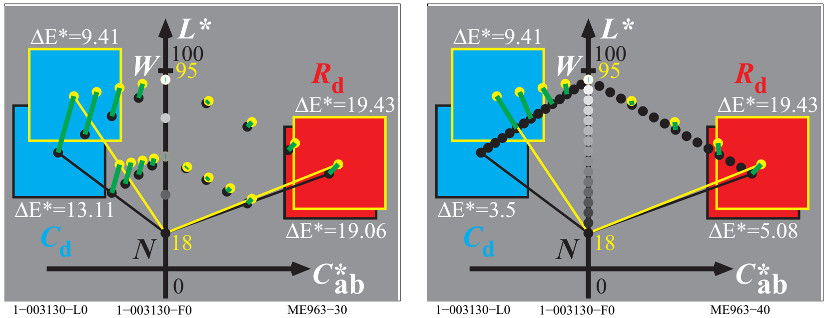


**Fig. 60: Affine colour reproduction and minimum colour difference $\Delta E*_{ab}$**

Fig. 60 shows the affine colour reproduction *(left)* and a reproduction with the smallest colour difference $\Delta E*_{ab}$ *(right)* between monitor colours *(yellow balls)* and standard printing colours *(black balls)*.

Fig. 60 *(left)* shows that for the hue cyan-blue 20% of the monitor colours and 30% of the printing colours are outside the common reproduction area. The affine colour reproduction uses the whole colour gamut of both devices.

Fig. 60 *(right)* shows the present solution of most colour management methods. The goal is the smallest colour difference $\Delta E*_{ab}$. In this case 30% of the cyan-blue printing area is not used. The ICC-colour management standard allows company specific solutions and therefore a wide variety of outputs may be produced for example by test charts according to DIN 33872-1 to -6, see http://www.ps.bam.de/33872E

For a filled out DIN-form of output questions see *(look olso for LE96 and similar)*
http://130.149.60.45/~farbmetrik/LE95

Any user can ask the device manufacturer for solutions in agreement with DIN 33872-1 to -6 or other international standards, for example ISO/IEC 15775.

This section may have shown that both the *device-independent hue* reproduction and the *affine* reproduction are possible. In a next step the *device-independent colour* reproduction may be based on CIE data of Fig. 58 on page 64 for optimal colours of maximum chromatic value $C_{AB}$ and section 21.

## 22 References

*Standards and similar publication*
CIE 13.3:1995, Method of measuring and specifying colour rendering of light sources.
CIE 15: 2004, Colorimetry, 3rd edition.
CIE 170-1:2006, Fundamental chromaticity diagram with physiological axes
CIE R1-47:2009, Hue angles of elementary colours, see http://div1.cie.co.at/
ISO 11664-4:2008(E)/CIE S 014-4/E:2007: Joint ISO/CIE Standard: Colorimetry — Part 4: CIE 1976 *L*a*b** Colour Space
DIN 33872-1 to -6 (2010), Information technology - Office machines - Method of specifying relative colour reproduction with YES/NO criteria, see http://www.ps.bam.de/33872E
ISO/IEC TR 24705 (2005) Information technology - Office machines - Method of specifying relative colour reproduction with YES/NO criteria

*Author publications*
Evans, R. M. and S. B. Swenholt (1967), Chromatic Strength of Colors; Dominant Wavelength and Purity, J. opt. Soc. Amer. 57, S. 1319-1324
Holtsmark, T. and Valberg, A. (1969), Colour discrimination and hue, Nature, Volume 224, October 25, S. 366-367.
Miescher, K. (1948), Neuermittlung der Urfarben und deren Bedeutung für die Farbordnung, Helv. Physiol. Acta 6, C12-C13
Miescher, K., Richter, K. und Valberg, A. (1982), Farbe und Farbsehen, Beschreibung von Experimenten fuer die Farbenlehre, Farbe + Design, no. 23/24
Newhall, S.M., D. Nickerson and D.B. Judd (1943), Final report of the O.S.A. subcommittee on the spacing of the Munsell colors. J. opt. Soc. Amer. 33, S. 385-418
Richter, K. (1979), BAM-Forschungsbericht Nr. 61, Beschreibung von Problemen der höheren Farbmetrik mit Hilfe des Gegenfarbsystems, 99 Seiten, ISSN 0172-7613
Richter, K. (1980), Cube root colour spaces and chromatic adaptation, Color Research and Application 5, no. 1, pages 25-43
Richter, K. (1985), BAM-Forschungsbericht Nr. 115, Farbempfindungsmerkmal Elementarbuntton und Buntheitsabstände als Funktion von Farbart und Leuchtdichte von In- und Umfeld, 118 Seiten, ISBN 3-88314-420-7



Richter, K. (1996), Computergrafik und Farbmetrik - Farbsysteme, *PostScript* und geräteunabhängige CIE-Farben, VDE-Verlag, 288 pages with about 500 colour figures and many additional references, see

http://www.ps.bam.de/buche
Richter, K (2011) ISO-CIE trend for the description of colour threshold data by new coordinates based on the device independent elementary colour coordinates of the report CIE R1-47:2009, see
http://130.149.60.45/~farbmetrik/CIE_ISO_10.PDF
Valberg, A. (2005), Light, Vision, Color, Wiley, ISBN 0470 849037, 462 pages.

## 23 Acknowledgements and Technical Remarks

The *Karl Miescher-Foundation for Colour Science Support* has supported this Book *Colour and Colour Vision* in German and English, and internet versions in additional languages

Since 2000 the professors *H. Kaase* and *S. Voelker* have continuously supported the exhibition *Colour and Colour Vision* at the department Lighting Technology of the Berlin University of Technology (TU).

***Remarks about the history of the exhibition Colour and Colour Vision***
During the years 1963/64 the exhibition *Colour and Colour Vision* has been developed by *K. Richter* under the leadership of *Dr. Karl Miescher* in the Laboratory of Colour Metrics at the Physical Institute of the University of Basle/ Switzerland. The colour exhibition was shown for six months at the *Swiss National Exhibition Expo 64* in Lausanne/CH. After the *Expo 64* the colour exhibition was shown for 30 years in the high school *Mathematisch-Naturwissenschaftliches Gymnasium* in Basle.

In 2000 the exhibition was rebuild with financial support of the *Karl Miescher-Foundation* at the Berlin University of Technology. In Berlin *K. Richter* has continuously enlarged the exhibition by some new colour developments in the field of colour information technology. Since 2000 many student and people with interests in colour visited the exhibition.

***Notes to the former editions and the edition 2012***
In 1964 the first edition comes without colour figures for the *Swiss National Exhibition Expo 64* in Lausanne and in languages German, French and Italian.

In 1982 after the second edition in 1978 the third edition with 50 colour figures comes in the colour journal “Farbe + Design” in German. In addition a special print comes in German and English. Coauthor of this edition was *Prof. Dr. Arne Valberg*, Trondheim/Norway.

The fourth edition 2012 comes with 135 colour figures, which in addition show new developments in the field of colour information technology. There are versions for offset, monitor, and printer output, and internet versions in German and English. In addition internet versions are intended in the languages French, Spanish, and Italian.

For download of the last internet editions and the order of offset versions see http://130.149.60.45/~farbmetrik/color

***Purposes and applications of the special print 2012***
The special prints serve for educational purposes and as introduction in the field of colour science. Different application fields of colour are connected without basic knowledge on colour but with some technical knowledge, for example

Visual basics and properties of colour vision
Colour measurement and colour metrics
*Relative Elementary Colour System RECS* in colour information technology.

For additional studies a colour book (only in German) is recommended with the title *Computer graphic and colorimetry - Colour systems, PostScript, and device independent CIE colours*. This book was edited by the VDE-Verlag in 1996 and has descriptions of about 500 colour figures in German and English. The colour figures may be used separately for educational purposes. The PDF files of this book and the colour figures are available as free download, see http://130.149.60.45/~farbmetrik/buche.html

The secretariat of the department Lighting Technology at the Berlin University of Technology may arrange guides on request through the exhibition *Colour and Colour Vision*, see
http://www.li.tu-berlin.de


Prof. Dr. Klaus Richter, Walterhoeferstrasse 44, D-14165 Berlin, Germany
Internet: http://130.149.60.45/~farbmetrik/
Fax: +49 30 84509039, email: klaus.richter@me.com

*Purposes and applications of improved versions 2013 in different languages*

For the translation from english into other languages I thank especially
*Prof. Dr. Manuel Melgosa* (University of Granada, Spain)
email: mmelgosa@ugr.es.
His translation into Spanish produces many questions and suggestions. This leads to improved internet versions 2013 in all five languages.



# 24 Test charts and technical Remarks

**Names of the test charts with 7 characters,**

Examples: *PE40S0S, PG7011S, PG7311L , PF4611P, PG7911P*

The first character describes a large file folder (here *P*). The second describes the language (E=English, G=German, F=French, S=Spanish, I=Italian).

The followwing two numbers include the range 00 to 99. The last number 0 produces the output of an *sRGB* display. The last numbers 3 or 6 define an output in offset print on the paper *L* with the two separations *CMYK* and *CMY0*. The last number 9 defines a printer output on the paper *A* (=APCO) with the separation *CMYK*.

The following two letters *S0* define a start output *(S0)* with mixed *rgb* and *cmyk* data in the file. Or the two numbers *00* or *01* define an *rgb* transfer for the output of device colours *(00)* or elementary colours *(01)*. Or the two numbers *10* and *11* define an *rgb-3D* linearisation for the output of device colours *(10)* or elementary colours *(11)*.

The last letter *S, L,* or *P* defines the output of an *sRGB* display *(S),* or in offset print on paper *L (L),* or of a printer on the paper *A (P)*.

**Test chart on the front cover**

*PE7011S, PE7311L, PE7911P:*
16 and 8 step elementary hue circle with the elementary colours according to CIE R1-47 and DIN 33872-1 to 6

**Test charts in the annex**

1. Output *S* without separation and *L* and *P* with the separation *CMYK*

*PE1011S, PE1311L, PE1911P:*
Test chart 1 for colour rendering with 54 colours of the *RECS*-colour system.

*PE40S0S, PE4000S, PE4001S, PE4010S, PE4011S*
*PE43S0L, PE4300L, PE4301L, PE4310L, PE4311L*
*PE49S0P, PE4900P, PE4901P, PE4910P, PE4911P:*
1080 colours for colour measurement and for the steering of the output.

*TE7011S, TE7311L, TE7911P:*
Achromatic test chart according to *ISO/IEC 15775, ISO/IEC TR 24705* and *ISO 9241-306,* Annex *D.*

*TE8011S, TE8311S, TE8911S:*
Chromatic test chart with an ISO/IEC image according to ISO/IEC 15775, ISO/IEC TR24705 and ISO 9241-306, annex E.

2. Outputs *L* and *P* with the separation *CMY0*

*PE46S0L, PE4600L, PE4601L, PE4610L, PE4611L*
*PE46S0P, PE4600P, PE4601P, PE4610P, PE4611P:*
1080 colours for colour measurement and for the steering of the output

3. Outputs *L* and *P* with the two separations *CMYK* and *CMY0*

*PE2311L*, *PE2311P:*
Test chart 2 for colour rendering with metameric colours for D65 and D50.

*PE3311L*, *PE3311P:*
Test chart 3 for colour rendering with metameric colours for A and P4000,

**Test charts on the inner back cover**

*PE91S0S*, *PE91S0L*, *PE91S0P:*
Table with CIE data of a 48 step colour circle.

*PE9011S*, *PE9311L*, *PE9911L:*
5 and 16 step colour seriesfor the elementyary colour rot $R_e$ according to DIN 33872-4.

**Technical remarks about the table at the inner back cover**:

For a 48 step hue circle the table shows in column 2 the *rgb* input data and CIELAB-colour measurement data *LabCh**. In column 3 the data are interpolated for the next even number of a CIELAB-hue angle $h_{ab}$ (0< i=$h_{ab}$ <360). The $rgb_s$-system (s=standard) relates the $rgb_s$-data $(1\ 0\ 0)_s$, $(1\ 1\ 0)_s$, $(0\ 1\ 0)_s$, $(0\ 1\ 1)_s$, $(0\ 0\ 1)_s$, and $(1\ 0\ 1)_s$ to the hue angles 30, 90, 150, 210, 270, and 330 degrees. Similar according to CIE R1-47 the $rgb_e$-system (e=elementary) relates the $rgb_e$-data $(1\ 0\ 0)_e$, $(1\ 1\ 0)_e$, $(0\ 1\ 0)_e$, $(0\ 1\ 1)_e$, $(0\ 0\ 1)_e$, and $(1\ 0\ 1)_e$ to the hue angles 26, 92, 162, 217, 272, and 329 degrees.

In addition for example for the sRGB system the output of the file

http://130.149.60.45/~farbmetrik/RE69/RE69L0NP.PDF

produces the CIELAB data as function of the hue angle *i* (0<= *i* <=360). For any *rgb*-data set (except *r*=*g*=*b*) it is valid according to DIN 33872-1:

$$i = 360 \text{ atan } \{[r \sin(30) + g \sin(150) - b \sin(270)]/[r \cos(30) + g \cos(150)]\}$$

The index *i* produces tables with the angle *i* between 0 and 360 degree, and the CIELAB-data *LabCh*,* and the related *rgb* data for the device colour or the elementary colour output system.



In applications the intended CIELAB-colour data are calculated for any hue angle *i* from the CIELAB data *LabCh** of colours with maximum chroma $C^*_{ab}$, and of white *W* and black *N*. To produce an intended colour the data $rgb_{dd}$ (device to device output) and $rgb_{de}$ (device to elementary output) use a 3D-linearization in the CIELAB-colour space.

For more information on output linearization of displays, offset print and printers see a so called “white report” for a draft standard document on output linearization

http://130.149.60.45/~farbmetrik/outlin

It is intended that the proposed report CIE R8-09 will be an extended summary of this report on output linearization.

**Test chart 1 for color rendering: 54 standard colours for D65; laser printer *(CMYK); rgb−>rgb*de***

| | | | | | | | | | |
|---|---|---|---|---|---|---|---|---|---|
| 01: R00Y_100_100$_e$ | 02: R25Y_100_100$_e$ | 03: R50Y_100_100$_e$ | 04: R75Y_100_100$_e$ | 05: Y00G_100_100$_e$ | 06: Y25G_100_100$_e$ | 07: Y50G_100_100$_e$ | 08: Y75G_100_100$_e$ | 09=10: G00B_100_100$_e$ | **Series: maximum m** |
| 10: G00B_100_100$_e$ | 11: G25B_100_100$_e$ | 12: G50B_100_100$_e$ | 13: G75B_100_100$_e$ | 14: B00M_100_100$_e$ | 15: B25R_100_100$_e$ | 16: B50R_100_100$_e$ | 17: B75R_100_100$_e$ | 18=01: R00Y_100_100$_e$ | **maximum m** |
| 19: R00Y_100_050$_e$ | 20: R50Y_100_050$_e$ | 21: Y00G_100_050$_e$ | 22: Y50G_100_050$_e$ | 23: G00B_100_050$_e$ | 24: G50B_100_050$_e$ | 25: B00R_100_050$_e$ | 26: B50R_100_050$_e$ | 27=19: R00Y_100_050$_e$ | **whitish w** |
| 28: R00Y_075_050$_e$ | 29: R50Y_075_050$_e$ | 30: Y00G_075_050$_e$ | 31: Y50G_075_050$_e$ | 32: G00B_075_050$_e$ | 33: G50B_075_050$_e$ | 34: B00R_075_050$_e$ | 35: B50R_075_050$_e$ | 36=28: R00Y_075_050$_e$ | **central z** |
| 37: R00Y_050_050$_e$ | 38: R50Y_050_050$_e$ | 39: Y00G_050_050$_e$ | 40: Y50G_050_050$_e$ | 41: G00B_050_050$_e$ | 42: G50B_050_050$_e$ | 43: B00R_050_050$_e$ | 44: B50R_050_050$_e$ | 45=37: R00Y_050_050$_e$ | **blackish n** |
| 46: NW_000$_e$ | 47: NW_013$_e$ | 48: NW_025$_e$ | 49: NW_038$_e$ | 50: NW_050$_e$ | 51: NW_063$_e$ | 52: NW_075$_e$ | 53: NW_088$_e$ | 54: NW_100$_e$ | **grey g** |

see similar files: http://130.149.60.45/~farbmetrik/PE19/PE19.HTM
technical information: http://www.ps.bam.de or http://130.149.60.45/~farbmetrik

TUB registration: 20130201-PE19/PE19L0FP.PDF /.PS
application for measurement of laser printer output, separationcmyn6* (CMYK)
TUB material: code=rha4ta

PE49S0P

http://130.149.60.45/~farbmetrik/PE49/PE49L0NP.PDF /.PS; start output
N: no 3D-linearization (OL) in file (F) or PS-startup (S), page 1/2

see similar files: http://130.149.60.45/~farbmetrik/PE49/PE49.HTM
technical information: http://www.ps.bam.de or http://130.149.60.45/~farbmetrik

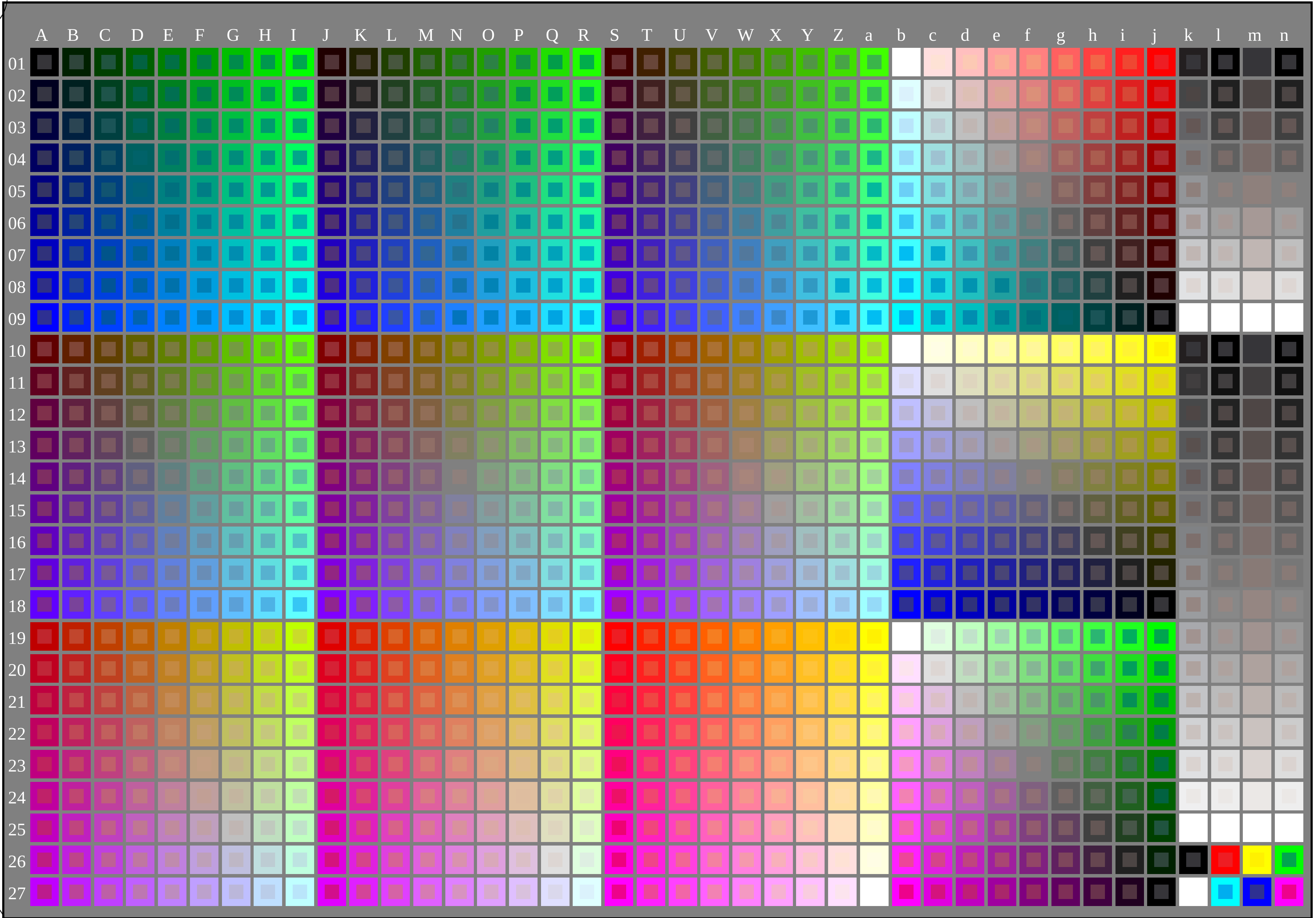


TUB registration: 20130201-PE49/PE49L0NP.PDF /.PS
application for measurement of laser printer output

TUB material: code=rha4ta

1-003030-L0 PE490-7N Test chart G with 1080 colours; 9 or 16 step colour scales; data in column (A−n): **rgb (A_j+k26_n27), 000n (k), w (l), nnn0 (m), www (n) + cmy0(all)**

TUB-test chart PE49; standard test chart
1080 standard colours; image technology

input: *rgb/cmyk −> rgb/cmyk*
output: no change

PE4900P

http://130.149.60.45/~farbmetrik/PE49/PE49L0NP.PDF /.PS; transfer output
N: no 3D-linearization (OL) in file (F) or PS-startup (S), page 2/2

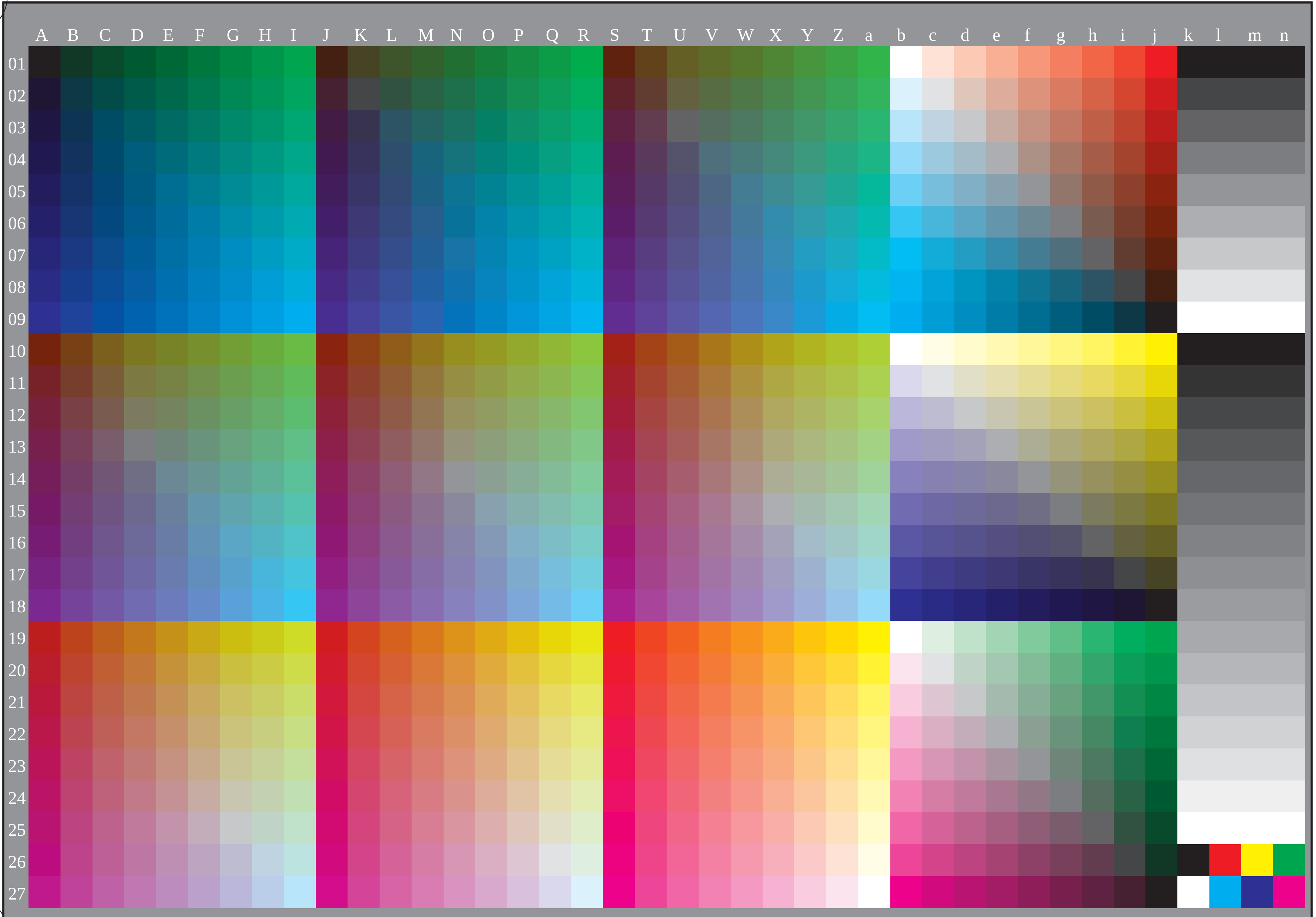


see similar files: http://130.149.60.45/~farbmetrik/PE49/PE49.HTM
technical information: http://www.ps.bam.de or http://130.149.60.45/~farbmetrik

TUB registration: 20130201-PE49/PE49L0NP.PDF /.PS
application for measurement of laser printer output, separationcmyn6 (CMYK)
TUB material: code=rha4ta

1-003130-L0 PE490-70

TUB-test chart PE49; standard test chart
1080 standard colours, 3D=0, de=0, *cmyk*

input: *rgb/cmyk* −> $rgb_d$
output: transfer to $cmyk_d$

1-003130-F0

PE4901P

http://130.149.60.45/~farbmetrik/PE49/PE49L0NP.PDF /.PS; transfer output
N: no 3D-linearization (OL) in file (F) or PS-startup (S), page 2/2

see similar files: http://130.149.60.45/~farbmetrik/PE49/PE49.HTM
technical information: http://www.ps.bam.de or http://130.149.60.45/~farbmetrik

TUB registration: 20130201-PE49/PE49L0NP.PDF /.PS
application for measurement of laser printer output, separationcmyn6 (CMYK)

TUB material: code=rha4ta

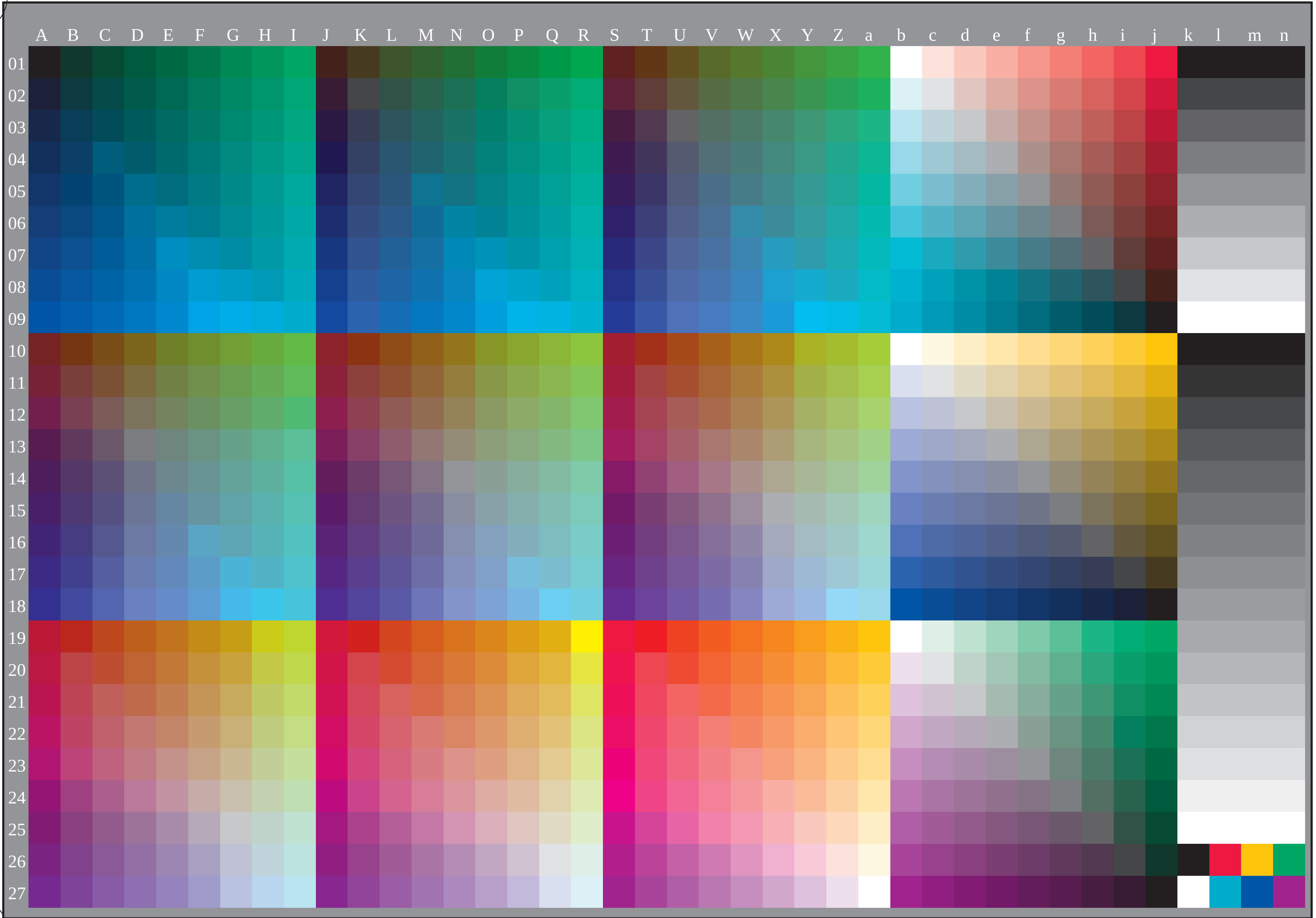

1-013130-L0 PE490-71

TUB-test chart PE49; standard test chart
1080 standard colours, 3D=0, de=1, *cmyk*

input: *rgb/cmyk* −> $rgb_e$
output: transfer to $cmyk_e$

1-013130-F0

http://130.149.60.45/~farbmetrik/PE49/PE49L0FP.PDF /.PS; 3D-linearization
F: 3D-linearization PE49/PE49LE30FP.DAT in file (F), page 2/2

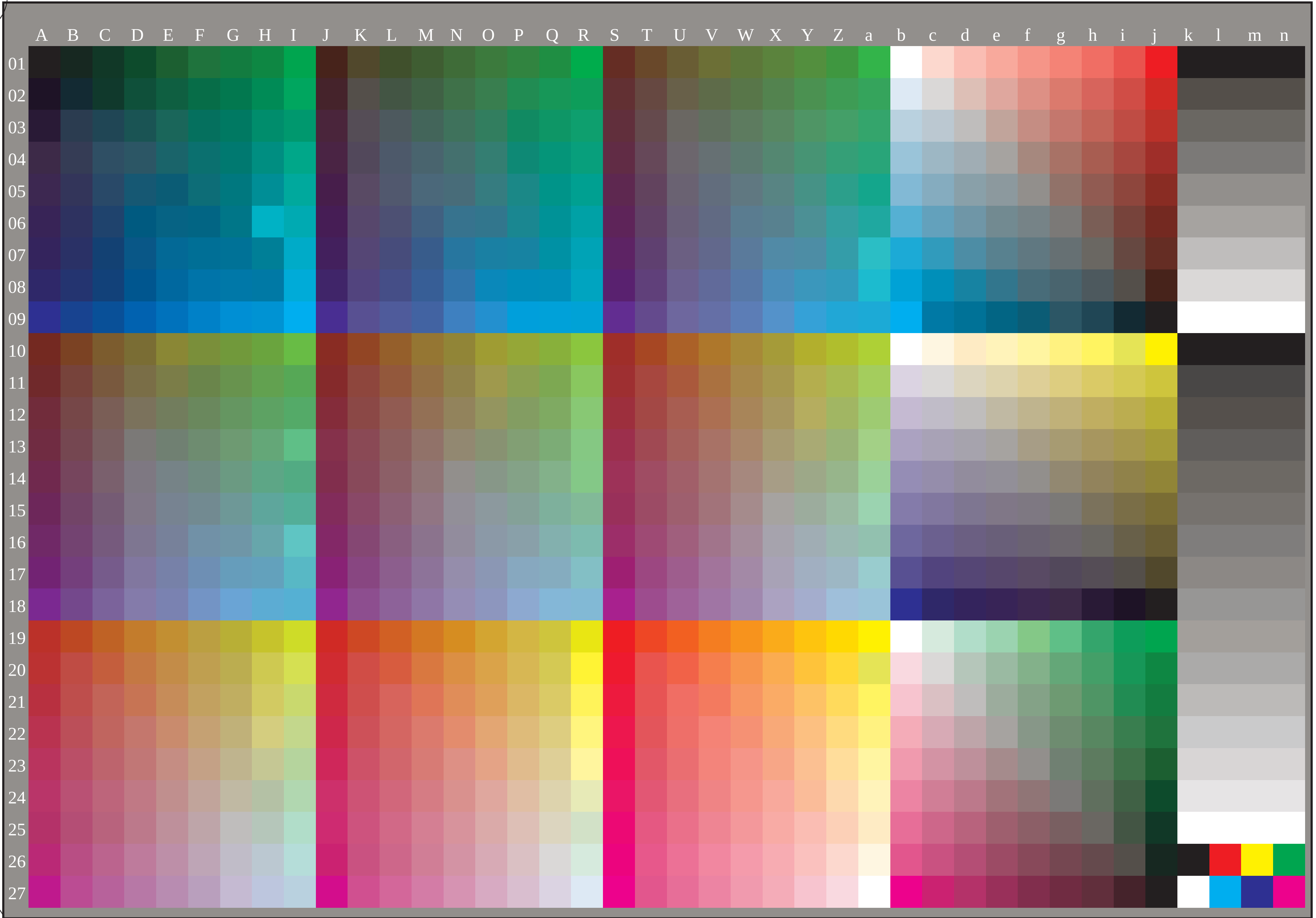


1-103130-L0

PE490-72

TUB-test chart PE49; standard test chart
1080 standard colours, 3D=1, de=0, *cmyk**

input: *rgb/cmyk* −> $rgb_{dd}$
output: 3D-linearization to $cmyk^*_{dd}$

1-103130-F0

see similar files: http://130.149.60.45/~farbmetrik/PE49/PE49.HTM
technical information: http://www.ps.bam.de or http://130.149.60.45/~farbmetrik

TUB registration: 20130201-PE49/PE49L0FP.PDF /.PS
application for measurement of laser printer output, separationcmyn6* (CMYK)

TUB material: code=rha4ta

PE4911P

http://130.149.60.45/~farbmetrik/PE49/PE49L0FP.PDF /.PS; 3D-linearization
F: 3D-linearization PE49/PE49LE30FP.DAT in file (F), page 2/2

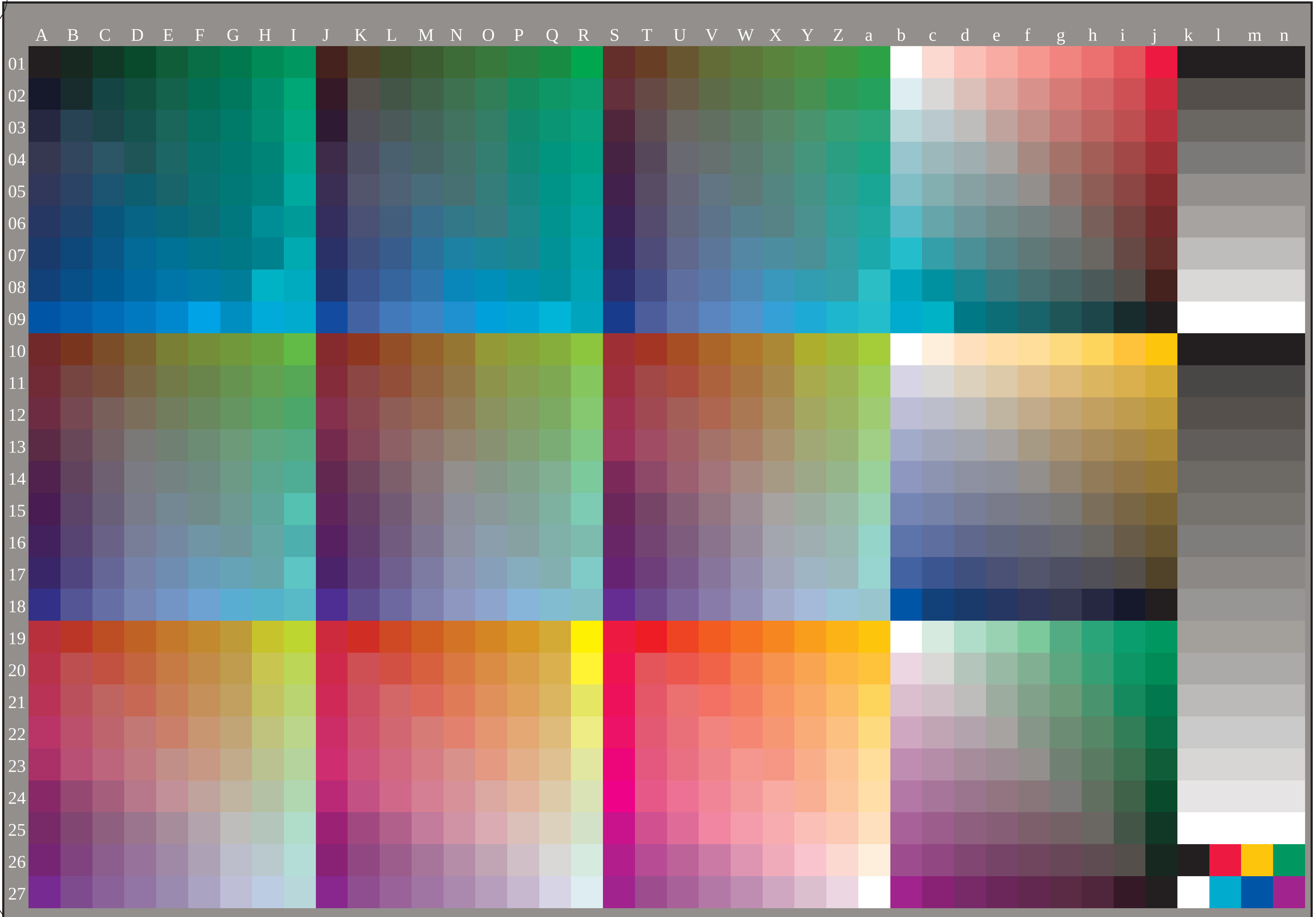


see similar files: http://130.149.60.45/~farbmetrik/PE49/PE49.HTM
technical information: http://www.ps.bam.de or http://130.149.60.45/~farbmetrik

TUB registration: 20130201-PE49/PE49L0FP.PDF /.PS
application for measurement of laser printer output, separationcmyn6* (CMYK)
TUB material: code=rha4ta

1-113130-L0 PE490-73

TUB-test chart PE49; standard test chart
1080 standard colours, 3D=1, de=1, *cmyk**

input: *rgb/cmyk* −> $rgb_{de}$
output: 3D-linearization to $cmyk^*_{de}$

1-113130-F0

http://130.149.60.45/~farbmetrik/TE79/TE79L0FP.PDF /.PS; 3D-linearization
F: 3D-linearization TE79/TE79LE30FP.DAT in file (F), page 2/2

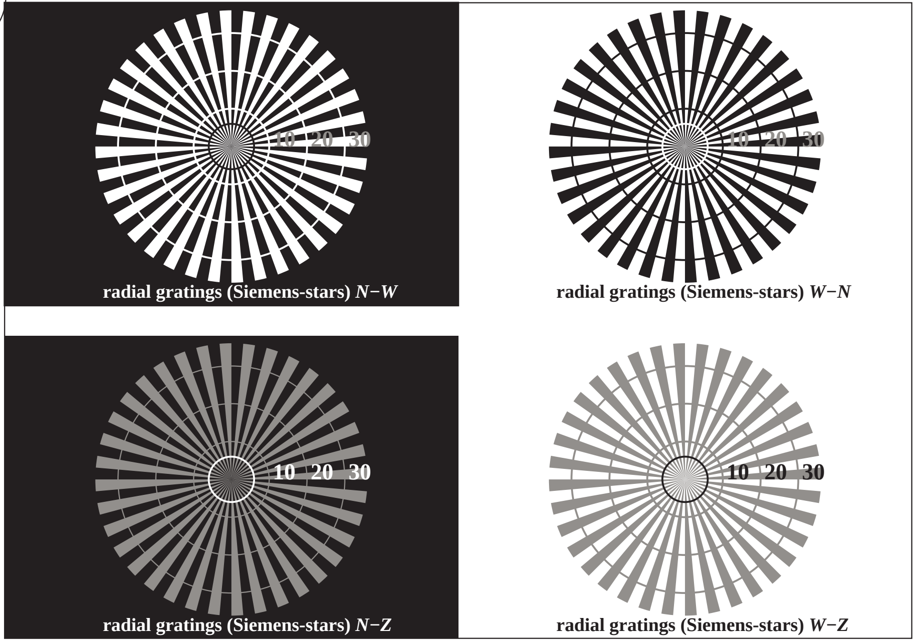


TE790−3, Picture C1Wde: Element A: radial gratings *N−W*, *W−N*, *N−Z* and *W−Z*; PS operator: *rgb/cmy0*

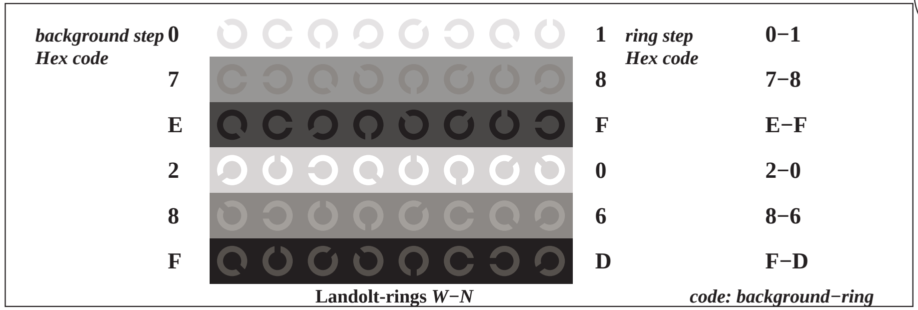


TE791−1, Picture C4Wde: Element D: Landolt-rings *W-N*; PS operator: *rgb/cmy0*

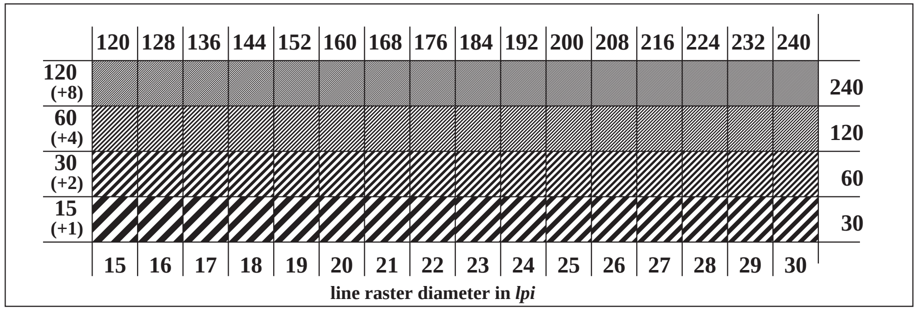


TE791−3, Picture C5Wde: Element E: Line raster under 45° (or 135°); PS operator: *rgb/cmy0*

| $L^*/Y_{intended}$ (absolute) | 18.0/18.0 | 37.3/37.3 | 56.7/56.7 | 76.1/76.0 | 95.4/95.4 | $N_0$ (min.) | $W_1$ (max.) |
|---|---|---|---|---|---|---|---|
| $w^*=l^*_{CIELAB,\,r}$ (relative) $w^*_{input}$ $w^*_{output}$ | 0,000 | 0,250 | 0,500 | 0,750 | 1,000 | $N_0$ (min.) | $W_1$ (max.) |

TE790−5, Picture C2Wde: Element B: 5 visual equidistant *L**-grey steps + *N0* + *W1*; PS operator: *rgb/cmy0*

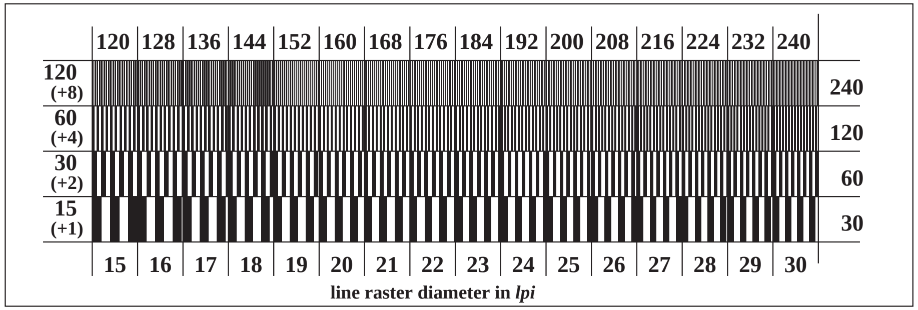


TE791−5, Picture C6Wde: Element F: Line raster under 90° (or 0°); PS operator: *rgb/cmy0*

| $L^*/Y_{intended}$ (absolute) | 18.0/18.0 | 23.2/23.2 | 28.3/28.3 | 33.5/33.5 | 38.6/38.6 | 43.8/43.8 | 49.0/49.0 | 54.1/54.1 | 59.3/59.3 | 64.4/64.4 | 69.6/69.6 | 74.8/74.8 | 79.9/79.9 | 85.1/85.1 | 90.2/90.2 | 95.4/95.4 |
|---|---|---|---|---|---|---|---|---|---|---|---|---|---|---|---|---|
| No. and Hex code | 00;F | 01;E | 02;D | 03;C | 04;B | 05;A | 06;9 | 07;8 | 08;7 | 09;6 | 10;5 | 11;4 | 12;3 | 13;2 | 14;1 | 15;0 |
| $w^*=l^*_{CIELAB,\,r}$ (relative) $w^*_{input}$ $w^*_{output}$ | 0,000 | 0,067 | 0,133 | 0,200 | 0,267 | 0,333 | 0,400 | 0,467 | 0,533 | 0,600 | 0,667 | 0,733 | 0,800 | 0,867 | 0,933 | 1,000 |

TE790−7, Picture C3Wde: Element C: 16 visual equidistant *L**-grey steps; PS operator: *rgb/cmy0*

test chart TE79; ME16(ISO 9241−306), 3(ISO/IEC 15775) input: *w/rgb/cmyk −> rgb*$_{de}$
achromatic test chart *N*, 3D=1, de=1, *cmyk** output: 3D-linearization to *cmyk**$_{de}$

see similar files: http://130.149.60.45/~farbmetrik/TE79/TE79.HTM
technical information: http://www.ps.bam.de or http://130.149.60.45/~farbmetrik

TUB registration: 20130201-TE79/TE79L0FP.PDF /.PS
application for measurement of laser printer output, separationcmyn6* (CMYK)
TUB material: code=rha4ta

http://130.149.60.45/~farbmetrik/TE89/TE89L0FP.PDF /.PS; 3D-linearization
F: 3D-linearization TE89/TE89LE30FP.DAT in file (F), page 2/2

see similar files: http://130.149.60.45/~farbmetrik/TE89/TE89.HTM
technical information: http://www.ps.bam.de or http://130.149.60.45/~farbmetrik


TE890−3, Picture D1Wde: Flower motif, 14 CIE-test colours and 2 + 16 grey steps (sf); ; *PS* operator *4 colorimage*

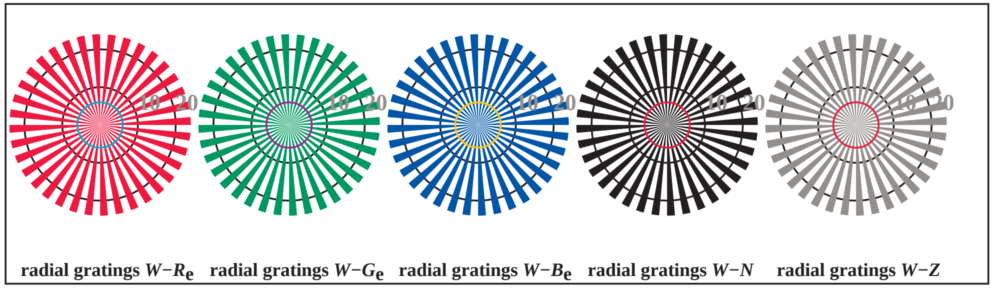

TE890−5, Picture D2Wde: radial gratings *W−R*e; *W−G*e; *W−B*e; *W−N*; *PS* operator *rgb−>rgb*de *setrgbcolor*

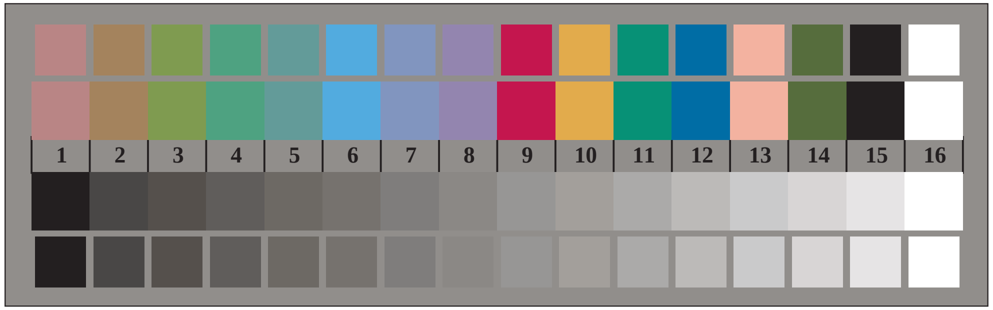
TE890−7, Picture D3Wde: 14 CIE-test colours and 2 + 16 grey steps (sf); *rgb/cmy0−>rgb*de *setrgbcolor*

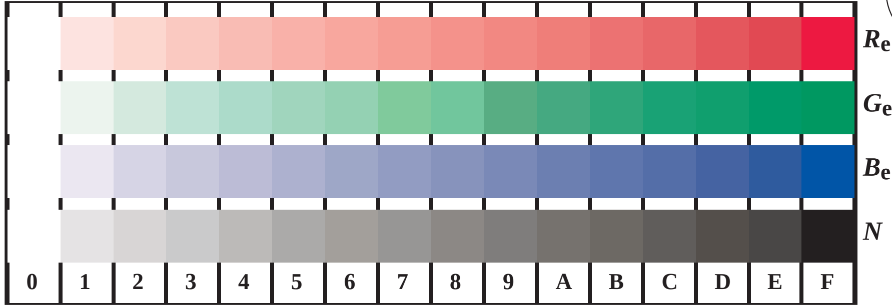

TE891−1, Picture D4Wde: 16 equidistant steps *W−R*e; *W−G*e; *W−B*e; *W−N*; *rgb/cmy0−>rgb*de *setrgbcolor*

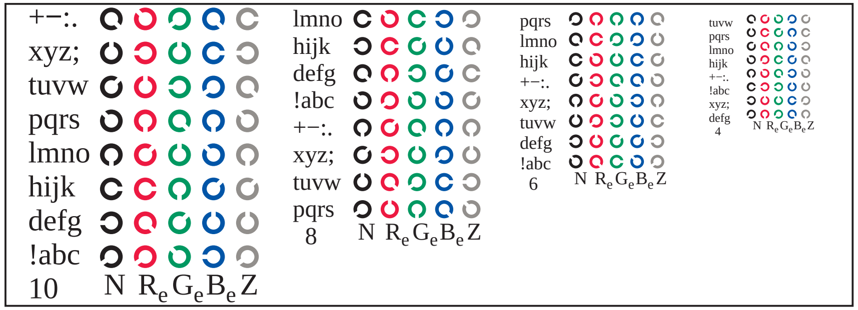

TE891−3, Picture D5Wde: Sript and Landolt-rings *N*; *R*e; *G*e; *B*e; *Z*; *PS* operator *rgb−>rgb*de *setrgbcolor*

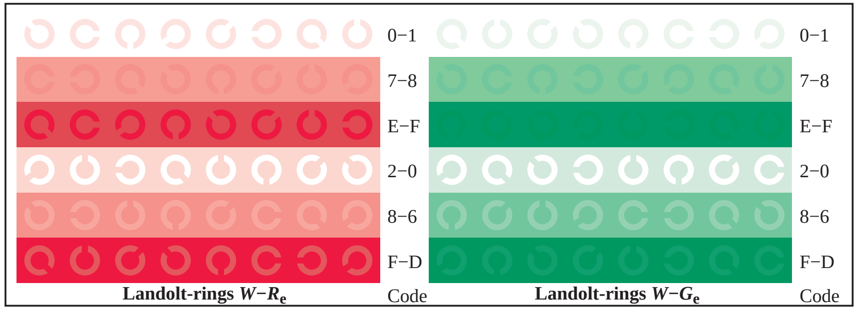

TE891−5, Picture D6Wde: Landolt-rings *W−R*e; *W−G*e; *PS* operator *rgb−>rgb*de *setrgbcolor*

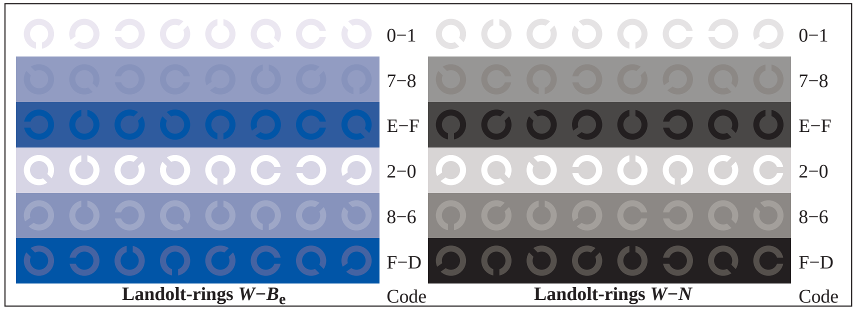

TE891−7, Picture D7Wde: Landolt-rings *W−B*e; *W−N*; *PS* operator *rgb−>rgb*de *setrgbcolor*

TUB registration: 20130201-TE89/TE89L0FP.PDF /.PS
application for measurement of laser printer output, separationcmyn6* (CMYK)

TUB material: code=rha4ta

test chart TE89; 4(ISO/IEC 15775 + ISO/IEC TR 24705)
chromatic test chart *RGB*

input: *rgb/cmyk −> rgb*de
output: 3D-linearization to *cmyk**de

http://130.149.60.45/~farbmetrik/PE46/PE46L0NP.PDF /.PS; start output
N: no 3D-linearization (OL) in file (F) or PS-startup (S), page 1/2

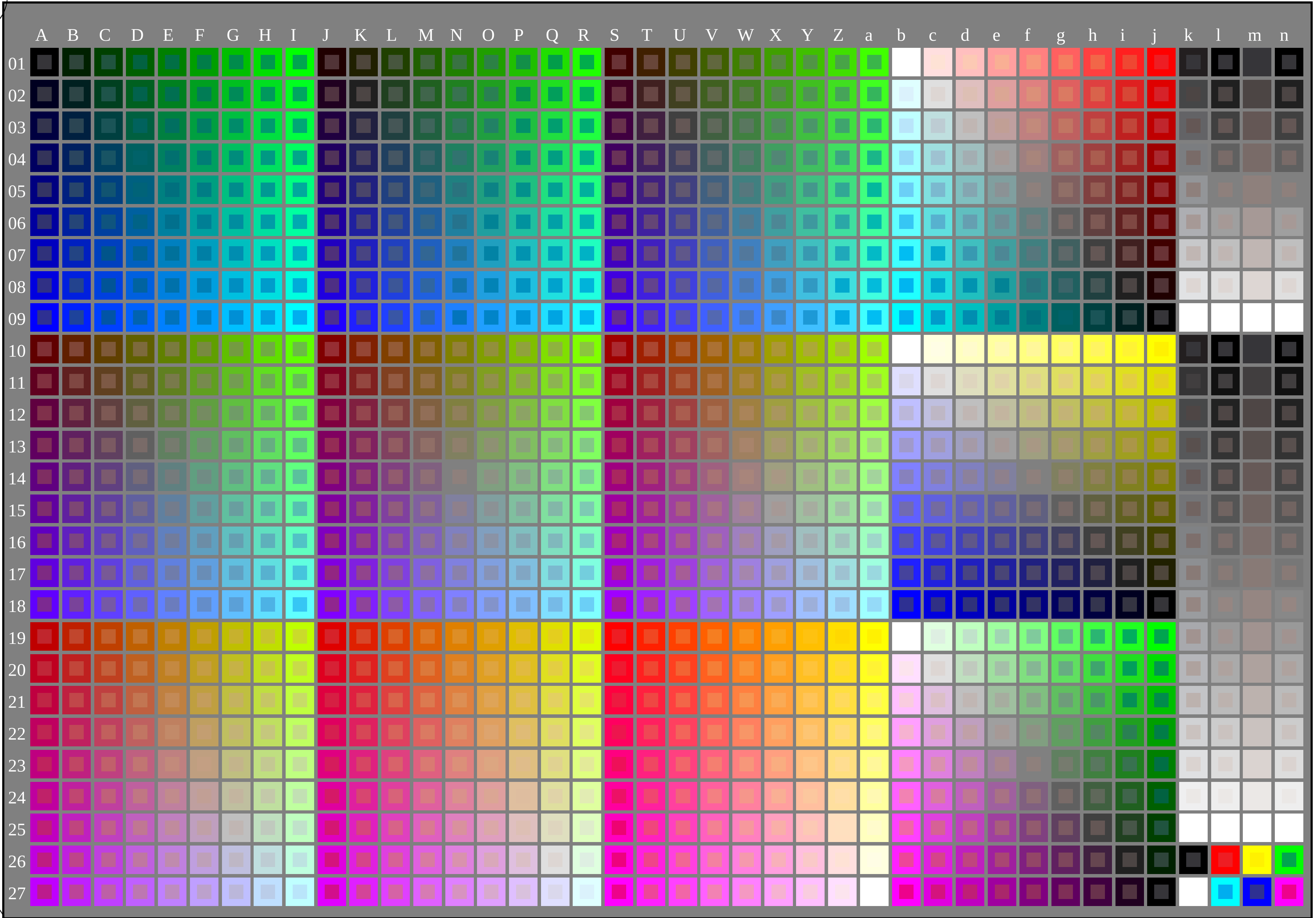


see similar files: http://130.149.60.45/~farbmetrik/PE46/PE46.HTM
technical information: http://www.ps.bam.de or http://130.149.60.45/~farbmetrik

TUB registration: 20130201-PE46/PE46L0NP.PDF /.PS
application for measurement of offset print output

TUB material: code=rha4ta

1−003031−L0 PE460−7N Test chart G with 1080 colours; 9 or 16 step colour scales; data in column (A−n): **rgb (A_j+k26_n27), 000n (k), w (l), nnn0 (m), www (n) + cmy0(all)**

TUB-test chart PE46; standard test chart
1080 standard colours; image technology

input: *rgb/cmyk −> rgb/cmyk*
output: no change

PE4600P

http://130.149.60.45/~farbmetrik/PE46/PE46L0NP.PDF /.PS; transfer output
N: no 3D-linearization (OL) in file (F) or PS-startup (S), page 2/2

see similar files: http://130.149.60.45/~farbmetrik/PE46/PE46.HTM
technical information: http://www.ps.bam.de or http://130.149.60.45/~farbmetrik

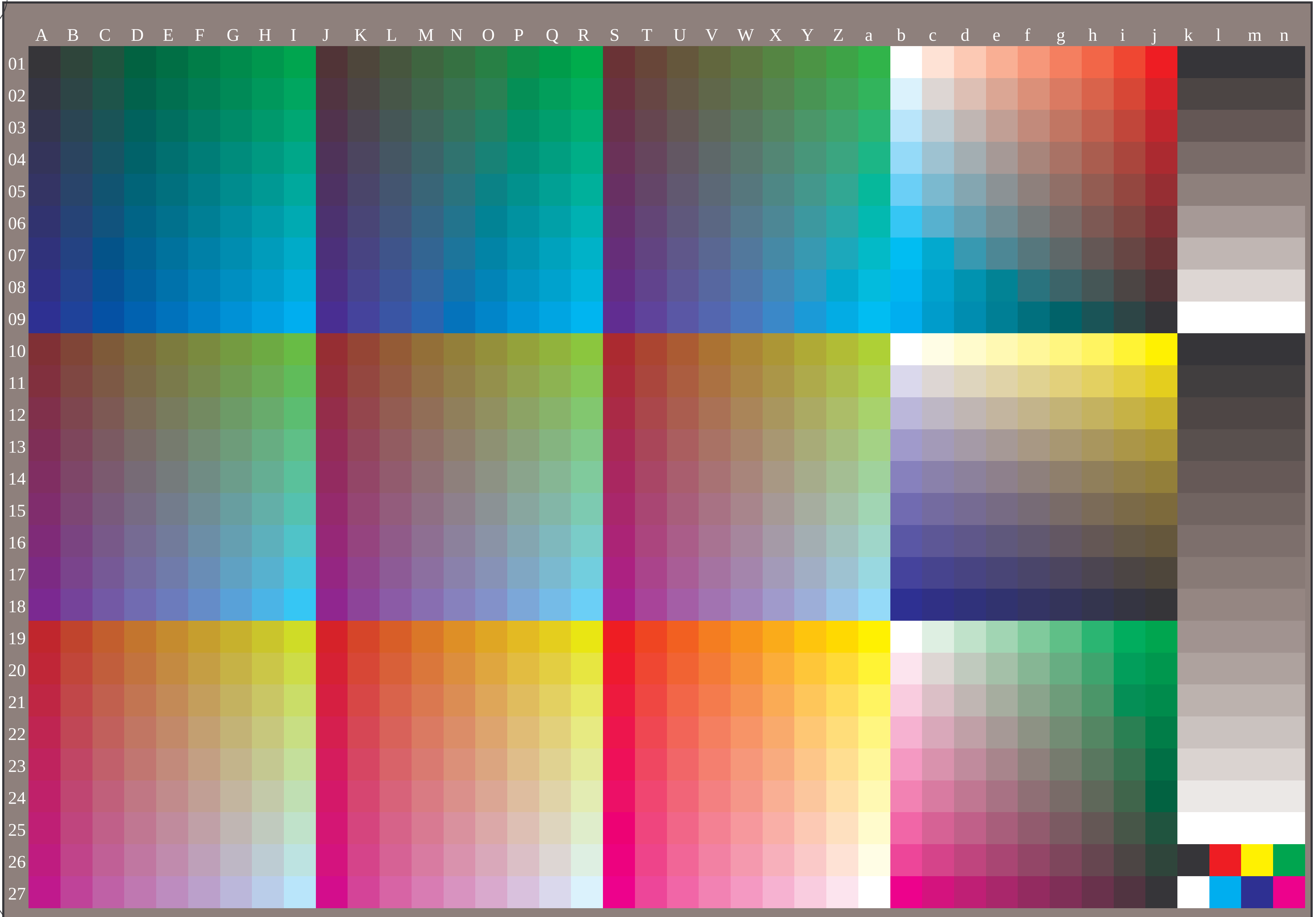


TUB registration: 20130201-PE46/PE46L0NP.PDF /.PS
application for measurement of offset print output, separationcmy0 (CMY0)

TUB material: code=rha4ta

1-003131-L0 PE460-70

TUB-test chart PE46; standard test chart
1080 standard colours, 3D=0, de=0, *cmy0*

input: *rgb/cmyk* −> *rgb*$_d$
output: transfer to *cmy0*$_d$

1-003131-F0

PE4601P

http://130.149.60.45/~farbmetrik/PE46/PE46L0NP.PDF /.PS; transfer output
N: no 3D-linearization (OL) in file (F) or PS-startup (S), page 2/2

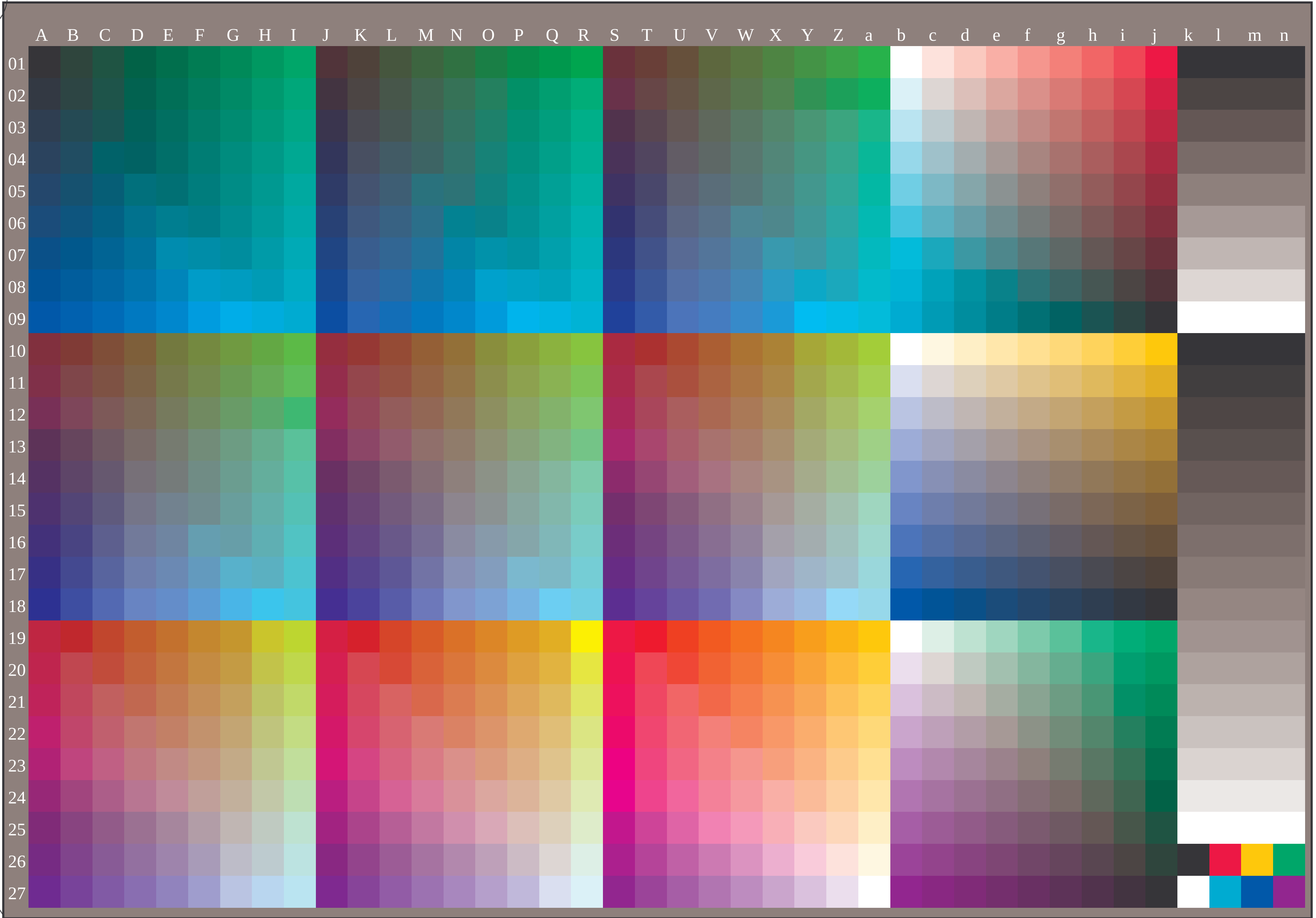

see similar files: http://130.149.60.45/~farbmetrik/PE46/PE46.HTM
technical information: http://www.ps.bam.de or http://130.149.60.45/~farbmetrik

TUB registration: 20130201-PE46/PE46L0NP.PDF /.PS
application for measurement of offset print output, separationcmy0 (CMY0)

TUB material: code=rha4ta

1-013131-L0 PE460-71

TUB-test chart PE46; standard test chart
1080 standard colours, 3D=0, de=1, *cmy0*

input: *rgb/cmyk* −> *rgb*$_e$
output: transfer to *cmy0*$_e$

1-013131-F0

PE4610P

http://130.149.60.45/~farbmetrik/PE46/PE46L0FP.PDF /.PS; 3D-linearization
F: 3D-linearization PE46/PE46LE30FP.DAT in file (F), page 2/2

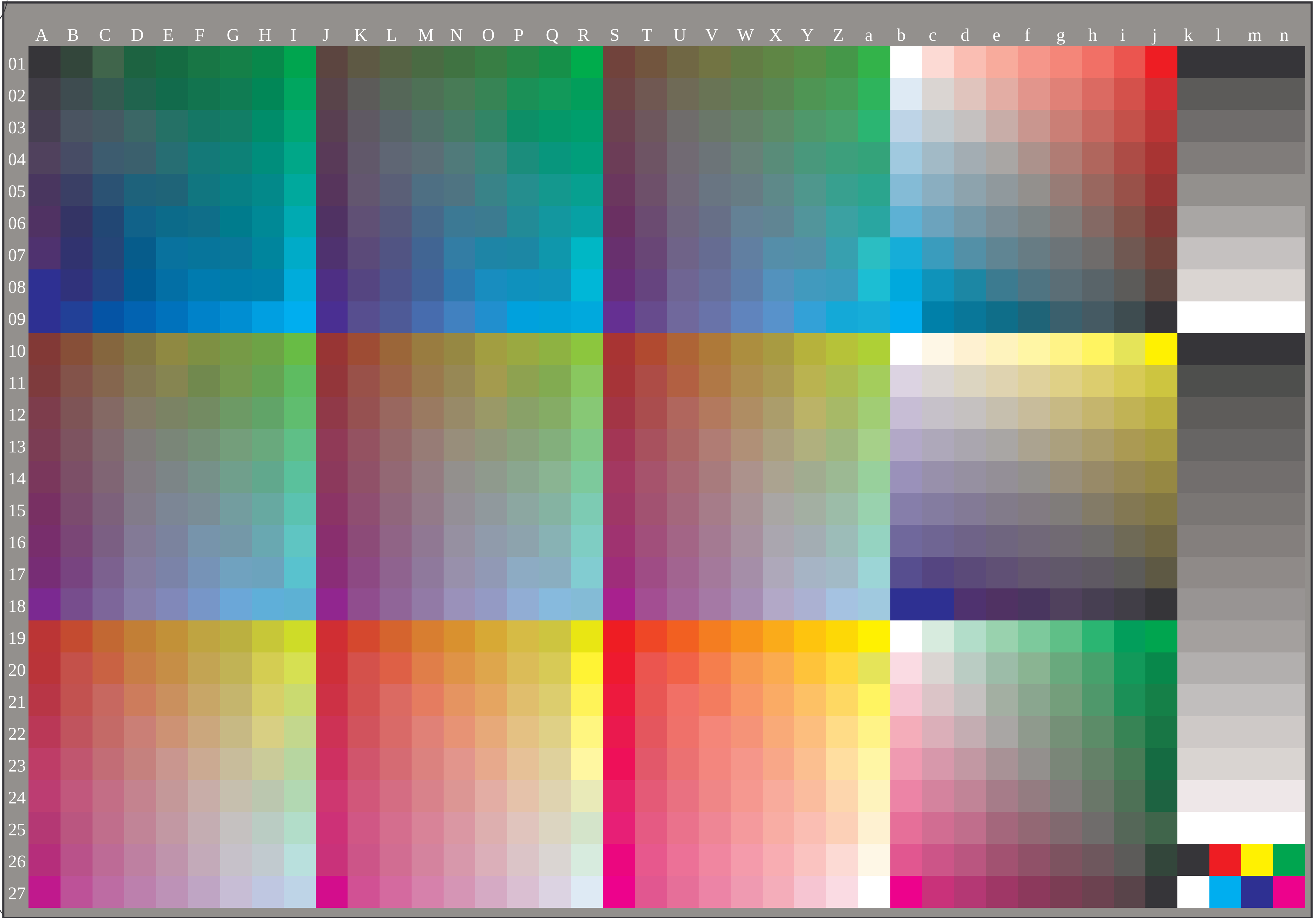


see similar files: http://130.149.60.45/~farbmetrik/PE46/PE46.HTM
technical information: http://www.ps.bam.de or http://130.149.60.45/~farbmetrik

TUB registration: 20130201-PE46/PE46L0FP.PDF /.PS
application for measurement of offset print output, separationcmy0* (CMY0)

TUB material: code=rha4ta

1-103131-L0 PE460-72

TUB-test chart PE46; standard test chart
1080 standard colours, 3D=1, de=0, *cmy0**

input: *rgb/cmyk* −> $rgb_{dd}$
output: 3D-linearization to $cmy0*_{dd}$

1-103131-F0

http://130.149.60.45/~farbmetrik/PE46/PE46L0FP.PDF /.PS; 3D-linearization
F: 3D-linearization PE46/PE46LE30FP.DAT in file (F), page 2/2

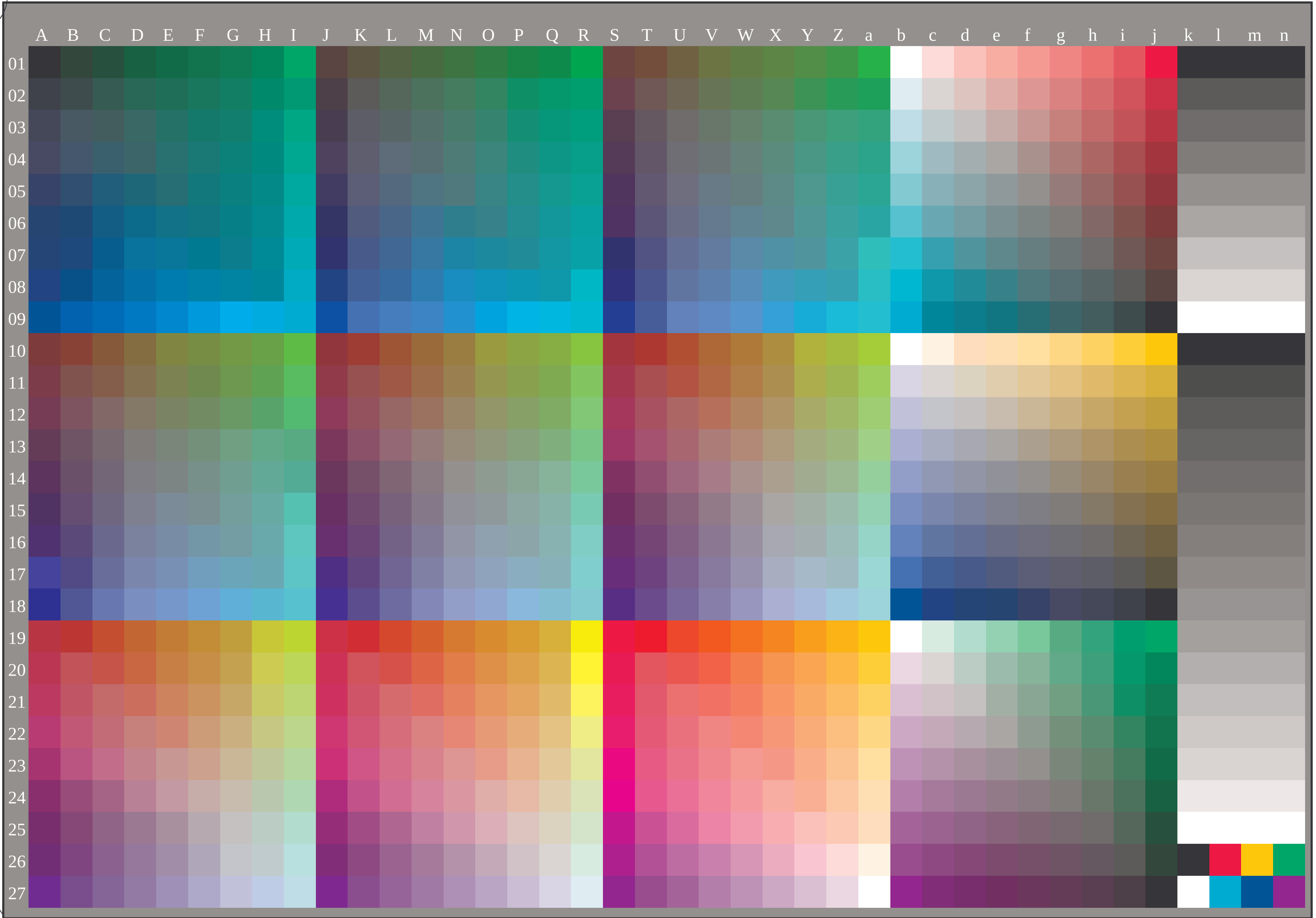


see similar files: http://130.149.60.45/~farbmetrik/PE46/PE46.HTM
technical information: http://www.ps.bam.de or http://130.149.60.45/~farbmetrik

TUB registration: 20130201-PE46/PE46L0FP.PDF /.PS
application for measurement of offset print output, separationcmy0* (CMY0)

TUB material: code=rha4ta

1-113131-L0 PE460−73

TUB-test chart PE46; standard test chart
1080 standard colours, 3D=1, de=1, *cmy0**

input: *rgb/cmyk* −> $rgb_{de}$
output: 3D-linearization to $cmy0*_{de}$

1-113131-F0

PE2911L

http://130.149.60.45/~farbmetrik/PE29/PE29L0FP.PDF /.PS; 3D-linearization
F: 3D-linearization PE29/PE29LE30FP.DAT in file (F), page 2/2

## Test chart 2 for color rendering: metameric colours D65 and D50; laser printer *(CMYK); rgb−>rgb*de

**Series: metameric m D65**

01: R00Y_075_050*e, 02: R50Y_075_050*e, 03: Y00G_075_050*e, 04: Y50G_075_050*e, 05: G00B_075_050*e, 06: G50B_075_050*e, 07: B00R_075_050*e, 08: B50R_075_050*e, 09=10: R00Y_075_050*e

**central z D65/D50**

10: R00Y_075_050*e, 11: R50Y_075_050*e, 12: Y00G_075_050*e, 13: Y50G_075_050*e, 14: G00B_075_050*e, 15: G50B_075_050*e, 16: B00R_075_050*e, 17: B50R_075_050*e, 18=01: R00Y_075_050*e

**metameric m D50**

19: R00Y_075_050*e, 20: R50Y_075_050*e, 21: Y00G_075_050*e, 22: Y50G_075_050*e, 23: G00B_075_050*e, 24: G50B_075_050*e, 25: B00R_075_050*e, 26: B50R_075_050*e, 27=19: R00Y_075_050*e

**metameric m D65**

28: NW_000*e, 29: NW_013*e, 30: NW_025*e, 31: NW_038*e, 32: NW_050*e, 33: NW_063*e, 34: NW_075*e, 35: NW_088*e, 36=28: NW_100*e

*Lab*N0*=17.7, 0.6, 0.6
*Lab*W0*=95.4, 1.3, −4.9
*Lab*N*=24.3, −5.6, −6.8
*Lab*W*=95.6, 1.4, −5.0

**grey g D65/D50**

37: NW_000*e, 38: NW_013*e, 39: NW_025*e, 40: NW_038*e, 41: NW_050*e, 42: NW_063*e, 43: NW_075*e, 44: NW_088*e, 45=37: NW_100*e

*Lab*N0*=17.7, 0.6, 0.6
*Lab*W0*=95.4, 1.3, −4.9
*Lab*N1*=17.7, 0.8, 0.6
*Lab*W1*=95.4, 0.8, −4.9

**metameric m D50**

46: NW_000*e, 47: NW_013*e, 48: NW_025*e, 49: NW_038*e, 50: NW_050*e, 51: NW_063*e, 52: NW_075*e, 53: NW_088*e, 54: NW_100*e

*Lab*N1*=17.7, 0.8, 0.6
*Lab*W1*=95.4, 0.8, −4.9
*Lab*N*=24.0, −5.6, −7.3
*Lab*W*=95.5, 0.9, −5.0

see similar files: http://130.149.60.45/~farbmetrik/PE29/PE29.HTM
technical information: http://www.ps.bam.de or http://130.149.60.45/~farbmetrik

TUB registration: 20130201-PE29/PE29L0FP.PDF /.PS
application for measurement of laser printer output, separationcmyn6* (CMYK)

TUB material: code=rha4ta

1−113130−L0 PE290−73

TUB-test chart PE29; colour rendering
54 colours; metameric for D65&D50, 3D=1, de=1, *cmyk**

input: *rgb/cmyk −> rgb*de
output: 3D-linearization to *cmyk**de

1−113130−F0

# Test chart 3 for color rendering: metameric colours A and P4000; laser printer *(CMYK); rgb−>rgb*de

| | | | | | | | | | |
|---|---|---|---|---|---|---|---|---|---|
| 01: R00Y_075_050*e | 02: R50Y_075_050*e | 03: Y00G_075_050*e | 04: Y50G_075_050*e | 05: G00B_075_050*e | 06: G50B_075_050*e | 07: B00R_075_050*e | 08: B50R_075_050*e | 09=10: R00Y_075_050*e | Series: metameric m A |
| 10: R00Y_075_050*e | 11: R50Y_075_050*e | 12: Y00G_075_050*e | 13: Y50G_075_050*e | 14: G00B_075_050*e | 15: G50B_075_050*e | 16: B00R_075_050*e | 17: B50R_075_050*e | 18=01: R00Y_075_050*e | central z A/P4000 |
| 19: R00Y_075_050*e | 20: R50Y_075_050*e | 21: Y00G_075_050*e | 22: Y50G_075_050*e | 23: G00B_075_050*e | 24: G50B_075_050*e | 25: B00R_075_050*e | 26: B50R_075_050*e | 27=19: R00Y_075_050*e | metameric m P4000 |
| 28: NW_000*e | 29: NW_013*e | 30: NW_025*e | 31: NW_038*e | 32: NW_050*e | 33: NW_063*e | 34: NW_075*e | 35: NW_088*e | 36=28: NW_100*e | metameric m A<br>*Lab*N0*=17.8, 1.3, 0.7<br>*Lab*W0*=95.3, 0.3, −4.9<br>*Lab*N*=23.1, −3.5, −9.1<br>*Lab*W*=95.4, 0.3, −5.0 |
| 37: NW_000*e | 38: NW_013*e | 39: NW_025*e | 40: NW_038*e | 41: NW_050*e | 42: NW_063*e | 43: NW_075*e | 44: NW_088*e | 45=37: NW_100*e | grey g A/P4000<br>*Lab*N0*=17.8, 1.3, 0.7<br>*Lab*W0*=95.3, 0.3, −4.9<br>*Lab*N1*=17.7, 1.0, 0.7<br>*Lab*W1*=95.3, 0.6, −5.0 |
| 46: NW_000*e | 47: NW_013*e | 48: NW_025*e | 49: NW_038*e | 50: NW_050*e | 51: NW_063*e | 52: NW_075*e | 53: NW_088*e | 54: NW_100*e | metameric m P4000<br>*Lab*N1*=17.7, 1.0, 0.7<br>*Lab*W1*=95.3, 0.6, −5.0<br>*Lab*N*=23.7, −5.0, −8.0<br>*Lab*W*=95.5, 0.6, −5.1 |

see similar files: http://130.149.60.45/~farbmetrik/PE39/PE39.HTM
technical information: http://www.ps.bam.de or http://130.149.60.45/~farbmetrik

TUB registration: 20130201-PE39/PE39L0FP.PDF /.PS
application for measurement of laser printer output, separationcmyn6* (CMYK)
TUB material: code=rha4ta

TUB registration: 20130201-PE99/PE99L0NP.PDF /.PS
application for measurement of laser printer output, separationcmyn6 (CMYK)

TUB material: code=rha4ta

**Data of Maximum color M in colorimetric system Laser printer output; separation cmyn6*, D65 for input or output; Six hue angles of the 60 degree standard colours *RYGCBM*$_s$: $h_{ab,ds}$ = 30.0, 90.0, 150.0, 210.0, 270.0, 330.0; Six hue angles of the device colours *RYGCBM*$_d$: $h_{ab,d}$ = 33.5, 100.6, 155.5, 235.2, 290.8, 348.9; Six hue angles of the elementary colours *RYGCBM*$_e$: $h_{ab,e}$ = 25.5, 92.3, 162.2, 217.0, 271.7, 328.6**

| $h_{ab,d}$ | $h_{ab,s}$ | $h_{ab,e}$ | *rgb**dd64M | | | *LAB**ddx64M (x=LabCh) | | | | | *rgb**ddx361M | | | *LAB**ddx361M (x=LabCh) | | | | | *rgb**dsx361M | | | *LAB**dsx361M (x=LabCh) | | | | | *rgb**dex361M | | | *LAB**dex361M | | | | |
|---|---|---|---|---|---|---|---|---|---|---|---|---|---|---|---|---|---|---|---|---|---|---|---|---|---|---|---|---|---|---|---|---|---|---|
| 33.4 | 30.0 | 25.4 | 1.0 | 0.0 | 0.0 | 47.5 | 57.2 | 37.8 | 68.6 | 33.4 | 1.0 | 0.0 | 0.0 | 47.6 | 57.2 | 37.9 | 68.6 | 33 | 1.0 | 0.0 | 0.158 | 47.7 | 56.3 | 32.5 | 65.0 | 30 | 1.0 | 0.0 | 0.263 | 47.6 | 56.1 | 26.7 | 62.1 | 25 |
| 42.1 | 37.5 | 33.8 | 1.0 | 0.125 | 0.0 | 51.9 | 54.3 | 49.2 | 73.2 | 42.1 | 1.0 | 0.117 | 0.0 | 51.7 | 54.6 | 48.5 | 73.0 | 41 | 1.0 | 0.05 | 0.0 | 49.4 | 56.3 | 42.4 | 70.5 | 37 | 1.0 | 0.0 | 0.012 | 47.6 | 57.2 | 37.5 | 68.4 | 33 |
| 52.8 | 45.0 | 42.1 | 1.0 | 0.25 | 0.0 | 58.2 | 41.8 | 55.1 | 69.2 | 52.8 | 1.0 | 0.25 | 0.0 | 58.3 | 41.8 | 55.2 | 69.2 | 52 | 1.0 | 0.158 | 0.0 | 53.6 | 51.1 | 51.1 | 72.2 | 45 | 1.0 | 0.125 | 0.0 | 52.0 | 54.3 | 49.2 | 73.3 | 42 |
| 63.7 | 52.5 | 50.5 | 1.0 | 0.375 | 0.0 | 64.6 | 29.8 | 60.4 | 67.3 | 63.7 | 1.0 | 0.367 | 0.0 | 64.2 | 30.6 | 60.1 | 67.5 | 63 | 1.0 | 0.24 | 0.0 | 57.8 | 42.8 | 54.8 | 69.6 | 52 | 1.0 | 0.216 | 0.0 | 56.6 | 45.2 | 53.9 | 70.3 | 49 |
| 73.8 | 60.0 | 58.8 | 1.0 | 0.5 | 0.0 | 70.5 | 19.2 | 66.2 | 69.0 | 73.8 | 1.0 | 0.5 | 0.0 | 70.5 | 19.2 | 66.3 | 69.0 | 73 | 1.0 | 0.332 | 0.0 | 62.5 | 34.0 | 58.9 | 68.0 | 60 | 1.0 | 0.32 | 0.0 | 61.8 | 35.2 | 58.4 | 68.2 | 58 |
| 80.7 | 67.5 | 67.2 | 1.0 | 0.625 | 0.0 | 74.9 | 11.4 | 70.7 | 71.6 | 80.7 | 1.0 | 0.617 | 0.0 | 74.6 | 12.0 | 70.5 | 71.5 | 80 | 1.0 | 0.416 | 0.0 | 66.6 | 26.5 | 62.5 | 67.9 | 67 | 1.0 | 0.412 | 0.0 | 66.4 | 26.9 | 62.3 | 67.9 | 66 |
| 91.5 | 75.0 | 75.6 | 1.0 | 0.75 | 0.0 | 82.9 | −2.0 | 76.9 | 77.0 | 91.5 | 1.0 | 0.75 | 0.0 | 83.0 | −1.9 | 77.0 | 77.0 | −268 | 1.0 | 0.521 | 0.0 | 71.3 | 18.0 | 67.1 | 69.5 | 75 | 1.0 | 0.532 | 0.0 | 71.6 | 17.3 | 67.5 | 69.7 | 75 |
| 96.8 | 82.5 | 83.9 | 1.0 | 0.875 | 0.0 | 87.6 | −9.0 | 75.7 | 76.3 | 96.8 | 1.0 | 0.867 | 0.0 | 87.3 | −8.5 | 75.9 | 76.4 | 96 | 1.0 | 0.639 | 0.0 | 75.8 | 10.1 | 71.6 | 72.3 | 82 | 1.0 | 0.655 | 0.0 | 76.9 | 8.4 | 72.5 | 73.0 | 83 |
| 100.5 | 90.0 | 92.3 | 1.0 | 1.0 | 0.0 | 91.5 | −15.8 | 84.6 | 86.1 | 100.5 | 1.0 | 1.0 | 0.0 | 91.6 | −15.7 | 84.7 | 86.2 | 100 | 1.0 | 0.732 | 0.0 | 81.8 | 0.0 | 76.3 | 76.3 | 90 | 1.0 | 0.769 | 0.0 | 83.7 | −3.0 | 76.8 | 76.9 | 92 |
| 101.4 | 97.5 | 101.0 | 0.875 | 1.0 | 0.0 | 92.8 | −18.1 | 89.4 | 91.2 | 101.4 | 0.883 | 1.0 | 0.0 | 92.7 | −17.9 | 89.1 | 90.9 | 101 | 1.0 | 0.88 | 0.0 | 87.8 | −9.3 | 76.2 | 76.7 | 97 | 1.0 | 0.996 | 0.0 | 91.5 | −15.5 | 84.4 | 85.8 | 100 |
| 103.9 | 105.0 | 109.7 | 0.75 | 1.0 | 0.0 | 90.1 | −21.3 | 86.0 | 88.6 | 103.9 | 0.75 | 1.0 | 0.0 | 90.1 | −21.3 | 86.0 | 88.7 | 103 | 0.738 | 1.0 | 0.0 | 89.2 | −22.5 | 84.4 | 87.4 | 105 | 0.684 | 1.0 | 0.0 | 84.7 | −27.5 | 76.7 | 81.5 | 109 |
| 115.0 | 112.5 | 118.5 | 0.625 | 1.0 | 0.0 | 79.9 | −31.7 | 67.9 | 75.0 | 115.0 | 0.633 | 1.0 | 0.0 | 80.6 | −31.1 | 69.2 | 75.9 | 114 | 0.659 | 1.0 | 0.0 | 82.7 | −29.4 | 73.0 | 78.8 | 112 | 0.595 | 1.0 | 0.0 | 77.8 | −34.4 | 65.0 | 73.6 | 117 |
| 127.3 | 120.0 | 127.2 | 0.5 | 1.0 | 0.0 | 70.9 | −41.7 | 54.8 | 68.9 | 127.3 | 0.5 | 1.0 | 0.0 | 71.0 | −41.7 | 54.8 | 68.9 | 127 | 0.574 | 1.0 | 0.0 | 76.3 | −36.2 | 62.8 | 72.6 | 120 | 0.501 | 1.0 | 0.0 | 71.0 | −41.6 | 54.9 | 68.9 | 127 |
| 134.7 | 127.5 | 136.0 | 0.375 | 1.0 | 0.0 | 66.5 | −47.5 | 48.0 | 67.6 | 134.7 | 0.383 | 1.0 | 0.0 | 66.9 | −47.1 | 48.5 | 67.7 | 134 | 0.503 | 1.0 | 0.0 | 71.2 | −41.5 | 55.2 | 69.1 | 127 | 0.366 | 1.0 | 0.0 | 66.2 | −48.2 | 47.6 | 67.8 | 135 |
| 144.7 | 135.0 | 144.7 | 0.25 | 1.0 | 0.0 | 60.6 | −57.2 | 40.4 | 70.1 | 144.7 | 0.25 | 1.0 | 0.0 | 60.6 | −57.2 | 40.5 | 70.1 | 144 | 0.372 | 1.0 | 0.0 | 66.4 | −47.8 | 47.9 | 67.7 | 135 | 0.25 | 1.0 | 0.0 | 60.6 | −57.1 | 40.5 | 70.1 | 144 |
| 151.0 | 142.5 | 153.4 | 0.125 | 1.0 | 0.0 | 57.0 | −62.2 | 34.4 | 71.1 | 151.0 | 0.133 | 1.0 | 0.0 | 57.3 | −61.8 | 34.8 | 71.0 | 150 | 0.284 | 1.0 | 0.0 | 62.3 | −54.6 | 42.7 | 69.4 | 142 | 0.073 | 1.0 | 0.0 | 55.9 | −64.4 | 33.0 | 72.5 | 152 |
| 155.5 | 150.0 | 162.2 | 0.0 | 1.0 | 0.0 | 54.3 | −67.6 | 30.8 | 74.3 | 155.5 | 0.0 | 1.0 | 0.0 | 54.3 | −67.6 | 30.8 | 74.4 | 155 | 0.146 | 1.0 | 0.0 | 57.6 | −61.3 | 35.5 | 70.9 | 150 | 0.0 | 1.0 | 0.147 | 53.8 | −65.9 | 21.1 | 69.3 | 162 |
| 160.8 | 157.5 | 169.0 | 0.0 | 1.0 | 0.125 | 53.8 | −66.4 | 23.0 | 70.2 | 160.8 | 0.0 | 1.0 | 0.117 | 53.9 | −66.4 | 23.5 | 70.6 | 160 | 0.0 | 1.0 | 0.035 | 54.2 | −67.3 | 28.6 | 73.2 | 157 | 0.0 | 1.0 | 0.251 | 53.8 | −63.0 | 12.7 | 64.4 | 168 |
| 168.5 | 165.0 | 175.9 | 0.0 | 1.0 | 0.25 | 53.7 | −63.1 | 12.8 | 64.4 | 168.5 | 0.0 | 1.0 | 0.25 | 53.8 | −63.1 | 12.8 | 64.4 | 168 | 0.0 | 1.0 | 0.192 | 53.8 | −64.7 | 17.4 | 67.1 | 165 | 0.0 | 1.0 | 0.331 | 54.4 | −59.3 | 4.2 | 59.5 | 175 |
| 179.9 | 172.5 | 182.7 | 0.0 | 1.0 | 0.375 | 54.7 | −56.8 | 0.0 | 56.8 | 179.9 | 0.0 | 1.0 | 0.367 | 54.7 | −57.2 | 0.8 | 57.3 | 179 | 0.0 | 1.0 | 0.288 | 54.1 | −61.4 | 8.6 | 62.1 | 172 | 0.0 | 1.0 | 0.405 | 54.8 | −55.6 | −2.1 | 55.7 | 182 |
| 189.8 | 180.0 | 189.6 | 0.0 | 1.0 | 0.5 | 55.0 | −51.4 | −8.9 | 52.2 | 189.8 | 0.0 | 1.0 | 0.5 | 55.0 | −51.4 | −8.8 | 52.2 | 189 | 0.0 | 1.0 | 0.375 | 54.8 | −56.7 | 0.0 | 56.8 | 180 | 0.0 | 1.0 | 0.497 | 55.0 | −51.5 | −8.6 | 52.3 | 189 |
| 204.4 | 187.5 | 196.4 | 0.0 | 1.0 | 0.625 | 55.3 | −44.1 | −20.0 | 48.5 | 204.4 | 0.0 | 1.0 | 0.617 | 55.3 | −44.6 | −19.3 | 48.8 | 203 | 0.0 | 1.0 | 0.464 | 55.0 | −53.0 | −6.4 | 53.5 | 187 | 0.0 | 1.0 | 0.553 | 55.2 | −48.6 | −13.9 | 50.7 | 195 |
| 214.4 | 195.0 | 203.2 | 0.0 | 1.0 | 0.75 | 55.2 | −39.5 | −27.1 | 47.9 | 214.4 | 0.0 | 1.0 | 0.75 | 55.2 | −39.4 | −27.0 | 47.9 | 214 | 0.0 | 1.0 | 0.544 | 55.2 | −49.1 | −13.1 | 50.9 | 195 | 0.0 | 1.0 | 0.615 | 55.3 | −44.7 | −19.2 | 48.8 | 203 |
| 221.9 | 202.5 | 210.1 | 0.0 | 1.0 | 0.875 | 54.4 | −36.7 | −33.0 | 49.4 | 221.9 | 0.0 | 1.0 | 0.867 | 54.5 | −36.9 | −32.6 | 49.4 | 221 | 0.0 | 1.0 | 0.604 | 55.3 | −45.5 | −18.3 | 49.1 | 202 | 0.0 | 1.0 | 0.69 | 55.3 | −41.8 | −23.8 | 48.2 | 209 |
| 235.1 | 210.0 | 216.9 | 0.0 | 1.0 | 1.0 | 53.1 | −30.0 | −43.1 | 52.5 | 235.1 | 0.0 | 1.0 | 1.0 | 53.1 | −29.9 | −43.0 | 52.5 | 235 | 0.0 | 1.0 | 0.694 | 55.3 | −41.6 | −24.0 | 48.2 | 210 | 0.0 | 1.0 | 0.792 | 55.0 | −38.6 | −29.0 | 48.4 | 216 |
| 237.9 | 217.5 | 223.8 | 0.0 | 0.875 | 1.0 | 53.1 | −27.9 | −44.7 | 52.7 | 237.9 | 0.0 | 0.883 | 1.0 | 53.1 | −28.0 | −44.5 | 52.8 | 237 | 0.0 | 1.0 | 0.792 | 55.0 | −38.6 | −29.1 | 48.5 | 217 | 0.0 | 1.0 | 0.888 | 54.3 | −36.1 | −34.1 | 49.8 | 223 |
| 241.3 | 225.0 | 230.6 | 0.0 | 0.75 | 1.0 | 52.9 | −25.9 | −47.5 | 54.1 | 241.3 | 0.0 | 0.75 | 1.0 | 52.9 | −25.8 | −47.5 | 54.2 | 241 | 0.0 | 1.0 | 0.904 | 54.2 | −35.4 | −35.4 | 50.2 | 225 | 0.0 | 1.0 | 0.957 | 53.6 | −32.5 | −39.7 | 51.5 | 230 |
| 247.2 | 232.5 | 237.5 | 0.0 | 0.625 | 1.0 | 50.5 | −20.8 | −49.5 | 53.7 | 247.2 | 0.0 | 0.633 | 1.0 | 50.7 | −21.1 | −49.3 | 53.8 | 246 | 0.0 | 1.0 | 0.97 | 53.5 | −31.8 | −40.7 | 51.8 | 232 | 0.0 | 0.916 | 1.0 | 53.1 | −28.6 | −44.1 | 52.7 | 237 |
| 254.9 | 240.0 | 244.3 | 0.0 | 0.5 | 1.0 | 46.1 | −13.3 | −49.4 | 51.1 | 254.9 | 0.0 | 0.5 | 1.0 | 46.2 | −13.2 | −49.3 | 51.2 | 254 | 0.0 | 0.801 | 1.0 | 53.0 | −26.7 | −46.3 | 53.6 | 240 | 0.0 | 0.686 | 1.0 | 51.7 | −23.3 | −48.5 | 54.0 | 244 |
| 262.6 | 247.5 | 251.2 | 0.0 | 0.375 | 1.0 | 41.4 | −6.3 | −49.2 | 49.6 | 262.6 | 0.0 | 0.383 | 1.0 | 41.7 | −6.7 | −49.2 | 49.8 | 262 | 0.0 | 0.63 | 1.0 | 50.7 | −20.9 | −49.4 | 53.8 | 247 | 0.0 | 0.568 | 1.0 | 48.6 | −17.2 | −49.5 | 52.6 | 250 |
| 272.6 | 255.0 | 258.0 | 0.0 | 0.25 | 1.0 | 36.8 | 2.2 | −48.5 | 48.6 | 272.6 | 0.0 | 0.25 | 1.0 | 36.9 | 2.2 | −48.5 | 48.6 | 272 | 0.0 | 0.499 | 1.0 | 46.1 | −13.1 | −49.3 | 51.2 | 255 | 0.0 | 0.449 | 1.0 | 44.2 | −10.4 | −49.4 | 50.6 | 258 |
| 281.4 | 262.5 | 264.8 | 0.0 | 0.125 | 1.0 | 35.0 | 9.4 | −46.3 | 47.3 | 281.4 | 0.0 | 0.133 | 1.0 | 35.2 | 8.9 | −46.5 | 47.4 | 280 | 0.0 | 0.386 | 1.0 | 41.8 | −6.8 | −49.2 | 49.8 | 262 | 0.0 | 0.353 | 1.0 | 40.6 | −4.7 | −49.2 | 49.5 | 264 |
| 290.8 | 270.0 | 271.7 | 0.0 | 0.0 | 1.0 | 32.5 | 16.9 | −44.6 | 47.7 | 290.8 | 0.0 | 0.0 | 1.0 | 32.6 | 16.9 | −44.5 | 47.7 | 290 | 0.0 | 0.283 | 1.0 | 38.1 | 0.0 | −48.8 | 48.9 | 270 | 0.0 | 0.261 | 1.0 | 37.3 | 1.5 | −48.6 | 48.7 | 271 |
| 299.2 | 277.5 | 278.8 | 0.125 | 0.0 | 1.0 | 31.6 | 23.6 | −42.2 | 48.4 | 299.2 | 0.117 | 0.0 | 1.0 | 31.7 | 23.2 | −42.3 | 48.4 | 298 | 0.0 | 0.188 | 1.0 | 36.0 | 5.8 | −47.5 | 48.0 | 277 | 0.0 | 0.169 | 1.0 | 35.7 | 7.0 | −47.2 | 47.8 | 278 |
| 307.8 | 285.0 | 285.9 | 0.25 | 0.0 | 1.0 | 31.0 | 30.5 | −39.3 | 49.8 | 307.8 | 0.25 | 0.0 | 1.0 | 31.0 | 30.6 | −39.3 | 49.9 | 307 | 0.0 | 0.078 | 1.0 | 34.1 | 12.3 | −45.8 | 47.5 | 285 | 0.0 | 0.065 | 1.0 | 33.9 | 13.1 | −45.6 | 47.5 | 285 |
| 317.5 | 292.5 | 293.0 | 0.375 | 0.0 | 1.0 | 34.2 | 38.2 | −35.0 | 51.8 | 317.5 | 0.367 | 0.0 | 1.0 | 34.0 | 37.8 | −35.3 | 51.7 | 316 | 0.018 | 0.0 | 1.0 | 32.4 | 17.9 | −44.2 | 47.8 | 292 | 0.026 | 0.0 | 1.0 | 32.4 | 18.4 | −44.1 | 47.9 | 292 |
| 324.4 | 300.0 | 300.1 | 0.5 | 0.0 | 1.0 | 37.2 | 43.1 | −30.8 | 53.0 | 324.4 | 0.5 | 0.0 | 1.0 | 37.2 | 43.2 | −30.8 | 53.1 | 324 | 0.136 | 0.0 | 1.0 | 31.6 | 24.3 | −41.9 | 48.5 | 300 | 0.139 | 0.0 | 1.0 | 31.5 | 24.4 | −41.9 | 48.6 | 300 |
| 330.6 | 307.5 | 307.2 | 0.625 | 0.0 | 1.0 | 39.1 | 48.4 | −27.2 | 55.6 | 330.6 | 0.617 | 0.0 | 1.0 | 39.0 | 48.1 | −27.4 | 55.4 | 330 | 0.238 | 0.0 | 1.0 | 31.1 | 29.9 | −39.6 | 49.7 | 307 | 0.235 | 0.0 | 1.0 | 31.1 | 29.8 | −39.7 | 49.7 | 306 |
| 338.7 | 315.0 | 314.3 | 0.75 | 0.0 | 1.0 | 41.8 | 55.1 | −21.4 | 59.1 | 338.7 | 0.75 | 0.0 | 1.0 | 41.9 | 55.2 | −21.4 | 59.2 | 338 | 0.343 | 0.0 | 1.0 | 33.4 | 36.3 | −36.2 | 51.4 | 315 | 0.335 | 0.0 | 1.0 | 33.2 | 35.8 | −36.5 | 51.2 | 314 |
| 343.9 | 322.5 | 321.4 | 0.875 | 0.0 | 1.0 | 45.6 | 60.1 | −17.3 | 62.6 | 343.9 | 0.867 | 0.0 | 1.0 | 45.4 | 59.8 | −17.5 | 62.4 | 343 | 0.456 | 0.0 | 1.0 | 36.2 | 41.5 | −32.3 | 52.7 | 322 | 0.439 | 0.0 | 1.0 | 35.8 | 40.8 | −32.9 | 52.5 | 321 |
| 348.9 | 330.0 | 328.6 | 1.0 | 0.0 | 1.0 | 48.1 | 65.4 | −12.7 | 66.6 | 348.9 | 1.0 | 0.0 | 1.0 | 48.2 | 65.4 | −12.7 | 66.7 | 348 | 0.612 | 0.0 | 1.0 | 38.9 | 47.9 | −27.6 | 55.4 | 330 | 0.584 | 0.0 | 1.0 | 38.5 | 46.8 | −28.4 | 54.8 | 328 |
| 350.7 | 337.5 | 335.7 | 1.0 | 0.0 | 0.875 | 49.5 | 66.1 | −10.7 | 67.0 | 350.7 | 1.0 | 0.0 | 0.883 | 49.5 | 66.1 | −10.8 | 67.0 | 350 | 0.723 | 0.0 | 1.0 | 41.3 | 53.8 | −22.7 | 58.4 | 337 | 0.696 | 0.0 | 1.0 | 40.7 | 52.3 | −24.0 | 57.6 | 335 |
| 354.2 | 345.0 | 342.8 | 1.0 | 0.0 | 0.75 | 49.3 | 64.5 | −6.5 | 64.8 | 354.2 | 1.0 | 0.0 | 0.75 | 49.3 | 64.6 | −6.5 | 64.9 | 354 | 0.902 | 0.0 | 1.0 | 46.2 | 61.3 | −16.3 | 63.5 | 345 | 0.848 | 0.0 | 1.0 | 44.9 | 59.1 | −18.2 | 61.9 | 342 |
| 361.9 | 352.5 | 349.9 | 1.0 | 0.0 | 0.625 | 48.0 | 61.8 | 2.1 | 61.8 | 361.9 | 1.0 | 0.0 | 0.633 | 48.1 | 62.0 | 1.6 | 62.0 | 361 | 1.0 | 0.0 | 0.83 | 49.5 | 65.6 | −9.1 | 66.3 | 352 | 1.0 | 0.0 | 0.964 | 48.6 | 65.6 | −12.1 | 66.8 | 349 |
| 370.0 | 360.0 | 357.0 | 1.0 | 0.0 | 0.5 | 47.8 | 58.9 | 10.4 | 59.9 | 370.0 | 1.0 | 0.0 | 0.5 | 47.8 | 59.0 | 10.4 | 59.9 | 370 | 1.0 | 0.0 | 0.657 | 48.3 | 62.6 | 0.0 | 62.6 | 360 | 1.0 | 0.0 | 0.828 | 49.5 | 65.6 | −9.0 | 66.2 | 352 |
| 378.9 | 367.5 | 364.1 | 1.0 | 0.0 | 0.375 | 47.4 | 56.8 | 19.5 | 60.0 | 378.9 | 1.0 | 0.0 | 0.383 | 47.4 | 57.0 | 18.9 | 60.1 | 378 | 1.0 | 0.0 | 0.547 | 47.9 | 60.2 | 7.4 | 60.6 | 367 | 1.0 | 0.0 | 0.659 | 48.4 | 62.7 | −0.1 | 62.7 | 359 |
| 386.2 | 375.0 | 371.2 | 1.0 | 0.0 | 0.25 | 47.5 | 55.9 | 27.5 | 62.3 | 386.2 | 1.0 | 0.0 | 0.25 | 47.6 | 55.9 | 27.6 | 62.4 | 386 | 1.0 | 0.0 | 0.43 | 47.6 | 58.0 | 15.5 | 60.0 | 375 | 1.0 | 0.0 | 0.519 | 47.8 | 59.5 | 9.2 | 60.2 | 368 |
| 391.3 | 382.5 | 378.3 | 1.0 | 0.0 | 0.125 | 47.6 | 56.3 | 34.2 | 65.9 | 391.3 | 1.0 | 0.0 | 0.133 | 47.7 | 56.4 | 33.8 | 65.7 | 390 | 1.0 | 0.0 | 0.323 | 47.5 | 56.6 | 22.9 | 61.0 | 382 | 1.0 | 0.0 | 0.408 | 47.5 | 57.6 | 17.1 | 60.0 | 376 |
| 393.4 | 390.0 | 385.4 | 1.0 | 0.0 | 0.0 | 47.5 | 57.2 | 37.8 | 68.6 | 393.4 | 1.0 | 0.0 | 0.0 | 47.6 | 57.2 | 37.9 | 68.6 | 393 | 1.0 | 0.0 | 0.158 | 47.7 | 56.3 | 32.5 | 65.0 | 390 | 1.0 | 0.0 | 0.263 | 47.6 | 56.1 | 26.7 | 62.1 | 385 |

rgb*dd rgb*ds rgb*de

1−003730−L0 PE990−70 LAB*la0, YN=0%, XYZnw=3.9, 4.1, 4.1, 84.7, 89.6, 93.9, LAB*nw=23.9, 0.0, 0.0, 95.8, 0.0, 0.0

Output: Laser printer output; separation cmyn6*, D65, page 8/33

TUB-test chart PE99; hue code: H*$_d$=R00Y$_d$
48 step hue circles; *rgb−LabCh**tables, *cmyk*

input: *rgb/cmyk* −> *rgb*$_d$
output: transfer to *cmyk*$_d$

see similar files: http://130.149.60.45/~farbmetrik/PE99/PE99.HTM
technical information: http://www.ps.bam.de or http://130.149.60.45/~farbmetrik

1−003730−F0

http://130.149.60.45/~farbmetrik/PE99/PE99L0FP.PDF /.PS; start output
F: 3D-linearization PE99/PE99LE30FP.DAT in file (F), page 1/2

**Input and Output: Printer Reflective System FRS06a for relative CIELAB hue $h_{ab,a,rel}$ = $h_{ab}$/360 = 31/360 = 0.08**

***H***₋ = R00Y₋*

**Data for any device (d) or elementary (e) colour:**
*HIC*₋*
**hue text for the colours of this page:**
*H*₋ = R00Y₋*
**triangle lightness *T****

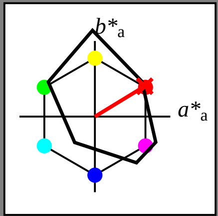


| FRS06a; adapted (a) CIELAB data | | | | | |
|---|---|---|---|---|---|
| *Name* | *L*=L*a* | *a*a* | *b*a* | *C*ab,a* | *h*ab,a* |
| $R_{-,Ma}$ | 32.5 | 62.3 | 46.4 | 77.7 | 36 |
| $Y_{-,Ma}$ | 82.7 | −3.1 | 113.9 | 114.0 | 91 |
| $G_{-,Ma}$ | 39.4 | −61.8 | 45.8 | 76.9 | 143 |
| $C_{-,Ma}$ | 47.8 | −26.8 | −34.2 | 43.4 | 231 |
| $B_{-,Ma}$ | 10.1 | 55.1 | −61.0 | 82.2 | 312 |
| $M_{-,Ma}$ | 34.5 | 80.6 | −33.9 | 87.5 | 337 |
| $N_{-,Ma}$ | 6.2 | 0.0 | 0.0 | 0.0 | 0 |
| $W_{-,Ma}$ | 91.9 | 0.0 | 0.0 | 0.0 | 0 |
| $R_{-,CIE}$ | 39.9 | 58.7 | 27.9 | 65.0 | 25 |
| $Y_{-,CIE}$ | 81.2 | −2.8 | 71.5 | 71.6 | 92 |
| $G_{-,CIE}$ | 52.2 | −42.4 | 13.6 | 44.5 | 162 |
| $B_{-,CIE}$ | 30.5 | 1.4 | −46.4 | 46.4 | 271 |

**Data for maximum colour (Ma):**
***LabCh*₋,Ma**: 48 66 40 77 31**
***HIC*₋,Ma**: R00Y_100_100₋**
***rgbic*₋,Ma**:**
**1.0 0.0 0.0 1.0 1.0**
**triangle lightness *T****

**%Gamut**
**$u^*_{rel}$ = 114**
**%Regularity**
**$g^*_{H,rel}$ = 28**
**$g^*_{C,rel}$ = 38**

| ORS20a; adapted (a) CIELAB data | | | | | |
|---|---|---|---|---|---|
| *H*₋* | *L*=L*a* | *a*a* | *b*a* | *C*ab,a* | *h*ab,a* |
| R00Y_100_100₋ | 48.4 | 66.1 | 40.2 | 77.3 | 31 |
| R25Y_100_100₋ | 56.8 | 48.0 | 50.5 | 69.6 | 46 |
| R50Y_100_100₋ | 68.6 | 25.0 | 63.9 | 68.6 | 68 |
| R75Y_100_100₋ | 80.6 | 4.8 | 77.2 | 77.3 | 86 |
| Y00G_100_100₋ | 90.2 | −9.6 | 88.2 | 88.7 | 96 |
| Y25G_100_100₋ | 83.2 | −18.4 | 79.9 | 81.9 | 102 |
| Y50G_100_100₋ | 73.3 | −31.7 | 62.7 | 70.2 | 116 |
| Y75G_100_100₋ | 62.0 | −49.7 | 43.2 | 65.8 | 139 |
| G00B_100_100₋ | 55.8 | −65.2 | 33.8 | 73.4 | 152 |
| G25B_100_100₋ | 59.3 | −50.3 | −9.0 | 51.0 | 190 |
| G50B_100_100₋ | 63.0 | −30.5 | −42.0 | 51.9 | 234 |
| G75B_100_100₋ | 45.7 | −5.7 | −44.6 | 44.9 | 262 |
| B00R_100_100₋ | 27.5 | 25.9 | −47.3 | 53.9 | 298 |
| B25R_100_100₋ | 38.3 | 52.6 | −28.5 | 59.8 | 331 |
| B50R_100_100₋ | 49.5 | 73.5 | −9.0 | 74.0 | 353 |
| B75R_100_100₋ | 48.9 | 69.3 | 12.9 | 70.4 | 10 |

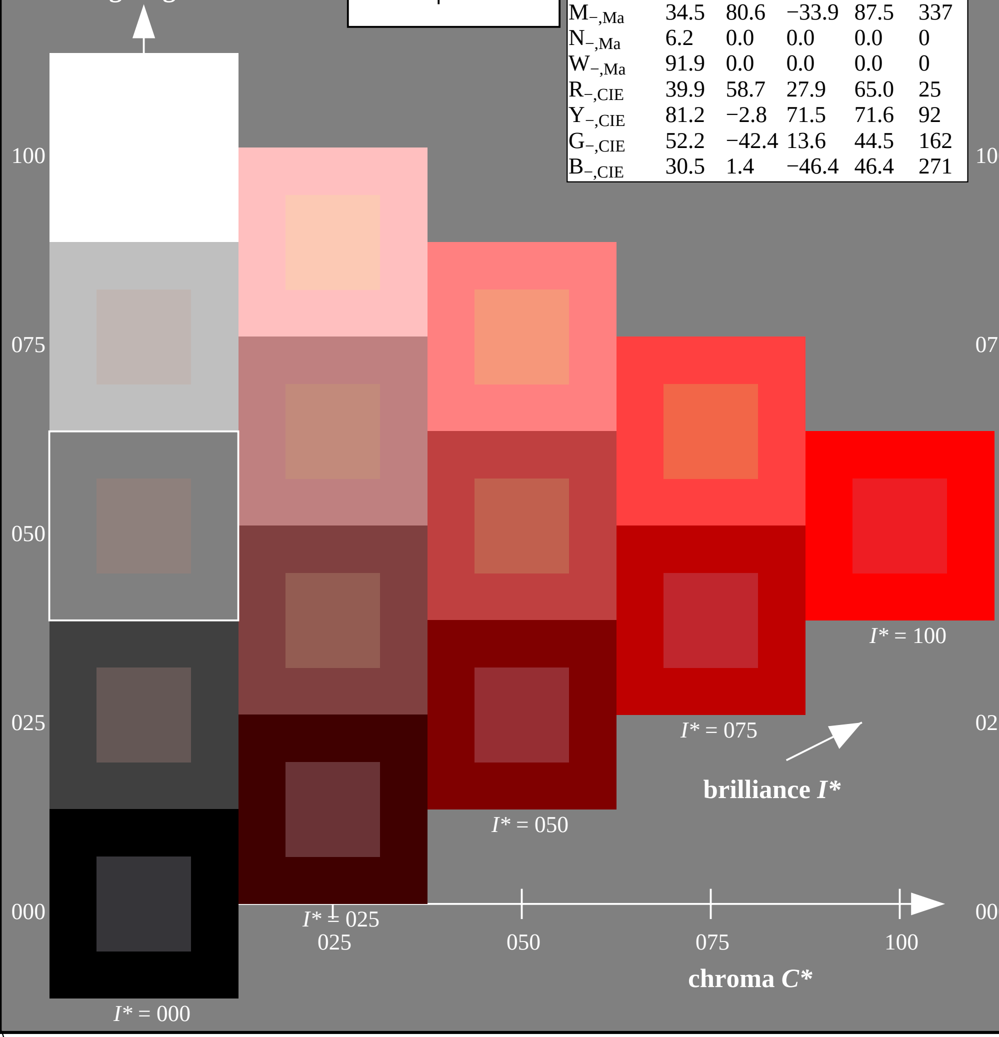


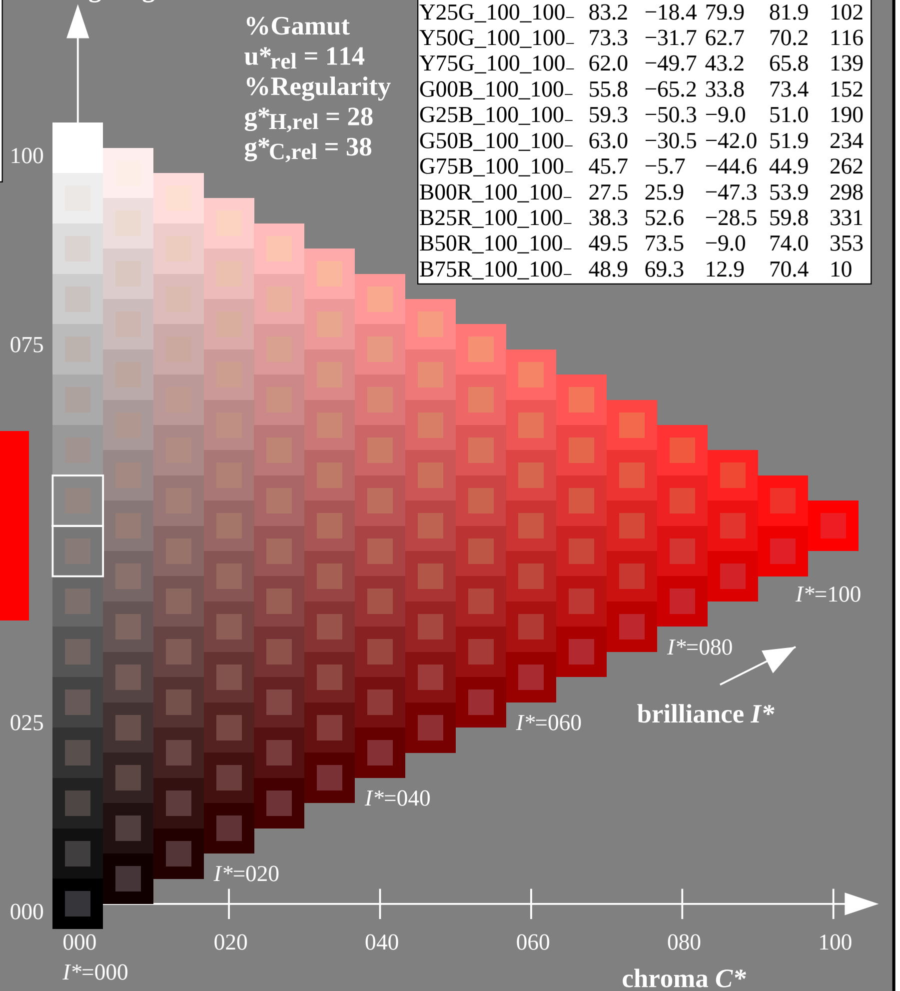


see similar files: http://130.149.60.45/~farbmetrik/PE99/PE99.HTM
technical information: http://www.ps.bam.de or http://130.149.60.45/~farbmetrik

TUB registration: 20130201-PE99/PE99L0FP.PDF /.PS
application for measurement of laser printer output

TUB material: code=rha4ta

1−113030−L0 PE990−7N

TUB-test chart PE99; hue code: H*₋=R00Y₋
Test chart according to DIN 33872

input: *rgb/cmyk −> rgb/cmyk*
output: no change